Biased Antagonists of CXCR4 Avoid the Development of Antagonist Tolerance

BY

BEN HITCHINSON
B.Sc. (Hons), University of Teesside, 2010
M.Res., Imperial College London, 2011

THESIS

Submitted as partial fulfilment of the requirements
for the degree of Doctor of Philosophy in Biochemistry and Molecular Genetics
in the Graduate College of the
University of Illinois at Chicago, 2019

Chicago, Illinois.

Defence Committee:

Vadim Gaponenko, Advisor and Chair
Steven J. Ackerman, Biochemistry and Molecular Genetics
Michael Caffrey, Biochemistry and Molecular Genetics
Nissim Hay, Biochemistry and Molecular Genetics
Angela Tyner, Biochemistry and Molecular Genetics
Andrei Gartel, Medicine

To my parents, Anthony and Tracy Hitchinson. This thesis is dedicated to you. You taught me to work hard and use my head, you guided me, you supported me, and despite the distance you never felt far away.

ACKNOWLEDGMENTS

The work presented in this thesis was made possible by the contributions of a significant number of people. Firstly, it would not have been possible without the ideas, patience and steadfast belief of Dr. Vadim Gaponenko. As my advisor, I would like to thank him for his generosity towards me during my time in the lab, where I have been fortunate to learn a range of new techniques. I would also like to thank him for his academic tutelage, for giving me the opportunity to complete my Ph.D and for his guidance throughout graduate school.

This work was also made possible by the contributions and suggestions of my thesis committee; Professor Angela Tyner, Professor Steven Ackerman, Dr. Michael Caffrey, Professor Nissim Hay and Dr. Andrei Gartel. I would like to thank them for their scientific guidance in subjects ranging from cell biology to biophysical characterisation of proteins, and I am indebted to them for giving up their time to do this. I would especially like to thank Professor Tyner, Professor Ackerman, and Dr. Gartel for allowing me to collaborate with their labs and to learn from them in the process. I am grateful to all of them for their time and support throughout my graduate school career.

The contributions of collaborators to this project is something I am very grateful for. I would especially like to thank Dr. Ben Ramirez, Professor Matthias Majetschak, Dr. Nadya Tarasova, Professor Brian Volkman, Dr. Sojin Shikano and Professor Nikolaus Heveker. Each of these people spent time and effort to train or help me and I sincerely appreciate it.

I would like to thank my lab mates both present and former: Dr. Boris Garnier, Dr. Otto Meyer, Dr. Tanmay Chavan, Dr. Russell Smith, Finn Mannerings, Anu Puppala, Ashley Priddey, Avik Banerjee and Dr. Hazem Abdelkarim. Each of these people taught me things I didn’t know, asked me questions that made me think, and made the work environment an enjoyable place. I would also like to thank my graduate school colleagues Dr. Stefanie Kall, Dr. Gaurang Bhide and Dr. Darren Wozniak, who were wonderful people to work alongside and learn from.

Finally, I would like to thank my friends and my family. I thank my wife Caitlin Hitchinson, née McDonald, for her love, her support and for making coming home at night the best part of the day whether experiments had succeeded or failed. I thank my in-laws Tom and Vickie McDonald for welcoming me into their family and for their support and kindness during this process. I thank my friends at home in Middlesbrough, even though they will never read this. And I thank my parents and my sister, who are the best people in the world. Without their love and support, I would never have survived this far from home.

Thank you.

Ben.

PREFIX

This thesis contains data and text that has previously been published in: "Biased antagonism of CXCR4 avoids antagonist tolerance." Hitchinson, B., J. M. Eby, X. Gao, F. Guite-Vinet, J. J. Ziarek, H. Abdelkarim, Y. Lee, Y. Okamoto, S. Shikano, M. Majetschak, N. Heveker, B. F. Volkman, N. I. Tarasova and V. Gaponenko (2018). Sci Signal 11(552). Reprinted with permission from AAAS.

AUTHOR CONTRIBUTIONS

The PRESTO-Tango and BRET assays in this thesis were performed by Jonathan Eby and Dr. Xianlong Gao in the lab of Professor Matthias Majetschak. Ca^{2+} flux experiments were performed by Dr. Joshua Ziarek in the lab or Professor Brian Volkman. NMR experiments with IT1t were performed by Dr. Hazem Abdelkarim, who also helped with sourcing of small molecule biased antagonists of CXCR4.

TABLE OF CONTENTS

LIST OF TABLES

LIST OF FIGURES

LIST OF ABBRIEVIATIONS

ACKR	Atypical chemokine receptor
AC	Adenylyl cyclase
Ala/A	Alanine
ALL	Acute lymphoid leukaemia
AML	Acute myeloid leukaemia
AMP	Adenosine monophosphate
ANOVA	Analysis of variance
Asn/N	Asparagine
Asp/D	Aspartic Acid
ATP	Adenosine triphosphate
B2AR	Beta-2-adrenergic receptor
BA	Beta-arrestin
BRET	Bioluminescence resonance energy transfer
BSA	Bovine serum albumin
cAMP	Cyclic adenosine monophosphate
CHO	Chinese hamster ovary cells
CREB1	Cyclic adenosine monophosphate responsive element binding protein 1
CXCL12	CXC-motif ligand 12
CXCR4	CXC-motif receptor 4
DAG	Diacylglycerol
DMEM	Dulbecco’s modified eagle media
DMSO	Dimethyl sulphoxide
DNA	Deoxyribonucleic acid
DOPR	Delta-opioid receptor

EC_{50}	Effective concentration 50
ECL	Extracellular loop
ELISA	Enzyme-linked immunosorbent assay
EM	Electron microscopy
ERK	Extracellular signal-regulated kinase
FDA	Food and Drug Administration
G protein	Guanine nucleotide binding protein
Gα	Guanine nucleotide binding protein alpha subunit
Gβ	Guanine nucleotide binding protein beta subunit
Gγ	Guanine nucleotide binding protein gamma subunit
GAPDH	Glyceraldehyde-3-phoshpate dehydrogenase
GDP	Guanine diphosphate
Glu/E	Glutamic acid
Gln	Glutamine
GPCR	G protein-coupled receptor
GRK	G protein-coupled receptor kinase
GTP	Guanine triphosphate
HEK	Human embryonic kidney cells
HSQC	Heteronuclear single quantum coherence spectroscopy
IC_{50}	Inhibitory concentration 50
ICL	Intracellular loop
ILE	Isoleucine
IMDM	Iscove's Modified Dulbecco's Medium
IP_3	Inositol 1,4,5-trisphosphate
KOPR	Kappa-opioid receptor

Lys/K	Lysine
MAPK	Mitogen activated protein kinase
MOPR	Mu-opioid receptor
NAM	Negative allosteric modulator
NME	New molecular entity
NMR	Nuclear magnetic resonance
PAM	Positive allosteric modulator
PBS	Phosphate buffered saline
PE	Phycoerythrin
PEG	Polyethylene glycol
PHE	Phenylalanine
PI3K	Phosphatidylinositide 3-kinases
PKA	Protein kinase A
PKC	Protein kinase C
PRESTO-Tango	Parallel receptorome expression and screening via transcriptional output, with transcriptional activation following arrestin translocation
PTM	Post-translational modification
PTX	Pertussis toxin
RNA	Ribonucleic acid
RPMI	Roswell Park Memorial Institute medium
SD	Standard deviation
SDF1	Stromal derived factor 1
Ser/S	Serine
SPR	Surface plasmon resonance
STD-NMR	Saturation transfer difference nuclear magnetic resonance spectroscopy

Thr/T	Threonine
TM	Transmembrane
Tyr/Y	Tyrosine
V_{max}	Maximum velocity
WGA	Wheat germ agglutinin
WHIM	Warts, Hypogammaglobulinemia, Immunodeficiency, and Myelokathexis syndrome

SUMMARY

In this thesis, I present work that describes the investigation of the mechanism that causes tolerance to an FDA approved GPCR antagonist. The antagonist, AMD3100, is a competitive inhibitor of the CXCR4 chemokine receptor, a GPCR involved in embryonic development and immune response. CXCR4, along with its canonical chemokine CXCL12, is also implicated in the metastatic phenotype of at least 23 different cancers. It was proposed that AMD3100 could be used to inhibit metastasis or mobilise tumour cells from protective niches and sensitise these cells to chemotherapy. However, tolerance to AMD3100 develops rapidly, decreasing the ability of the drug to inhibit CXCR4 and sensitize them to chemotherapy.

In the first part of this thesis, I present cell biology data to support the notion that AMD3100 is an unbiased antagonist of CXCR4. I show that inhibition of CXCR4 endocytosis by prolonged exposure to AMD3100 causes receptor accumulation on the cell surface. I use biophysical techniques to show that the prolonged exposure of cells to AMD3100 leads to CXCR4 oligomerisation, causing a conformational change within the receptor. Ultimately, this conformational change leads to an altered interaction between the receptor and the antagonist, reducing the affinity of CXCR4 for AMD3100 in tolerant cells, thus allowing cells to overcome the effects of the antagonist.

In the second part of this thesis, I demonstrate that X4-2-6, a peptide derived from transmembrane helix 2 and extracellular loop 1 of CXCR4, is a biased antagonist of the receptor that inhibits G proteins but not β-arrestin1/2 and subsequent receptor endocytosis. Prolonged exposure of cells to X4-2-6 does not lead to accumulation of CXCR4 on the cell surface and avoids tolerance. I demonstrated that the mechanism of X4-2-6 biased antagonism is through forming a ternary complex with the receptor and the chemokine CXCL12 that allows for chemokine activation of arrestins but inhibits activation of G proteins.

I. INTRODUCTION

1.1 The Problem of Drug Tolerance

Each year, the United States Food and Drug Administration (FDA) approves approximately twenty new drugs for medical use [1]. These drugs, also called new molecular entities (NMEs), must pass rigorous preclinical and clinical tests to demonstrate both safety and efficacy. Efficacy refers to capacity of a drug to produce an effect. On average, the cost in research and development outlays to bring a drug to market is $2.9 billion [2]. The process is lengthy and most potential drugs fail in clinical trials due to low efficacy, with only 13.8% of drug development programs resulting in the approval of a NME [3]. Despite the monumental efforts it takes to bring a NME to market, the success of any approved drug can be significantly limited by a number of factors, including genetic variations of individual patients that has been linked to differences in patient response to anti-hypertensive drugs, resistance to antibiotics during the treatment of bacterial infections, and the development of tolerance to pain relieving medications [4].

Tolerance is the diminished pharmacological effect of a drug after repeated, prolonged or chronic exposure [5]. The result is a significant reduction in drug efficacy over time, which can be problematic when higher doses of a drug are required to elicit a response but also have the potential to induce undesirable side effects. The development of tolerance has been demonstrated for multiple classes of drugs including alcohols, opioids and chemotherapies, and has been observed in health conditions such as peptic ulcer disease, gastroesophageal reflux, schizophrenia and opioid addiction [6-12]. Yet most preclinical studies only assess the efficacy of a drug after acute administration and do not consider the potential for the development of tolerance [13]. Additionally, there are very few studies that provide strategies to avoid the reduction in drug efficacy over time. Understanding the mechanisms which cause tolerance may contribute to the development of drugs that avoid a reduction in efficacy over time and provide new therapeutic options for diseases where antagonist tolerance is a significant problem.

1.2 G Protein-Coupled Receptors

1.2.1 G Protein-Coupled Receptors as drug targets

More than 30% of all FDA approved drugs target a single protein family, the G protein-coupled receptors (GPCRs) [14, 15]. GPCRs are the largest family of membrane proteins in the human genome, with more than 800 receptors identified that can be classified into five main subfamilies: The Rhodopsin family (class A), the Secretin family (class B), the Glutamate family (class C), the Frizzled family (class F), and the Adhesion Family [16]. GPCRs are attractive drug targets because the abundance of these receptors and expression in virtually all tissues means they direct most physiological processes in human health and disease [17-19]. Additionally, their localisation to the plasma membrane of cells facilitates the binding of drugs from the extracellular space. Currently there are more than 700 drugs that target 134 GPCRs, suggesting there is still ample opportunity for GPCR drug development [15]. Thus, understanding the structure, function and signalling mechanisms of GPCRs and how tolerance to GPCR drugs develops is of great pharmacologic interest.

1.2.2 G Protein-Coupled Receptors as Molecular Switches

GPCRs primarily localise to the plasma membrane of cells where upon binding of a variety of extracellular ligands, they stimulate intracellular signalling. The diversity of GPCR ligands are legion and include photons, ions, odorants, vitamins, peptide hormones, chemical hormones, proteins, neurotransmitters and even metabolites [20-22]. Yet despite this all GPCRs share the same general architecture. GPCRs are comprised of an extracellular N-terminus, seven transmembrane (TM) α-helicies connected by three extracellular and three intracellular loops, and an intracellular C-terminus. The N-terminus, extracellular loops that connect the TM domains and the TM helical bundle itself, often serve as the binding site for ligands. The intracellular C-terminus and intracellular loops are sites for effector binding. Because binding of an extracellular

ligand induces intracellular signalling, GPCRs can be considered allosteric proteins, an observation that has propelled the modern theory of GPCR activation discussed later in this thesis.

In the simplest scheme of GPCR signalling, an extracellular activating ligand (or agonist) binds an inactive GPCR (R) and "switches on" the receptor (R*) to promote its interaction with a heterotrimeric Guanine nucleotide binding protein (G protein) consisting of α, β and γ subunits (figure 1) [23-25]. The "switched on" receptor facilitates the activation of the Gα subunit by promoting exchange of GDP for GTP, and the GTP-bound Gα dissociates from the Gβγ subunits that remain as a heterodimer. The active, GTP-bound Gα can then modulate intracellular second messengers e.g. cAMP production, before hydrolysis of GTP to GDP renders the protein in its inactive state. The Gβγ heterodimer mediates other downstream signalling e.g. mitogen activated protein kinase (MAPK), phosphatidylinositide 3-kinases (PI3K) etc.

Subsequently, the "switched on" GPCR is phosphorylated on its C-terminus by protein kinases and G protein-coupled receptor kinases (GRKs), leading to the recruitment of adapter proteins called arrestins. Three arrestins make up the arrestin family, namely visual arrestin (arrestin-1) that couples to rhodopsin, and β-arrestin1 (BA1, arrestin-2) and β-arrestin2 (BA1, arrestin-3) that are ubiquitously expressed [26]. The recruitment of arrestins causes receptor desensitisation by inhibiting further G protein coupling and promoting receptor internalization by connecting receptors to endocytic machinery. This "switches off" the receptor which can then be either recycled to the plasma membrane or targeted for degradation.

For some receptors, recruitment of arrestins also triggers G protein-independent signalling by scaffolding for signalling proteins [27]. Thus, arrestins function to both regulate G protein signalling and initiate a parallel set of G protein-independent signals. The two consecutive pathways of G protein and arrestin are considered paradigmatic for all GPCRs, but receptors can also engage many other signal transduction mechanisms e.g. JAK/STAT signalling, to initiate cellular responses [28, 29].

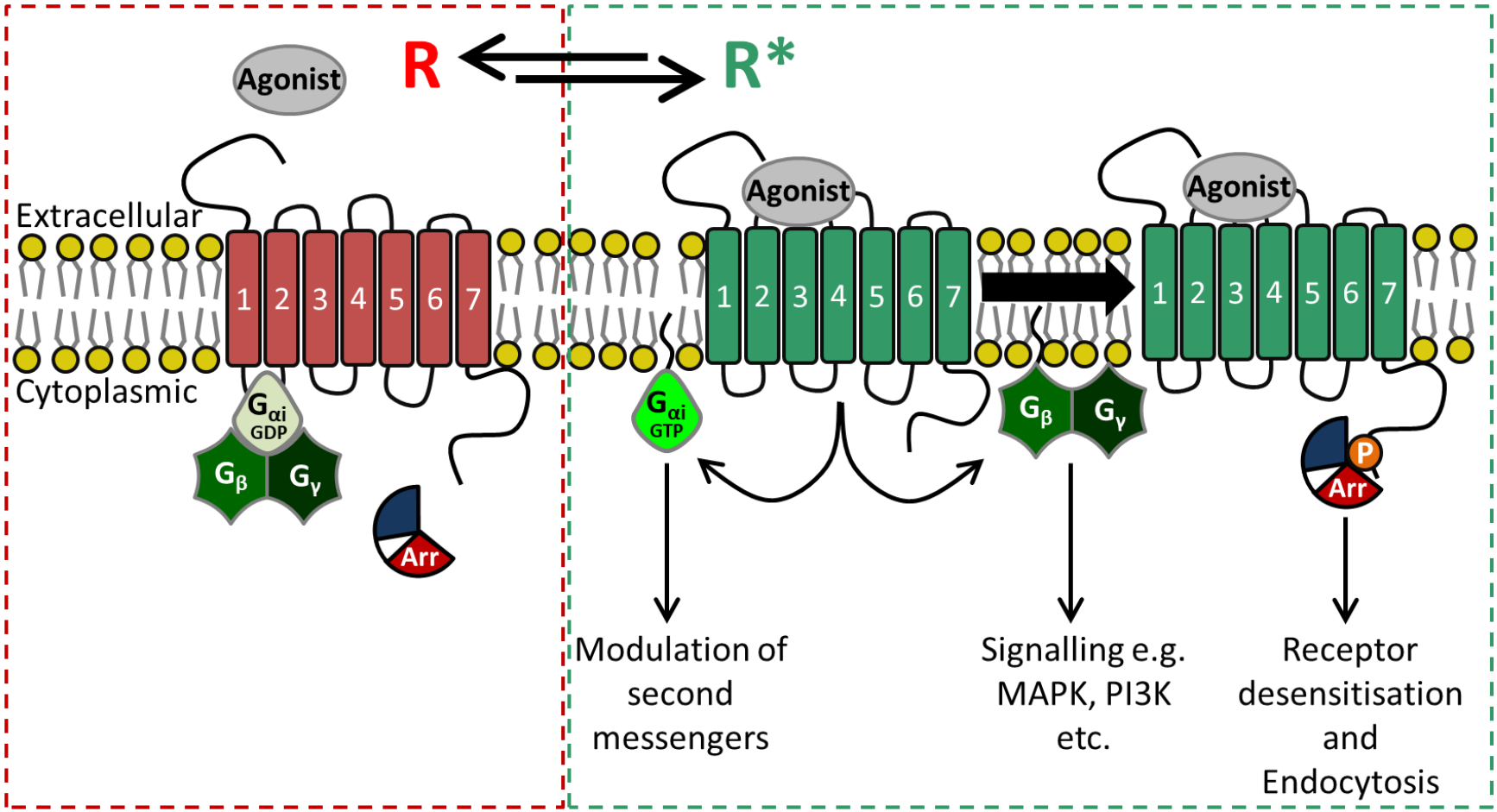

Figure 1: The paradigm of G protein-coupled receptors as signalling switches.

Upon ligand binding, GPCRs undergo a conformational change from an off (R) state to an on (R*) state. This allows for activation of G proteins and subsequently the recruitment of arrestins.

1.2.2 Functional Selectivity and Ligand Bias at G Protein-Coupled Receptors

While the two-state model of GPCR activation is sufficient to define a simple R to R* transition, increasing evidence is available to suggest that GPCRs are not simple on/off switches and can adopt multiple conformations beyond R and R*. The observation that membrane extracts containing GPCRs, such as the δ opioid receptor (DOPR) or the β2-adrenergic receptor (B2AR), could activate G proteins *in vitro* in the absence of ligands provided the first evidence to suggest that GPCRs could adopt an active conformation in the absence of an agonist, hinting that receptors had basal activity [30-32]. These findings also suggested that receptors existed in a conformational equilibrium but did not disprove the two-state model. However, the discovery of agonists of the same receptor that had different efficacies and that yielded different potencies in G protein and arrestin assays supported the notion that the conformational equilibrium of receptors incorporated intermediate states between R and R* [33-35]. It is this conformational equilibrium that is believed to drive the new paradigms and rich pharmacology of GPCR ligands [36].

The current paradigm states that GPCRs exist in a conformational equilibrium, sampling a range of conformations between R and R* at rest [32]. Ligands bind to a GPCR and shift the conformational distribution of the receptor to establish a new equilibrium that leads to a distinct biological outcome (figure 2). These ligands can fall into a broad range of categories depending upon the extent to which they modulate the biological response. For example, an agonist binds extracellularly to promote a conformation of the receptor that leads to coupling and activation of intracellular effectors i.e. an agonist shifts the conformational equilibrium of the receptor towards the R* state. Partial agonists also promote the R* state, but the maximum response is lower than caused by agonist binding. Inverse agonists lower activity below that of the basal state and thus stabilize the R conformation. Antagonists do not affect the equilibrium or basal activity but compete to inhibit the effects of other ligands that bind at the same site.

The dynamic equilibrium of GPCR conformations is also believed to underlie the phenomenon of ligand bias. Historically, GPCRs were classified based on the G protein with which they coupled e.g. Gαi, Gαs, Gαq etc., and agonists were thought to activate the entire signalling repertoire of a receptor [28, 37-39]. However, some GPCRs couple to more than one G protein and some ligands show a preference to activate one pathway over another [40-43]. The greater efficacy of a ligand toward one pathway e.g. G proteins over another, e.g. arrestin, is known as ligand bias and is dependent on the ability of ligands to bind to receptor conformations that preferentially couple to specific effectors.

In addition to the ligands discussed which interact with the receptor orthosteric site i.e. the binding site of the endogenous receptor ligand, some GPCRs can be allosterically controlled by ligands and drugs. These allosteric modulators fall into two categories: Negative allosteric modulators (NAMs) that negatively impact the function of orthosteric ligands, or positive allosteric modulators (PAMs) that enhance orthosteric ligand effects [44]. Additionally, agonist or antagonist molecules have been discovered that interact with both orthosteric and allosteric sites and these are classified as bitopic ligands [22]. Consideration of the ability of a ligand to stimulate or inactivate GPCRs and individual pathways to different extents is an important consideration during the drug development process. For example, activation of arrestins by opioid receptor agonist drugs is associated with unwanted depression of the respiratory system. This rich pharmacology can be harnessed when designing drugs to avoid unwanted side effects associated such as respiratory depression when targeting GPCRs.

1.2.3 Tolerance to G Protein-Coupled Receptor Drugs

Unfortunately, GPCRs often become tolerant to the drugs that target them, significantly limiting therapeutic options available to patients. Examples include tolerance to drugs targeting opioid, adrenergic and dopamine receptors [45-47]. Most studies of tolerance have focused on

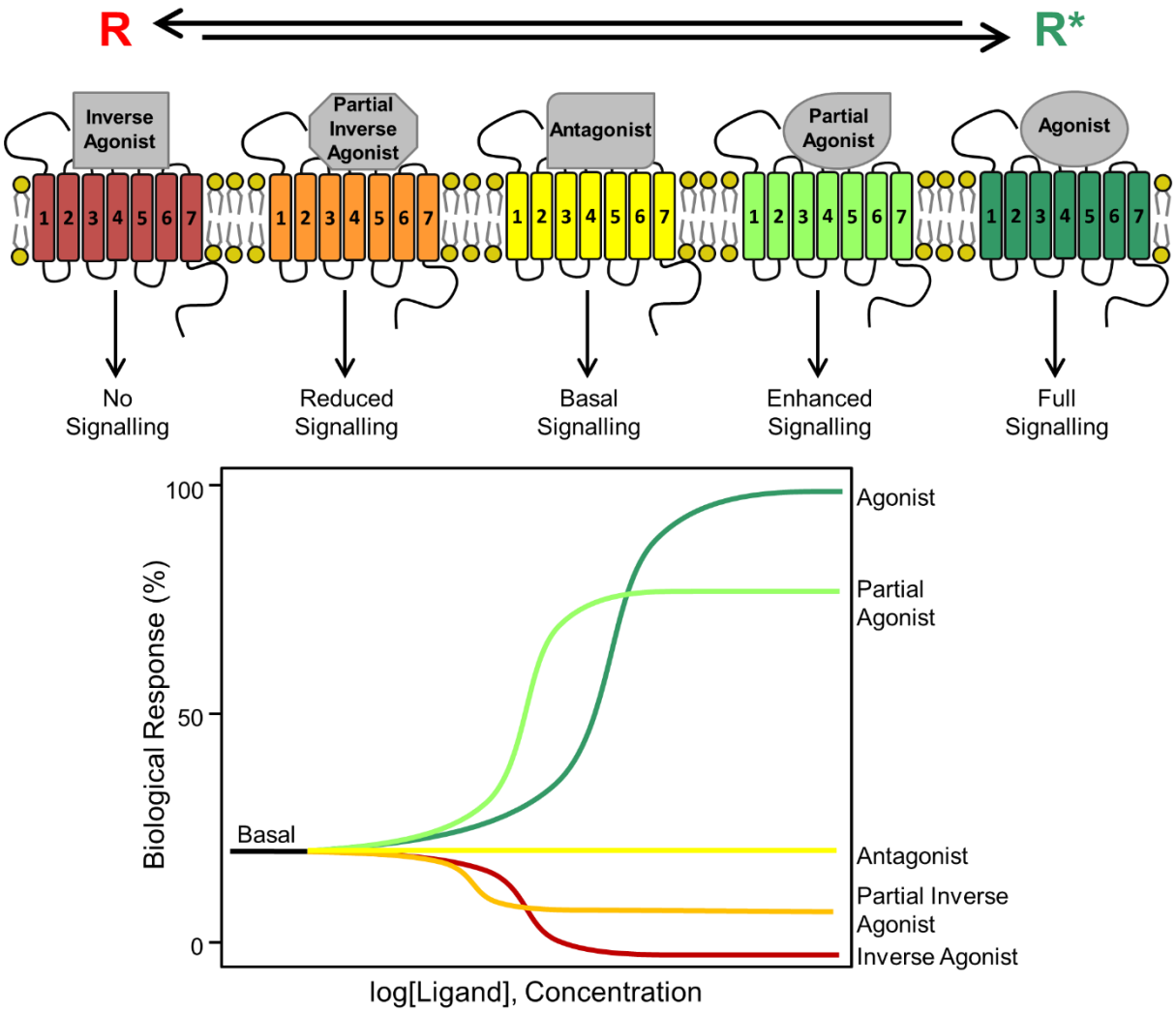

Figure 2: The pharmacology of GPCR ligands.

GPCRs can adopt more conformations than R and R*, which can subsequently be stabilised or induced by different ligands. Each class of ligand has distinct functional outputs and different biological responses.

opioid receptor agonists that activate receptor function. There are three classical opioid receptors, the DOPR, κ-opioid receptor (KOPR) and μ-opioid receptor (MOPR), with the most clinically relevant opioid drugs acting as agonists of MOPRs to elicit analgesic effects [48]. Studies of opioid tolerance have highlighted two possible mechanisms of agonist tolerance: Internalisation and impaired receptor recycling to the cell surface reducing the concentration of receptor that can be targeted, and reduced receptor occupancy by the drug [49]. It has therefore been of significant pharmacological interest to develop biased agonists of opioid receptors that activate G protein pathways related to the analgesic effects of receptor signalling but not BA pathways that would remove the receptor from the cell surface and is linked to respiratory depression. Despite reported tolerance to antagonists of GPCRs, there are very few studies providing strategies to avoid it. Antagonist tolerance has been observed for AMD3100, the only FDA approved inhibitor of the GPCR CXCR4 [50, 51].

1.3 The Chemokine Receptor CXCR4 and Drug Tolerance

1.3.1 An Introduction to CXCR4

C-X-C chemokine receptor type 4 (CXCR4) is a class A GPCR that belongs to a subfamily of 20 receptors, collectively known as chemokine receptors. Chemokine receptors are differentially expressed in a variety of tissues and on all leukocytes. The functions of these GPCRs is critical for cell migration during development, immune cell homeostasis, cell migration during immune response and the recruitment of immune cells in disease [52]. These receptors direct the migration of cells towards increasing concentrations of endogenous ligands, small chemotactic cytokines called chemokines. The 20 chemokine receptors and 48 known chemokines can be subdivided into families based on the spacing of the first two conserved cysteines within the chemokine amino acid sequence e.g. C-, CC-, CXC- and CX3C- [53]. Most receptors only bind ligands from the same family but can be promiscuous in the number of ligands they bind, with some receptors able

to bind as many as different 10 chemokines [54]. Additionally, some chemokines can activate multiple receptors. The majority of chemokine receptors couple to the pertussis toxin (PTX)-sensitive Gαi-class of G proteins, that when activated inhibit the activity of adenylate cyclase isoforms to inhibit the production of cAMP. They are then subject to regulation by BAs. Chemokine receptor signalling has been implicated in a number of diseases, including autoimmune disorders, viral infections and cancer metastasis [52]. Yet only two FDA approved drugs target this family; the CCR5 antagonist maraviroc and the CXCR4 antagonist AMD3100 [55].

CXCR4 is of particular interest for drug development because it is a coreceptor for T-trophic HIV cellular entry, causes Warts, Hypogammaglobulinemia, Immunodeficiency, and Myelokathexis (WHIM) syndrome, and receptor overexpression is observed in at least twenty-three different cancers where it is associated with a highly metastatic phenotype [56-59]. CXCR4 is involved in a large number of physiological processes, including embryonic development, homing and maintenance of hematopoietic stem cells, haematopoiesis and immune response, where CXCR4 drives chemotaxis of cells toward its only abundant cognate ligand CXCL12, also known as stromal derived factor 1 (SDF1) (figure 3) [60-66]. Many splice variants of CXCL12 exist, but the predominantly expressed variant is CXCL12-α, which once secreted and cleaved of its signal sequence contains 68 amino acids [67-69]. Genetic knockout of either CXCL12 or CXCR4 in mice results in embryonic lethality, defects in B cell lymphopoiesis and bone marrow colonization demonstrating the essential role of the chemokine-receptor pair in development [70, 71]. In the adult, CXCR4 is expressed in a variety of tissues but primarily those of the immune system to drive immune cell chemotaxis and response [72, 73].

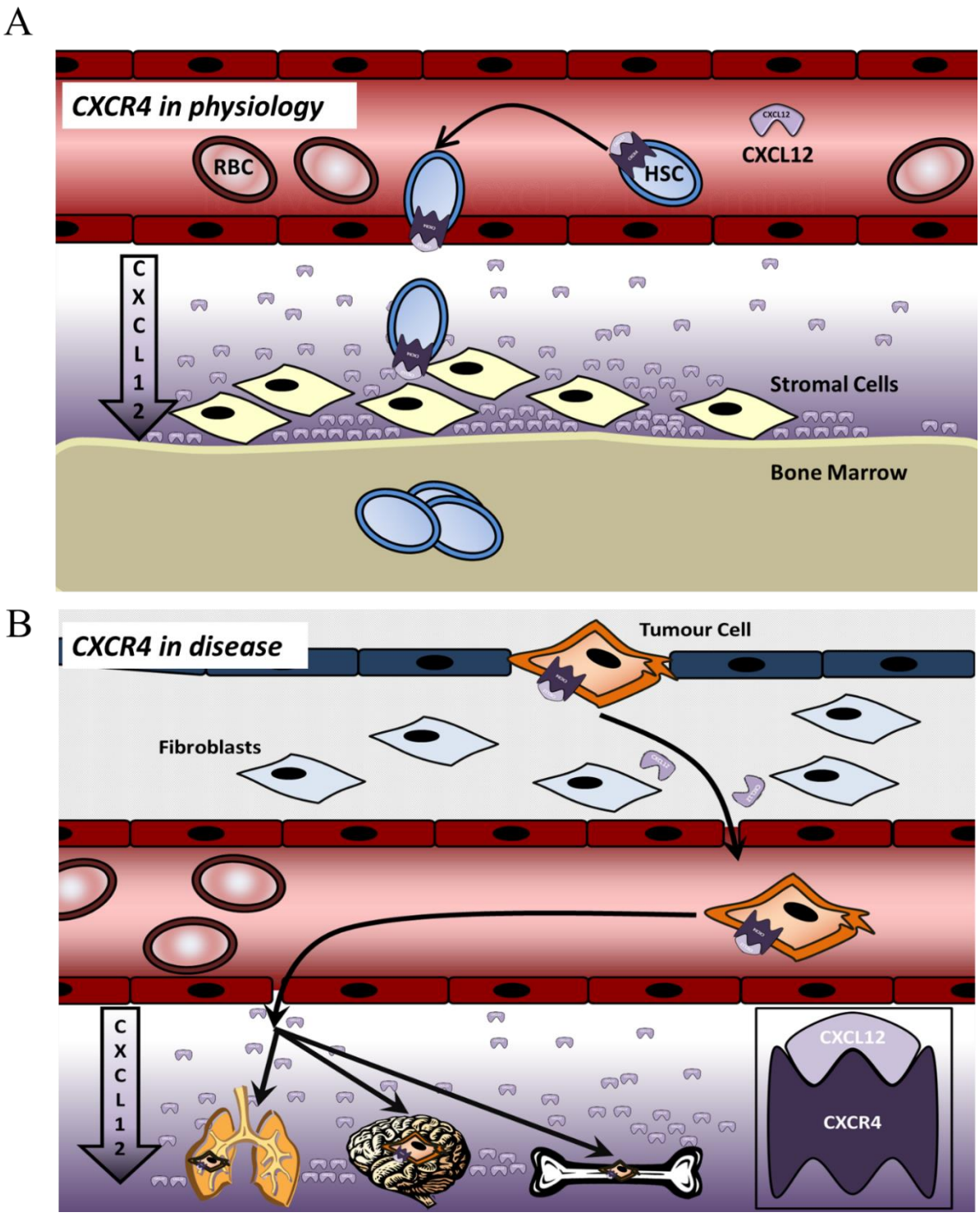

Figure 3: CXCR4 in physiology and disease.

(A) CXCR4 is expressed on a variety of tissues in normal physiology, including cells of the immune system e.g. haematopoietic stem cells (HSC). This drives cells into niches where the CXCL12 is highly expressed e.g. bone marrow. (B) This process can be hijacked by cancer cells that overexpress CXCR4 to drive metastasis to distant sites.

1.3.2 CXCR4-CXCL12 Signalling

Upon binding of the chemokine CXCL12, CXCR4 is activated. CXCL12 binding to CXCR4 is proposed to occur through a two-step process; first residues 12–17 in the N-loop of the chemokine are "lassoed" by the flexible N-terminal 2–36 residues of the receptor [74, 75]. This causes the receptor to undergo a conformational change that results in the insertion of the flexible N-terminus of CXCL12 into the CXCR4 transmembrane helical bundle. This facilitates the interaction of CXCL12 K1 with D97 and E288 of the receptor, chemokine residues S4 and Y7 with CXCR4 D187 [74, 75]. These residues have been shown to be crucial for chemokine-receptor activation [74, 76-79].

The binding of CXCL12 causes the receptor to adopt an active conformation and activates a number of signalling pathways downstream (figure 4) [80]. Almost immediately, the CXCR4 conformational change allows for the GTP-loading of the coupled Gα G protein. CXCR4 primarily couples to the PTX sensitive Gαi but can also couple to Gαq. Active, GTP-loaded Gαi dissociates from the Gβγ heterodimer and inhibits adenylyl cyclase and the subsequent production of cAMP. This in turn relieves PKA mediated inhibition of the Src family tyrosine kinases that can then activate the MAPK pathway [81-83]. The free Gβγ heterodimer activates PI3Ks, which regulates cell polarity, chemotaxis and cell adhesion via phosphorylation of AKT and activation of integrin signalling [84-87]. The Gβγ heterodimer also activates phospholipase C (PLC), which catalyses the hydrolysis of phosphatidylinositol 4,5-bisphosphate (PIP2) into inositol 1,4,5-trisphosphate (IP3) and diacylglycerol (DAG) [88]. IP3 is a soluble second messenger signalling molecule that binds to the inositol trisphosphate receptor (InsP3R) Ca^{2+} channel and results in Ca^{2+} mobilization from the intracellular stores [89]. DAG, which remains in the membrane, promotes the activation of protein kinase C (PKC) and MAPK [90].

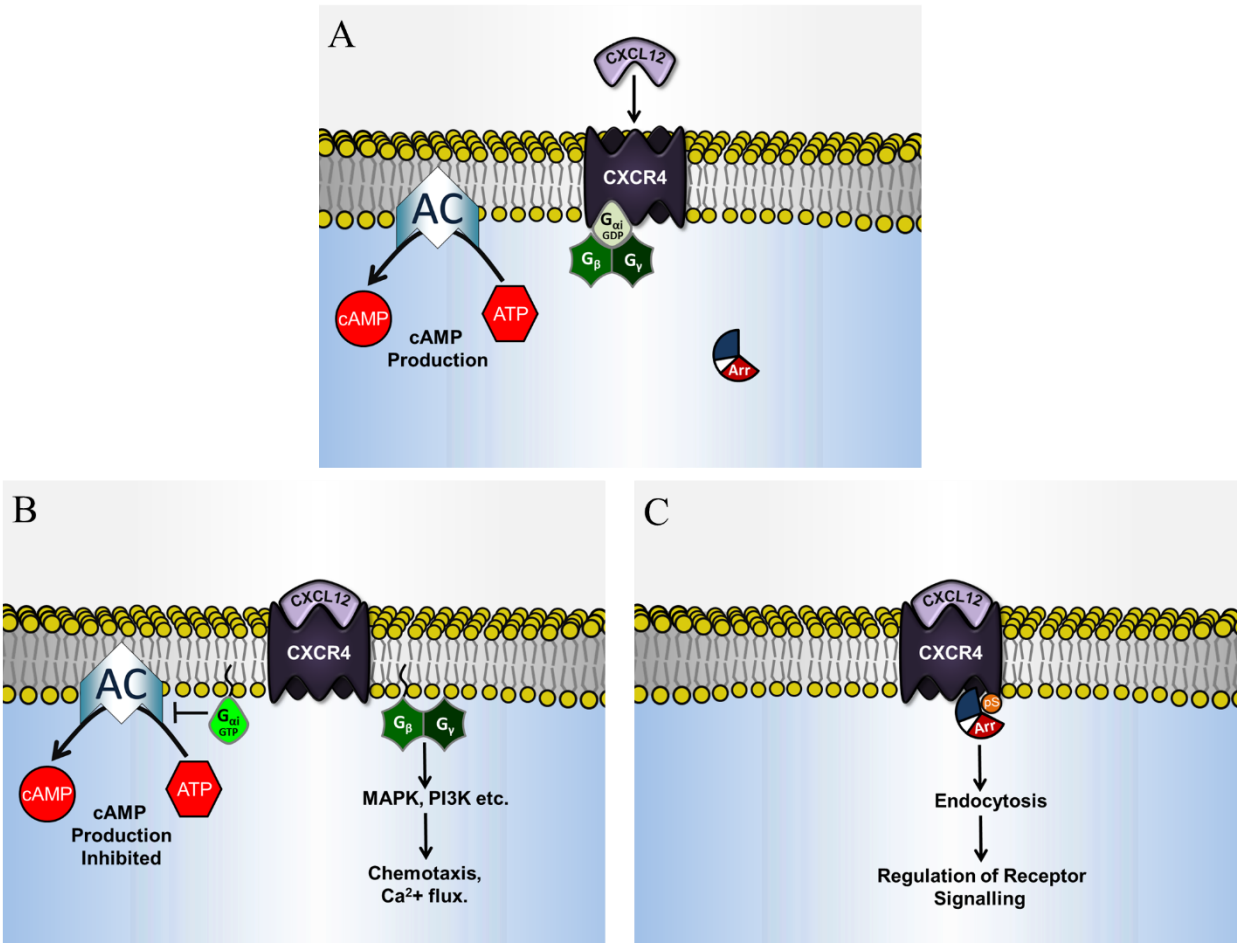

Figure 4: Paradigmatic CXCR4-CXCL12 signalling.

(A) When CXCR4 is in the R state, CXCL12 is not bound, Gαi is GTP loaded and BA is not recruited. (B) When CXCL12 binds CXCR4, the receptor adopts the R* conformation and Gαi is activated by GTP loading. Gαi-GTP dissociates from the Gβγ heterodimer. Gαi inhibits the production of cAMP by inhibiting adenylyl cyclase while Gβγ activated MAPK, PI3K etc. (C) Subsequent to G protein activation, CXCR4 is phosphorylated by kinases that allow for the recruitment of BA, endocytosis of the receptor and "switching off" of receptor signalling.

Subsequent to G protein activation, CXCR4 is rapidly phosphorylated on serine and threonine residues in the C-terminal tail of the receptor [88, 91-93]. This allows for the binding of BA1 and BA2, that couple the receptor to the AP2 adapter protein of the clathrin complex [94]. This ultimately leads to endocytosis, removing CXCR4 from the plasma membrane and regulating signalling [80]. The primary kinases that target CXCR4 are GRK2, GRK6 and PKC [91, 95-97]. Overexpression of GRK2 and/or BA2 enhances CXCL12-mediated CXCR4 endocytosis, while knockdown of GRK6 is associated with increased CXCR4 driven chemotaxis [96]. Truncation of the entire CXCR4 c-terminus eliminated internalisation of the receptor and increased receptor output, something that is closely replicated by germline mutations to the CXCR4 gene in WHIM syndrome [88, 92, 98-100]. Within the CXCR4 C-terminus there are 15 Ser and 3 Thr residues that can be phosphorylated [88, 91-93]. These residues are phosphorylated in a hierarchical manner [101]. Of note, Ser 324/325, Ser 330, Ser 338/339 and Ser 341 when mutated, reduce CXCL12-induced phosphorylation, desensitisation and internalisation of the receptor and are therefore crucial to regulation of receptor signalling [91-93, 101]. CXCR4 can also undergo CXCL12-independent phosphorylation and internalisation, through the process of heterologous desensitisation. In this scenario, activation of second messenger dependent kinases such as PKC by other GPCRs can result in phosphorylation of CXCR4.

After internalisation, CXCR4 can be recycled back to the plasma membrane or degraded. However, following CXCL12-mediated receptor internalisation, CXCR4 is usually degraded and is rarely recycled [102]. Following endocytosis, CXCR4 is ubiquitinated by the E3 ubiquitin ligase AIP4, sorted to the lysosome and degraded [103, 104].

While the process of BA recruitment is traditionally considered to turn off CXCR4 signalling following receptor activation, BA2 knock out mice display a decreased chemotactic response to CXCL12 [95]. It has been suggested that arrestins also function in cell signalling, by acting as scaffolds for signalling molecules [27, 97, 105]. Downstream of CXCR4, BA1 and BA2 have

been reported to be involved in CXCR4-mediated ERK activation after CXCL12 stimulation [97, 106]. This suggests that CXCR4 signalling may be a complex interplay between G protein and BA mediated processes.

1.3.3 Post-translational Modifications of CXCR4.

Beyond phosphorylation, CXCR4 is subjected to an assortment of other post-translational modifications (PTMs). These PTMs can alter protein behaviour, function and tracking. CXCR4 is subject to phosphorylation, sulphation, glycosylation, and ubiquitination [107]. On the extracellular side of the receptor, Asn 11 and Asn 176 both serve as sites for N-linked glycosylation of CXCR4 [108]. Proper glycosylation is crucial to CXCL12 binding and activation of the receptor [109, 110]. These modifications can also affect the behaviour of the receptor during sodium dodecyl sulphate-polyacrylamine gel electrophoresis (SDS-PAGE) analysis [111]. CXCR4 also undergoes tyrosine sulphation on Tyr 7, Tyr 12, and Tyr 21 within the receptor N-terminus, with all three sites implicated in chemokine binding [112].

1.3.4 FDA Approved Antagonists of CXCR4

The only CXCR4 antagonist that is currently approved by the FDA is AMD3100, also known as Mozobil or Plerixafor. AMD3100 is a small molecule composed of two 1,4,8,11-tetra-azacyclotetradecane (cyclam) moieties connected by a conformationally constraining phenylenebismethylene linker (figure 5a). It was initially discovered as an impurity that inhibited HIV cellular entry before the mechanism was uncovered as a specific blockade of CXCR4 [113-117]. This drug is approved for mobilization of haematopoietic stem cells from the bone marrow to the peripheral bloods, where they are collected by stem cell apheresis and used for autologous transplantation in patients with non-Hodgkin's lymphoma and multiple myeloma [118].

AMD3100 is considered an unbiased antagonist that inhibits G protein signalling and BA1/2-dependent endocytosis of CXCR4 with equal potency (figure 5b) [119].

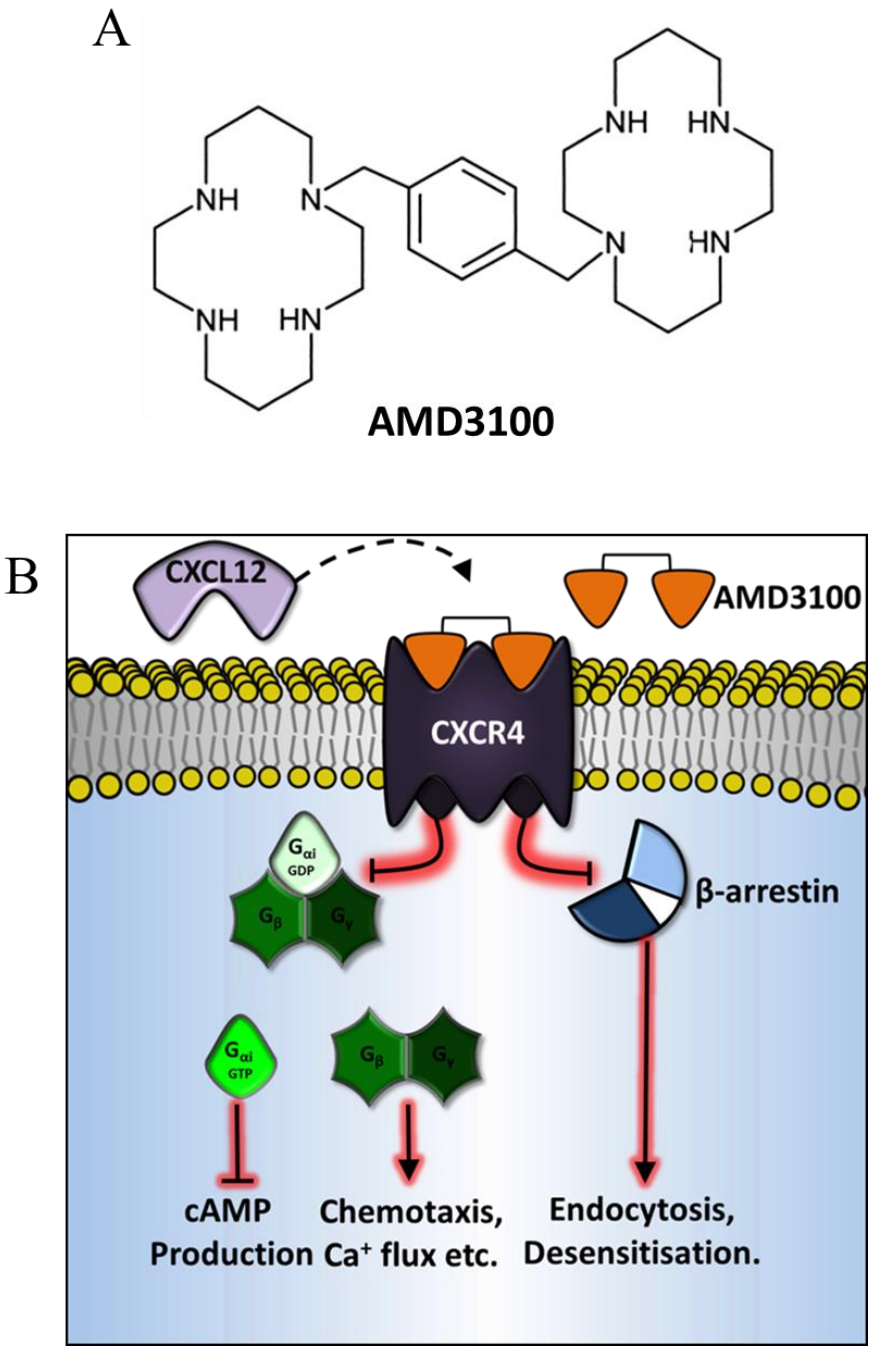

Figure 5: AMD3100 is an unbiased antagonist of CXCR4.

(A) Chemical structure of AMD3100. (B) Cartoon depiction of how AMD3100 inhibits CXCR4 in an unbiased manner, competing with CXCL12 for the orthotopic binding site. It inhibits both G protein signalling and BA-mediated endocytosis.

1.3.5 CXCR4 in cancer

A number of studies correlate high levels of CXCR4 expression in cancer with poor prognosis and resistance to chemotherapy [120-126]. Cancer cells overexpress CXCR4 which drives chemotaxis of cells to distant sites and establish metastatic disease in tissues with high levels of CXCL12 expression levels such as the brain, bone marrow and lungs [68, 127-129]. CXCR4 is the most commonly expressed chemokine receptor in cancer and is especially associated with hematopoietic malignancies like leukaemia. Leukaemia is a collection of haematopoietic cancers of different lineages that together cause approximately 23,000 deaths in the US annually [130].

Leukaemia including acute myeloid leukemia (AML) and acute lymphocytic leukaemia (ALL) often home to the bone marrow via CXCR4-CXCL12 chemotaxis, which provides a protective environment for the cells to avoid chemotherapy [60, 125, 131, 132]. This can provide a reservoir for leukaemic blasts that can ultimately lead to disease relapse. When tested in leukaemia patients, AMD3100 was expected to mobilize leukemic blasts, progenitor cells responsible for leukaemia relapse, from the bone marrow into the peripheral blood where they would be eliminated by chemotherapy. However, after prolonged treatment with the compound to keep cells in the peripheral blood, leukaemic blasts became tolerant to the drug and rehomed to the bone marrow where they were protected from killing [50, 51].

1.4 Statement of the problem and significance of the study

Despite reported tolerance to antagonists of multiple GPCRs, very few studies provide mechanistic insight and strategies to avoid it [50, 133, 134]. Tolerance to the only FDA–approved CXCR4 receptor antagonist AMD3100 can occur and significantly limits the potential to target the receptor in a variety of pathologies [50]. This tolerance is associated with increased receptor expression on the cell surface.

In this thesis, we have investigated the mechanism of tolerance to AMD3100 and developed strategies to avoid it. We hypothesize that accumulation of CXCR4 on the cell surface leads to the development of tolerance, at least in part, due to the inhibition of receptor endocytosis by AMD3100. Thus, we hypothesized that antagonists that inhibited G protein signalling but not receptor endocytosis would avoid the development of tolerance. Few compounds of this type, called biased antagonists, have been discovered [135, 136]. By understanding the mechanisms through which tolerance develops, we believe that future pharmaceutical development will benefit from rational design of inhibitors that avoid these processes.

II. MATERIALS AND METHODS

2.1 Antibodies

Western blotting was performed with antibodies from the following sources: BA1/2 (clone D24H9, #4674; Cell Signaling), CREB (86B10; Cell Signaling), CREB pSer133 (9198; Cell Signaling), CXCR4 (clone UMB2, AB124824; Abcam), CXCR4 (SAB3500383; Sigma-Aldrich), CXCR4 pSer324/325 (CP4251, ECM Biosciences), CXCR4 pSer339 (SAB4504153; Sigma-Aldrich), ERK1/2 (9102; Cell Signaling), pERK1/2 (9101; Cell Signaling), total Gai (AB102014; Abcam), GAPDH (60004- 1-Ig; Proteintech), HA (2-2.2.14; Thermo Fisher), rabbit anti-mouse (7076; Cell Signaling), and mouse anti-rabbit (7074; Cell Signaling).

Confocal microscopy was performed using antibodies from the following sources: BA2 (clone C16D9, #3857; Cell Signaling), CXCR4 (clone UMB2, AB124824; Abcam), Alexa Fluor 488 goat anti-rabbit (R37116; Thermo Fisher Scientific), Alexa Fluor 555 goat anti-mouse (A21422; Thermo Fisher Scientific).

For flow cytometry, staining was performed using antibodies from the following sources: PE-tagged CXCR4 4G10 monoclonal antibody (clone 4G10, sc-53534PE; Santa Cruz Biotechnology), PE-tagged CXCR4 12G5 monoclonal antibody (clone 12G5, 306506; BioLegend), PE- Mouse IgG2b, k Isotype control antibody (402204; BioLegend), and PE-Mouse IgG2a, k Isotype control antibody (400212; BioLegend).

For immuno-electron microscopy, CXCR4 staining was performed using 1:100 dilution of CXCR4 antibody (2B11; BD Bioscience).

For immunoprecipitation, 1 ml of anti-active Gai (26901; New East Biosciences) was used per 500 ml of sample.

2.2 Bioluminescence Resonance Energy Transfer.

BA2 recruitment to CXCR4 was measured by BRET. Briefly, the BRET signal was measured in cells co-transfected with 1.0 μg of BA2-GFP10 and 0.05 μg of CXCR4-Rluc or 0.05 μg of CXCR4-Rluc, completed to 2 μg per well with empty vector. BA2 recruitment was assessed by adding the ligands 10 min after the addition of coelenterazine 400A.

2.3 Cell Culture.

Jurkat, THP-1, Kasumi and CHO-K1 cells were obtained from the American Type Culture Collection (ATCC). HL60 and KG1 cells were a kind gift from the lab of Dr. Andrei Gartel. Jurkat cells were cultured in suspension, in culture media consisting of RPMI-1640 (Sigma-Aldrich) supplemented with 10% heat inactivated FBS (Sigma-Aldrich), 1% penicillin-streptomycin (ThermoFisher) solution and a final concentration of 2 mM L-Glutamine (ThermoFisher). THP-1 cells were cultured RPMI 1640 containing 10% FBS (Sigma-Aldrich), 1% penicillin-streptomycin and 0.05 mM 2-mercaptoethanol (ThermoFisher). Kasumi cells were cultured in suspension, in culture media consisting of RPMI-1640 (Sigma-Aldrich) supplemented with 20% heat inactivated FBS (Sigma-Aldrich), 1% penicillin-streptomycin (ThermoFisher) solution and a final concentration of 2 mM L-Glutamine (ThermoFisher). CHO-K1 cells cultured in F-12K media (Gibco) containing 10% FBS, 1% penicillin-streptomycin. All cells were maintained in a humidified environment containing 5% CO2 at 37°C. HL60 cells were cultured in suspension, in culture media consisting of IMEM (Gibco) supplemented with 10% heat inactivated FBS (Sigma-Aldrich), 1% penicillin-streptomycin (ThermoFisher) solution and a final concentration of 2 mM L-Glutamine (ThermoFisher). KG1 cells were cultured in media consisting of RPMI-1640 (Sigma-Aldrich) supplemented with 10% heat inactivated FBS (Sigma-Aldrich), 1% penicillin-streptomycin (ThermoFisher) solution and a final concentration of 2 mM L-Glutamine (ThermoFisher). MEF cells were cultured in media consisting of DMEM (Gibco)

supplemented with 10% FBS (Sigma-Aldrich), 1% penicillin-streptomycin (ThermoFisher) and a final concentration of 2 mM L-Glutamine (ThermoFisher).

For serum starvation, cells were cultured in media consisting of the specific base media indicated previously supplemented with 1% penicillin-streptomycin and a final concentration of 2 mM L-Glutamine.

2.4 Chemotaxis Assay

Cells were maintained in migration media consisting of the cell line base media, 2 mM L-Glutamine, 20 mM HEPES (pH 7.4) (ThermoFisher) and 0.1% Fraction V BSA (ThermoFisher) for six hours prior to the start of the assay. Cells were pre-incubated with vehicle or CXCR4 antagonists for 30 minutes, before 1 x 10^5 cells were seeded into the upper chamber of a 5 µM pore transwell plate (Corning). Cells were stimulated to migrate towards the lower chamber by migration media containing CXCL12. After 2.5 hours, cells in the lower chamber were counted using a Beckman Coulter flow cytometer and data plotted using GraphPad Prism 7.00 (GraphPad Software).

2.5 CHO and HEK293 Cell Transient Transfections

CHO and HEK293 cells were transfected with pcDNA3.1 constructs containing HA-tagged CXCR4 using Fugene transfection reagents (Promega). Cells were grown in normal culture media until 60% confluency was reached. A 1:2.5 ratio of DNA-Lipofectamine complexes were formed in OptiMEM media (Invitrogen), added to cells and incubated for 36-48 hours. Following the incubation, the cells were prepared for the appropriate assays.

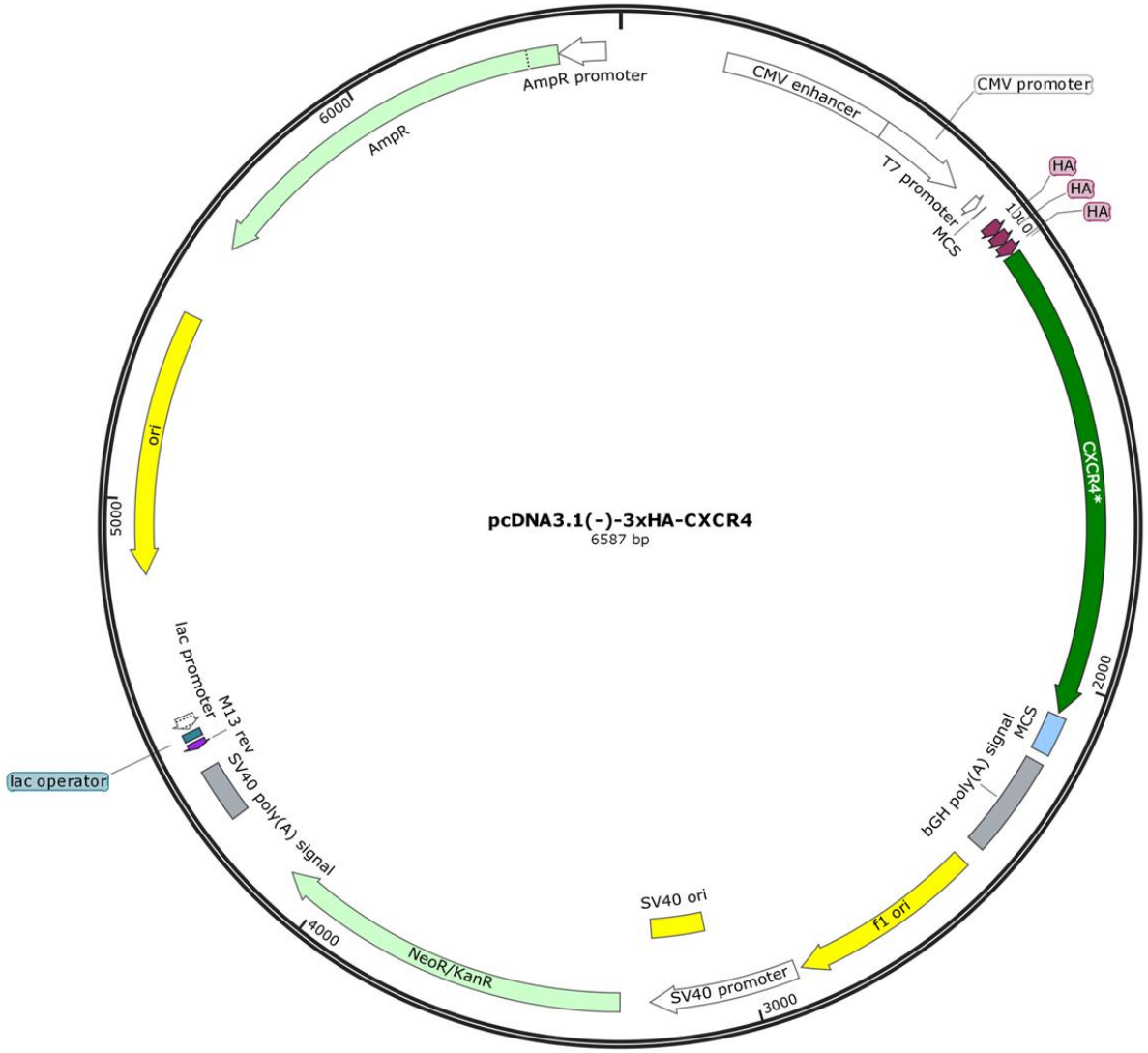

Figure 6: Recombinant pcDNA3.1 DNA construct encoding HA-tagged CXCR4.

The pcDNA3.1 backbone with cloned CXCR4 was used for transfections and to generate all CXCR4 mutant constructs.

2.6 Confocal Microscopy.

Jurkat cells (1 x 10^5) were serum starved for six hours then treated with CXCR4 inhibitors for 30 minutes prior to stimulation with 30 nM CXCL12 for 60 minutes. Cells were then pelleted by centrifugation and fixed in 4% paraformaldehyde. Cells were pelleted, washed and resuspended in PBS. On to a poly-lysine coated cover slip, 5 µL of cell suspension was smeared using a pipette tip. The sample was then blocked in PBS containing 5% BSA, 0.3% Triton X-100 for one hour at room temperature, prior to incubation overnight with a mouse monoclonal Anti-CXCR4 and rabbit monoclonal Anti-β-arrestin2 antibody at 4 °C in the same buffer. Coverslips were washed with ice-cold PBS, then stained with Anti-rabbit Alexa-fluor 488 and Anti-mouse Alexa-fluor 555 secondary antibodies for one hour at room temperature. Finally, coverslips were incubated with 0.5 µg/ml 4',6-Diamidino-2-Phenylindole, Dihydrochloride (DAPI) (ThermoFisher, D1306) for 10 minutes before being washed 3 x in PBS. Coverslips were mounted onto slides with ProLong Gold antifade reagent (ThermoFisher) and analysed on a Zeiss laser scanning 710 microscope.

CXCR4 antagonist preparation. To prepare stock concentrations of peptides, 2 mg of lyophilized X4-2-6 was incubated in a volume of DMSO that would represent 5% of the final volume of solution at 37°C for 30 minutes. The peptide was diluted to the final stock concentration using PBS before being applied to cells. AMD3100 octahydrochloride hydrate (Sigma-Aldrich) was prepared in PBS and SEN071 (MolPort) in DMSO.

2.7 CXCR4 phosphorylation assay.

Jurkat cells (1 x 10^6) were serum starved for six hours prior to treatment with vehicle, 1 µM AMD3100 or 10 µM X4-2-6 for 30 minutes. Cells were then stimulated with 30 nM CXCL12 for 30 minutes before harvesting and lysis in ice-cold RIPA buffer. CXCR4 phosphorylation was analyzed by SDS-PAGE and immunoblotting.

2.8 Cytotoxicity and Growth Assays.

Jurkat cells (1 x 10^4) were seeded into each well of a 96-well plate. Cells were then treated with increasing concentrations of CXCR4 antagonists or vehicle, each concentration in triplicate. Cell were incubated at 37 °C, 5% CO_2. Every twelve hours, cells were collected by centrifugation, media was aspirated and replaced with fresh media containing vehicle or CXCR4 antagonists. After 72 hours, cell media was replaced and 15 µl MTT dye (Promega) added to each well. Cells were incubated for 4 hours at 37°C, 5% CO_2 before 100 µL or stop solution was added to each well. Absorbance was recorded at 570 nM on a BioRad Model 680 Microplate Reader.

2.9 Dynasore treatment.

Jurkat cells were serum starved for 6 hours before treatment for one hour with 80 µM dynasore (Sigma-Aldrich), then washed 3 times with PBS. Cells were then prepared for the appropriate assays. Cell surface expression of CXCR4 was measured using anti-CXCR4-PE antibody clone 4G10 and flow cytometry, as described below. Chemotaxis assays were performed as described above, with chemotaxis stimulated by 30 nM CXCL12.

2.10 Electroporation of Jurkat Cells.

Jurkat cells (1 x 10^6) were centrifuged and resuspended in 100 µl Cell Line Nucleofector® Solution V (Lonza) containing, where relevant, pcDNA3.1-CXCR4 constructs or 300 nM Silencer® Select BA1 and BA2 siRNA (ThermoFisher). Cell-nucleic acid suspension was transferred to an electroporation cuvette (Lonza) and subjected to the Nucleofector® Program X-005 electroporation program using an Amaxa electroporator device. Cells were incubated in the cuvette for 10 minutes before being transferred into culture media consisting of RPMI-1640 (Sigma-Aldrich) supplemented with 10% heat inactivated FBS (Sigma-Aldrich), 1% penicillin-streptomycin (ThermoFisher) and a final concentration of 2 mM L-Glutamine (ThermoFisher). Cells were left for 24 hours before being subjected to the relevant assay.

2.11 Electron Microscopy.

Cells were subsequently fixed with 2% glutaraldehyde in 0.1 M Na-cacodylate and quenched with 50 mM NH4Cl in PBS, before being smeared onto a poly-lysine coated coverslip. After washing with PBS, the cells were treated anti-CXCR4 antibody or IgG control antibody. After overnight incubation, a secondary antibody conjugated to 11 nm gold particles was used to detect primary antibody. Samples were imaged on FEI Tecnai Spirit G2 transmission electron microscope at the Center for Advanced Microscopy and Nicon Imaging at Northwestern University.

2.12 ELISA

Jurkat cells (5×10^6) were serum starved for six hours in RPMI-1640, 1% penicillin-streptomycin, 2 mM L-Glutamine then stimulated with 100 µM Forskolin or vehicle for 30 minutes. Each sample was then treated with vehicle or CXCR4 antagonists, where indicated, for 30 minutes. Cells were exposed to 30 nM CXCL12 for a further period of 30 minutes. The direct cAMP ELISA kit (Enzo Life Sciences) was used to measure cAMP concentrations in cell lysates. The relative change of cAMP production was calculated using Assay Blaster! Software (ADI-28-0002) and results plotted using GraphPad Prism 7.00 (GraphPad Software) to determine the effects of CXCR4 inhibitors on cAMP production in response to CXCL12.

2.13 Endocytosis Assay.

Cells were serum-starved for 6 hours and incubated with vehicle or CXCR4 antagonist 30 minutes before stimulation with CXCL12. After the designated time, cells were washed 3 times in ice cold PBS containing 1% BSA. Cells were then incubated with phycoerythrin-tagged CXCR4 monoclonal antibodies 4G10 or 12G5 diluted to manufacturer recommendations in PBS

containing 1% BSA, or suitable isotype controls at 4°C for 20 minutes. Cells were washed twice in PBS before being fixed in PBS containing 4% paraformaldehyde. Cell surface expression of CXCR4 was determined via flow cytometry using a Beckman Coulter flow cytometer and data analyzed by WinMDI software.

2.14 ERK1/2 phosphorylation assay.

Cells (1×10^7) were serum-starved for six hours prior to the start of the assay. After starvation, cells were treated with vehicle (PBS) or 30 nM CXCL12 for several timepoints up to 30 minutes. Cells were harvested, washed three times in ice-cold PBS and lysed in RIPA buffer for analysis by SDS-PAGE and immunoblotting.

2.15 Gene Expression Analysis

Total RNA was extracted from cells using the RNeasy Mini Kit (Qiagen) following the manufacturer's instructions. Extracted RNA (5 µg) was reverse transcribed with and real-time quantitative PCR (RT-qPCR) was performed using SYBR-Green (BioRad) and gene specific primers (Table I) on a BioRad CFX Connect RT-PCR thermocycler.

TABLE I: RT-Q-PCR PRIMERS

Primer target	Primer direction	Primer sequence
CXCR4	Forward	CACGGAAACAGGGTTCCTTCA
	Reverse	AACCAGCGGTTACCATGGAG
GAPDH	Forward	GTCTCCTCTGACTTCAACAGCG
	Reverse	ACCACCCTGTTGCTGTAGCCAA

2.16 Immunoprecipitation.

To detect changes in GTP-loading of Gαi, 1 x 10^7 Jurkat cells were serum starved for 6 hours then treated with the indicated conditions. Cells were lysed by sonication in ice-cold IP lysis buffer (20 mM Tris-HCl pH 8.0, 140 nM NaCl, 2 mM EDTA) containing protease cocktail inhibitor (Santa Cruz) and phosphatase inhibitors (10 mM NaF, 1 mM Na3OV4), cell debris was pelleted, and the supernatant was collected. Cell lysates were incubated with the anti-active Gαi antibody overnight at 4°C, before addition of 5 µL protein A Dynabeads (ThermoFisher) for one hour at room temperature. Immunoprecipitated proteins were eluted from the beads using SDS-PAGE loading buffer lacking DTT (50 mM Tris-HCl pH 6.8, 2% SDS, 0.1 % bromophenol blue, 10% glycerol).

2.17 Molecular Modelling

The interactions between AMD3100 and CXCR4 dimer (PDB: 3ODU) or trimer (3OE8) were simulated by docking experiments using AutoDock vina [137]. The structure of AMD3100 was constructed using the ChemOffice software suite and optimised using MM2. Grid maps were generated with 0.375 Å spacing using a grid box of 44–100–44 Å. At least 9 models were generated and assessed for goodness of fit based on known interactions and STD-NMR data.

2.18 NMR Spectroscopy

2.18.1 Heternuclear Single Quantum Coherance Spectroscopy

^{1}H-^{15}N Heteronuclear Single Quantum Coherence (HSQC) experiments were performed on 50 µM recombinant human CXCL12 (Protein Foundry) and dissolved in PBS, pH 7.4, containing 10% D_2O. Experiments were carried out in the presence and absence of antagonists at the designated concentrations and/or 10 µg membranes preps from mammalian cells. All HSQC-NMR experiments were performed on a 900-MHz Bruker Avance Spectrometer equipped with a cryogenic probe. Data processing and analysis were carried out using NMRPipe [138]. The

chemical shift assignments were taken from the Biological Magnetic Resonance Data Bank (BMRB) database (http://www.bmrb.wisc.edu) using the 16142 BMRB identification number [139]. Changes in signal intensity were calculated by subtracting the signal intensity of experimental spectra (I) from control spectra (I_0) divided by I_0 and plotted as a ratio. Mean chemical shift difference was calculated as follows:

$$\Delta\delta_{NH} = \sqrt{\frac{(\Delta\delta^1 H_N)+(\Delta\delta^{15}N)^2/25}{2}}.$$

Changes in signal intensity and chemical shift perturbations (CSPs) higher than the sum of the average and one standard deviation were considered statistically significant.

2.18.2 Saturation Transfer Difference Spectroscopy

Saturation transfer difference experiments were performed on a Bruker 800 mHz Avance spectrometer equipped with a cryogenic probe. Saturation was achieved with a train of 50 ms Gaussian-shaped pulses applied at field strength of 100 Hz in the methyl region at −1 ppm. The duration of the saturation pulse was 1 s. Where relevant, experiments were performed with 100 µg of membrane preparation, 100 µM AMD3100 and or 125 µM IT1t. Experiments were run in a phosphate buffered saline (pH 7.6) solution, 10 % D_2O and carried out at room temperature.

2.19 Preparation of Membrane Fractions.

Jurkat cells (1 x 10^7) or CHO-cells (2 x 10^7) were collected and washed three times with PBS before lysis by sonication in 1 mL fractionation buffer (250 mM Sucrose, 20 mM HEPES pH 7.4, 10 mM KCl, 2 mM $MgCl_2$, 1 mM EDTA, 1 mM EGTA, protease cocktail inhibitor (SCBT), 10 mM NaF, 1 mM Na_3OV_4). Samples were centrifuged at 10,000 x g for 10 minutes and the supernatant transferred to a fresh ultracentrifuge tube. The sample was spun in a Beckman L8-80M centrifuge at 100,000 x g, for 1 hour at 4°C. The subsequent pellet was washed once in 500 µL fractionation buffer before being re-suspended in sterile PBS.

2.20 PRESTO-Tango Assay.

β-Arrestin2 recruitment to CXCR4 was measured by the PRESTO-Tango (parallel receptorome expression and screening via transcriptional output, with transcriptional activation following arrestin translocation) assay, as previously described [140]. Briefly, Tango plasmids were transfected into HTLA cells, both kindly provided by Professor Brian Roth, using Lipofectamine 3000 (ThermoScientific). One day after transfection, HTLA cells were plated onto Poly-L-Lysine pre-coated 96-well microplates and allowed to attach to the plate for 4 hours prior to treatment. Cells were treated with increasing concentrations of CXCL12 in the presence of vehicle, 1 μM AMD3100 or 10 μM X4-2-6 for one hour at 37°C, 5% CO2 in a humidified environment. Cells were then incubated with culture media with 100 μL 1:5 mixture of Bright-Glo (Promega) and 1x HBSS, 20 mM HEPES solution. Plates were incubated at room temperature before measuring luminescence on a Biotek Synergy II plate reader.

2.21 Prolonged Exposure to CXCR4 antagonists.

In culture media, cells were exposed to the indicated concentrations of CXCR4 antagonists. At 12-hour intervals, cells were pelleted by centrifugation, washed three times with PBS and fresh culture media containing CXCR4 antagonists was replenished. After 72 hours, cells were counted using a hemocytometer and prepared for subsequent assays.

2.22 Protein sequence alignment.

Amino acid sequences of proteins were acquired from the UniProt website and alignments performed using the MultAlin website and the ESPript 3.0 ENDscript server [141].

2.23 Site-Directed Mutagenesis.

CXCR4 mutant pcDNA3.1 constructs were made by using a QuikChange II site-directed mutagenesis kit (Agilent) in accordance with the manufacturer's instructions. The following primers were used to create each mutant:

TABLE II: SITE DIRECTED MUTAGENESIS PRIMERS

Mutant	Primer direction	Sequence
N119S	Forward	5'-GGCAGTCCATGTCATGACACAGTCAGC-3'
	Reverse	5'-ACACTGCTGTAGAGGCTGACTGTGTAGA-3'
D171N	Forward	5'-CTCCTGCTGACTATTCCCAACTTCATC-3'
	Reverse	5'-GACGTTGGCAAAGATGAAGTTGGGAA-3'
I261A	Forward	5'-TACTACATTGGGATCAGCGCGGACTCCTTC-3'
	Reverse	5'-AGGAGGATGAAGGAGTCCGCGCTGATCCC-3'
K239E/V242A/L264A	Forward	GGCGAAGAAAGCCGCGATGAGGATGGCTGTGGTCTCGAGGGCCTTGCG
	Reverse	CGCAAGGCCCTCGAGACCACAGCCATCCTCAGCGGCTTTCTTCGCC

2.24 Statistical Analysis.

Quantification of immunoblots was done using ImageJ [142], with at least 3 independent experiments performed per data set. Results are shown as a mean of those experiments ± standard deviation. At any data point, P-values were determined by the designated statistical test using GraphPad Prism 7.00 (GraphPad Software).

2.25 Western Blotting.

To detect changes in cell signalling, cells were lysed in ice-cold RIPA buffer (10 mM Tris-HCl, 140 nM NaCl, 1 mM EDTA, 1 % Triton X-100, 0.1 % sodium deoxycholate, 0.1% sodium dodecyl sulphate) containing protease cocktail inhibitor (Santa Cruz) and phosphatase inhibitors (10 mM NaF, 1 mM Na3OV4). Cells were lysed by sonication, cell debris was pelleted by centrifugation and the supernatant was collected. Total protein concentrations were measured. Samples were mixed with SDS-PAGE sample buffer and boiled at 90°C for 3 minutes. Proteins were separated by SDS-PAGE and transferred onto nitrocellulose membranes for detection with indicated antibodies. All immunoblots are representative of at least 3 independent experiments.

III. ELUCIDATING THE MECHANISM OF AMD3100 ANTAGONIST TOLERANCE

3.1 Tolerance to AMD3100 develops in a leukaemia cell line with high CXCR4 expression.

3.1.1 Jurkat cells develop tolerance to AMD3100 inhibition of CXCL12-mediated chemotaxis.

Previously, tolerance to AMD3100 was demonstrated in several leukaemia cell lines where after exposure to the antagonist for 72 hours, cells could undergo chemotaxis to CXCL12 even in the presence of the drug [50]. To independently verify these results and to investigate the development of tolerance in other leukaemia cell lines, we compared the potency of AMD3100 before and after 72 hours of exposure in the following cells: Jurkat (clone E6-1), HL60, Kasumi-1, KG1a and THP-1 (table 3). These lines were chosen because they represent both myeloid and lymphoid cell lineages of leukaemia.

In Jurkat T-lymphocytic leukaemia cells without pre-exposure, we found that AMD3100 inhibited chemotaxis with a relative median inhibitory concentration (IC_{50}) of 0.13 ± 0.09 μM (figure 7a). We found that Jurkat cells pre-exposed to AMD3100 for 72 hours became tolerant to the antagonist, reflected by an IC_{50} value of 2.73 ± 0.84 μM for the inhibition of CXCL12-mediated chemotaxis (figure 7a). In HL60 acute promyelocytic leukaemia cells, the IC_{50} concentration before and after 72 hours exposure increased slightly but was not significantly altered, at 0.09 ± 0.07 μM and 0.12 ± 0.08 μM, respectively (figure 7b). Likewise, in Kasumi-1 AML cells the IC_{50} value was 0.02 ± 0.01 μM without any previous exposure to AMD3100 and was unchanged after 72 hours, with an IC_{50} of 0.04 ± 0.02 μM (figure 7c). Additionally, the IC_{50} value remained unchanged before and after 72 hours AMD3100 exposure in acute myelogenous leukaemia KG-1a cells, with IC_{50} values of 0.63 ± 0.31 μM and 0.39 ± 0.25 μM respectively (figure 7d). Finally, AMD3100 inhibited CXCL12-mediated in THP-1 AML cells with an IC_{50} of 0.15 ± 0.04 μM, which remained unchanged after 72 hours pre-exposure to the drug, with an

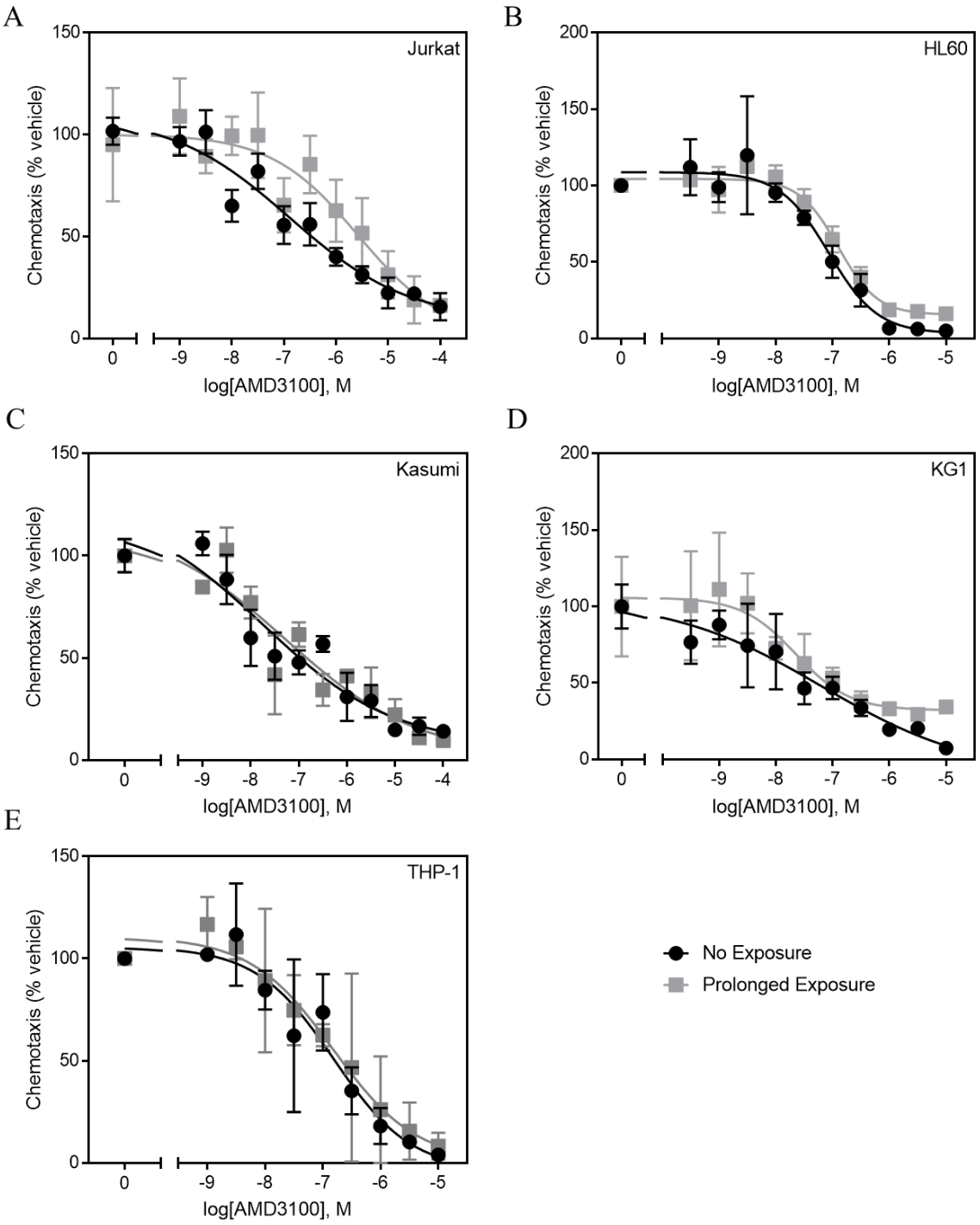

Figure 7: The development of tolerance to AMD3100 in a panel of leukaemia cell lines.

Transwell chamber assays to calculate IC_{50} values of AMD3100 for (A) Jurkat cell, (B) HL60 cell, (C) Kasumi-1 cell, (D) KG1 cell and (E) THP-1 cell chemotaxis toward 30 nM CXCL12.

IC_{50} of 0.15 ± 0.05 μM after 72 hours of exposure (figure 7e). These data suggested that not all cell lines become tolerance to the effects of AMD3100. Data points are means ± SD from two experiments performed in triplicate for each antagonist concentration.

TABLE III: COMPARISON OF AMD3100 IC_{50} VALUES FOR CXCL12-MEDIATED CHEMOTAXIS IN A PANEL OF LEUKAEMIA CELL LINES.

Cell Line	IC_{50} before exposure (μM)	IC_{50} after 72 hours exposure (μM)
HL60	0.09 ± 0.07	0.12 ± 0.08
Jurkat	0.13 ± 0.09	2.73 ± 0.84
Kasumi	0.02 ± 0.01	0.04 ± 0.02
KG1a	0.63 ± 0.31	0.39 ± 0.25
THP-1	0.15 ± 0.04	0.15 ± 0.05

3.1.2 Jurkat cells express high levels of CXCR4 compared to other leukaemia cell lines.

It is well established that CXCR4 expression varies between cell types and that increased CXCR4 expression is correlated with more aggressive leukaemia and disease relapse [143]. We hypothesized that the development of tolerance to AMD3100 in leukaemia cell lines was correlated with CXCR4 cell surface expression. To investigate the expression of CXCR4 in Jurkat, HL60, Kasumi-1, KG1a and THP-1 cell lines, we performed flow cytometry with CXCR4 specific antibodies. We found that Jurkat cells had the highest mean fluorescent intensity (MFI) of all 5 cell lines, suggesting these cells had the highest CXCR4 expression (figure 8a). This correlated with the development of tolerance in Jurkat cells. While tolerance was not easily observable in any other cell line, HL60 and Kasumi-1 cells both had CXCR4 expression on the cell surface (figure 8b, c). THP-1 cells expressed the lowest levels of CXCR4 than the other tested cell lines, while

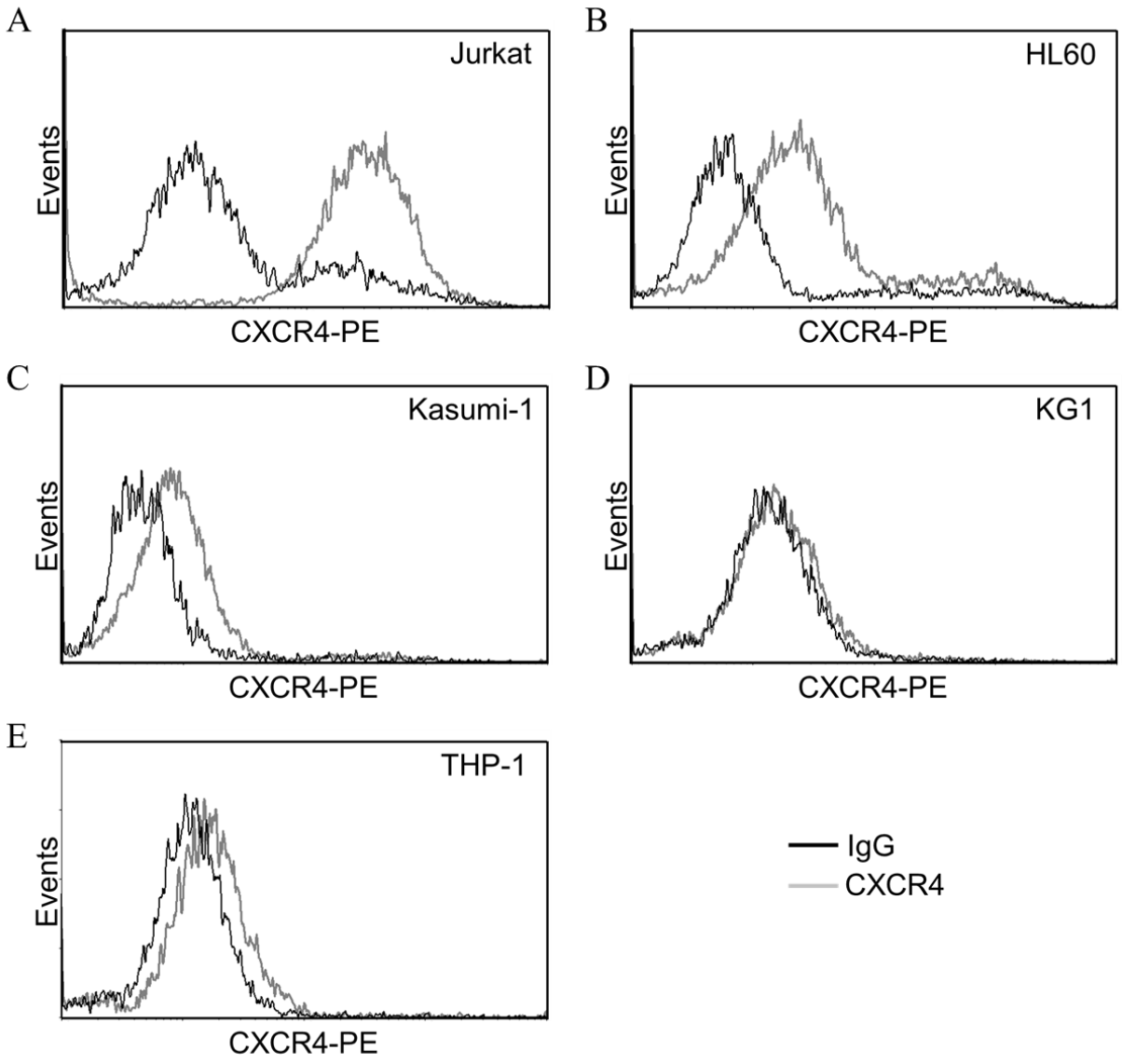

Figure 8: CXCR4 cell surface expression varies between leukaemia cell lines.

Flow cytometry analysis of CXCR4 cell surface expression using the anti-CXCR4 12G5 antibody in (A) Jurkat, (B) HL60, (C) Kasumi-1, (D) KG1 and (E) THP-1 cells.

the KG1a cell line had very little receptor expression (figure 8d, e). Based on these findings, we chose to investigate the mechanism of AMD3100 tolerance in Jurkat cells, where CXCR4 expression is high and the development of tolerance was clearly observed after 72 hours.

3.2 AMD3100 is an unbiased antagonist of CXCR4 that leads to antagonist tolerance

3.2.1 AMD3100 is an unbiased, competitive antagonist of CXCR4

Most investigations of GPCR drug tolerance have focused on opioid receptor agonists that, in contrast to antagonists, promote receptor activation and endocytosis [10, 144]. These studies have proposed impaired receptor expression at the cell surface or reduced receptor occupancy by the drug as possible mechanisms of agonist tolerance. Reports of tolerance to GPCR antagonists exist, for example those targeting cannabinoid, opioid, and dopamine D2 receptors, but very few studies provide insight into the mechanism. In order to investigate the mechanism of AMD3100 tolerance, we first investigated the pharmacology of AMD3100 in Jurkat cells. AMD3100 was initially described as an antagonist of CXCR4 capable of inhibiting HIV cellular entry, but several subsequent reports suggested the drug acted as a partial agonist [145-147]. Since AMD3100 was a potent inhibitor of chemotaxis in Jurkat cells, a process associated with G protein activation, we investigated the effect of AMD3100 on BA-mediated CXCR4 endocytosis by flow cytometry. When Jurkat cells were treated only with increasing concentrations of AMD3100, no change in the cell surface staining was observed, suggesting AMD3100 did not act as an agonist of CXCR4 (figure 9a). However, AMD3100 inhibited endocytosis stimulated by 30 nM CXCL12 with an IC_{50} of 0.3 ± 0.05 μM, and thus can be classified as an antagonist in the concentration range assayed (figure 9b). When the IC_{50} value of AMD3100 for endocytosis is compared to the IC_{50} value for chemotaxis, AMD3100 can be classified as an unbiased antagonist of CXCR4 in Jurkat cells (figure 9c). This is in line with the observation that AMD3100 binds at the orthosteric binding site to inhibit chemokine binding and receptor activation [114, 115, 148-150].

However, AMD3100 does not completely block CXCL12 binding to CXCR4 [150, 151]. In fact, some reports have suggested that AMD3100 may act in an allosteric manner [152]. In order to understand the mechanisms that underlie the development of antagonist tolerance to AMD3100, it is crucial to first understand the mechanism via which AMD3100 acts. To further characterise the pharmacology of AMD3100 in Jurkat cells, we investigated if AMD3100 acts as a competitive inhibitor of CXCL12-CXCR4 interaction. A competitive inhibitor is one that increases the K_m of a substrate without affecting the V_{max}. Often the binding site of a competitive inhibitor is the same as that of the substrate, but it is more accurate to say that the binding of a competitive inhibitor and the binding of substrate are mutually exclusive events [153]. If an inhibitor is competitive, the inhibitory effects can be overcome by increasing the concentration of the endogenous ligand. We hypothesized that AMD3100 blocks activation of CXCL12 by competing for the orthosteric site. To test this, we performed a chemotaxis assay with increasing concentrations of CXCL12 and a single concentration (1 µM) of AMD3100. In a chemotaxis assay, cells responded in a biphasic manner to increasing concentrations of CXCL12 (figure 9d). This is due to technical reasons (i.e. the ability to form a gradient at high concentrations over the distance of the chamber) and biological reasons (CXCL12 dimerises and can then function as an inhibitor of chemotaxis) [154]. The experiment resulted in a maximum chemotactic response of Jurkat cells at approximately 30 nM CXLC12 (figure 9d). However, in the presence of 1 µM AMD3100, the maximum response of Jurkat cells shifted to ~100 nM, indicating that increasing concentrations of CXCL12 could outcompete the inhibitory effects of AMD3100 and that the bicyclam is a competitive inhibitor.

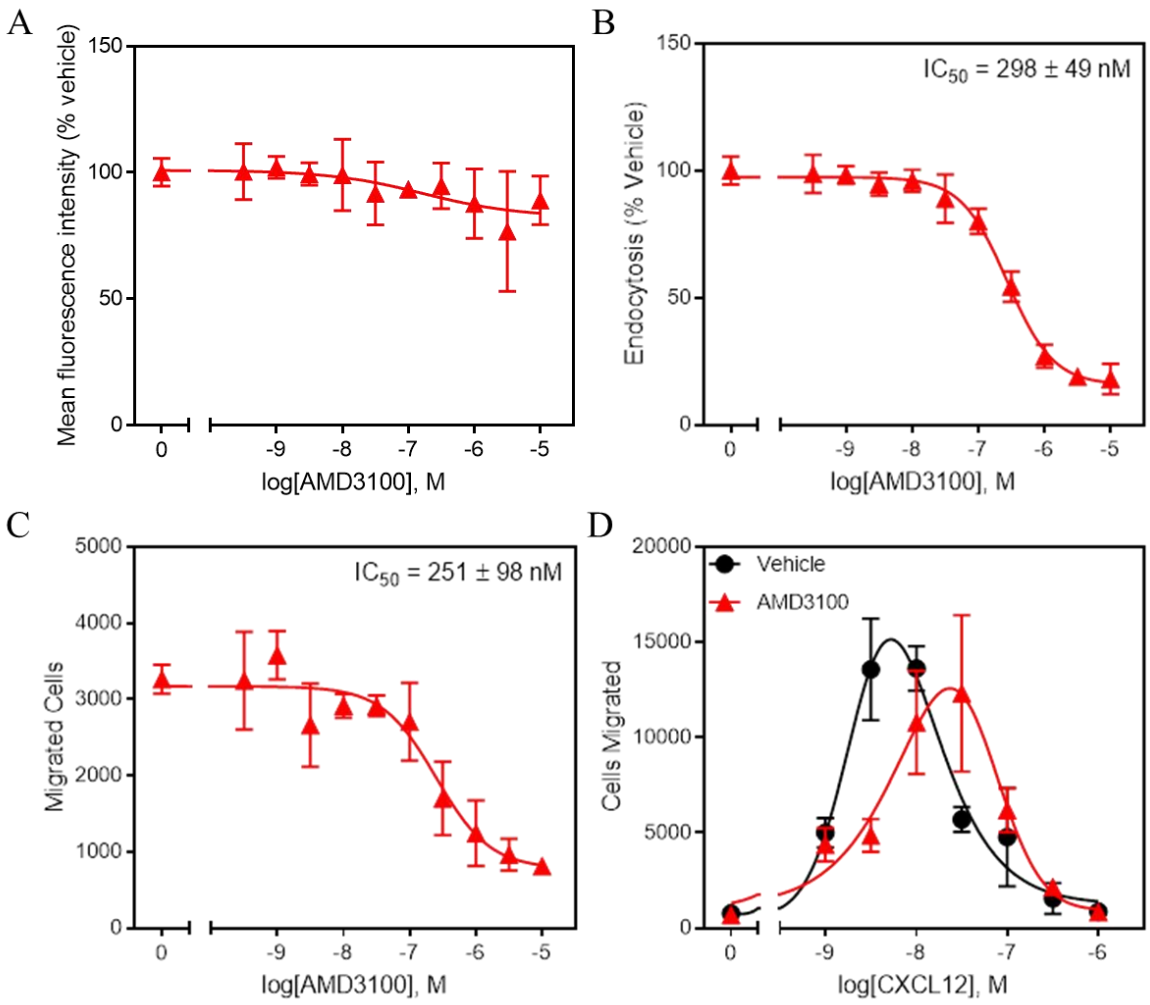

Figure 9: AMD3100 is an unbiased, competitive antagonist of CXCR4.

(A) Flow cytometry analysis of CXCR4 cell surface expression on Jurkat cells treated with increasing concentrations of AMD3100 and measured using the anti-CXCR4 antibody 4G10. (B) The IC_{50} values of AMD3100 for 30 nM CXCL12-mediated CXCR4 endocytosis in Jurkat cells. (C) IC_{50} values of AMD3100 for Jurkat cell chemotaxis toward 30 nM CXCL12. (D) Comparison of the biphasic chemotactic response of Jurkat cells in the absence and presence of 1 µM AMD3100.

3.2.2 Prolonged exposure to AMD3100 leads to CXCR4 accumulation on the surface of Jurkat cells and the development of antagonist tolerance

Studies investigating tolerance to GPCR agonist drugs have suggested that altered receptor expression at the cell surface has important consequences for the development of drug tolerance [155-157]. In line with those studies, Sison *et. al* showed that after prolonged exposure to AMD3100, CXCR4 expression was increased on the plasma membrane of several leukaemia cell lines [50]. Taken together with our previous data suggesting cells with high CXCR4 surface expression were susceptible to the development of antagonist tolerance, we hypothesized that the CXCR4 cell surface expression in Jurkat cells would be increased after exposure to AMD3100 for 72 hours. To test this hypothesis, we treated Jurkat cells with vehicle or AMD3100 every 12 hours for 72 hours, and measured CXCR4 cell surface expression at various time points using flow cytometry and the anti-CXCR4 antibody clone 4G10. Treating Jurkat cells with vehicle only for 72 hours had no effect on CXCR4 expression at the cell surface (figure 10a). Treatment of Jurkat cells with AMD3100 increased the expression of CXCR4 at the cell surface after as short as 12 hours of treatment. After 72 hours, cell surface expression of CXCR4 more than doubled compared to vehicle treated cells. This increase in cell surface CXCR4 was confirmed by Western blotting of Jurkat cell membrane fractions taken over the 72 hours treatment time course (figure 10a). Western blot analysis showed a ~50% increase in plasma membrane CXCR4, in contrast to flow cytometry estimates of a CXCR4 concentration that had more than doubled (figure 10b). This discrepancy may be explained by the use of different antibodies, each with different epitopes and affinities, for each experiment. The 4G10 antibody used for flow cytometry recognises an epitope in the N-terminus of the receptor [158]. However, the UMB-2 antibody used for Western blotting recognises a C-terminal epitope and does not recognise phosphorylated CXCR4 as demonstrated by the lack of receptor in the CXCL12 treated sample [101]. Despite the slight inconsistency, the

increase in CXCR4 cell surface expression is consistent with the ability of AMD3100 to inhibit CXCR4 endocytosis.

Given that CXCR4 expression levels in the plasma membrane are closely associated with receptor activity, we investigated whether the time dependent increase in CXCR4 caused by repeated dosing of Jurkat cells to AMD3100 correlated with an increased ability to overcome the effects of the drug [159-161]. We hypothesized that as CXCR4 expression increased over time, so would the ability of cells to overcome the inhibitory effects of AMD3100. To test this hypothesis, we measured the ability of Jurkat cells treated every 12 hours for 72 hours to overcome inhibition of CXCL12-mediated chemotaxis by 1μM AMD3100. We took cells every twelve hours, counted and seeded to ensure the same number of cells were used, and ran chemotaxis assays. After 24 hours pre-exposure to AMD3100, twice as many Jurkat cells were able to undergo chemotaxis toward CXLC12 in the presence of AMD3100 as when cells had no pre-exposure to the drug (figure 10a). This remained consistent across all subsequent timepoints and correlated with the increased expression of CXCR4 at the cell surface. These findings suggested that AMD3100 inhibition of CXCR4 endocytosis causes an accumulation of receptor at the plasma membrane and results in the development of antagonist tolerance.

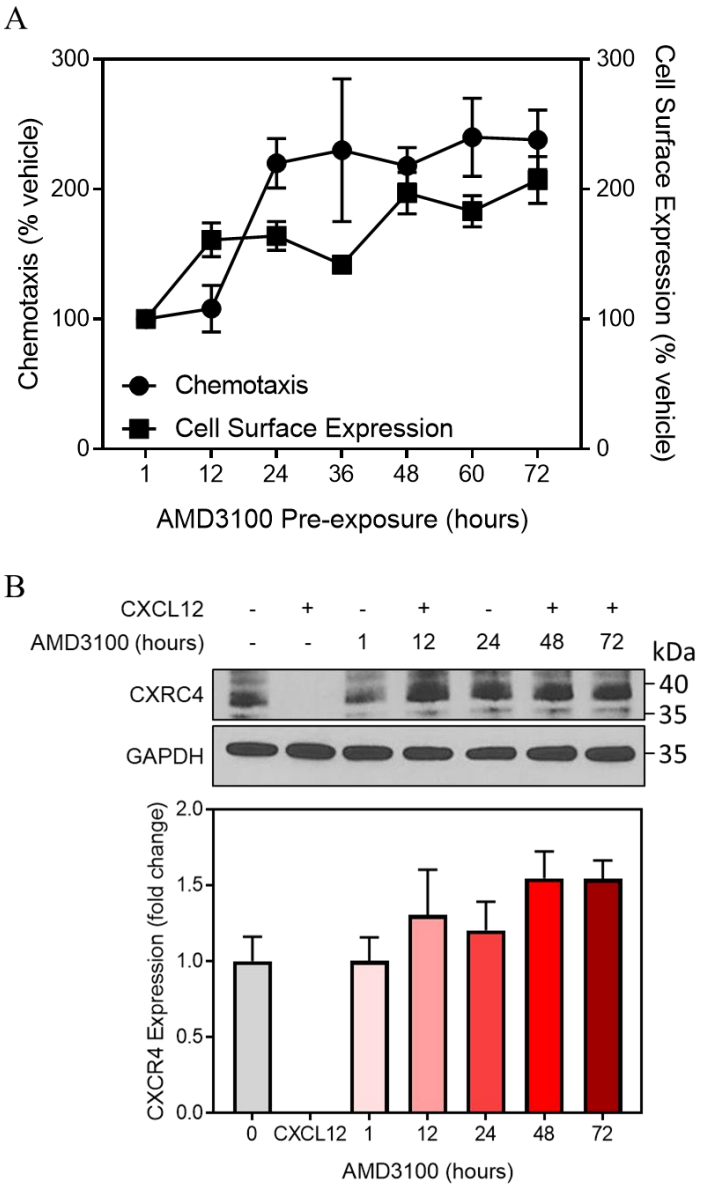

Figure 10: AMD3100 increases CXCR4 cell surface expression and leads to the development of antagonist tolerance.

(A) Comparison of CXCR4 cell surface expression in Jurkat cells treated with 1 μM AMD3100 every 12 hours for 72 hours and measured by flow cytometry using anti-CXCR4 4G10 antibody (■) plotted on the left Y axis, and the ability of those cells to overcome the inhibitory effects of 1 μM in a chemotaxis assay (●) plotted on the right Y axis. (B) Western blotting for CXCR4 in membrane fractions prepared from Jurkat cells treated with 1 μM AMD3100 every 12 hours for 72 hours using the anti-CXCR4 antibody UMB-2. GAPDH is provided as a loading control and used to normalise CXCR4 expression during ImageJ quantification, shown below the blot.

However, other mechanisms may contribute to the AMD3100-induced increase of CXCR4 cell surface expression. For example, we hypothesized that accelerated transcription of the CXCR4 gene might contribute to increased CXCR4 on the surface of cells treated with AMD3100. Multiple reports have suggested AMD3100 can act as a partial agonist of CXCR4 with weak activity [146, 147]. Weak partial agonists can inhibit autocrine signalling of full agonists. Jurkat cells produce and secrete CXCL12 which can signal through CXCR4 in an autocrine manner [162]. If AMD3100 inhibits this autocrine signalling to reduce CXCR4 activation relative to untreated cells, this could lead to a reduction in Gαi activity in resting Jurkat cells. In turn, this could release inhibition of AC, increasing intracellular cAMP. The increase in intracellular cAMP could activate cAMP dependent kinases, such as PKA or CREB. CXCR4 gene expression can be regulated by CREB activation owing to the presence of a CREB binding site within the CXCR4 promoter [163, 164]. Additionally, CREB is regulated by Ca^{2+} and Ca^{2+}-CaM kinase II, which can be affected by AMD3100 [165-167]. We hypothesized that if AMD3100 acted to inhibit autocrine activity of CXCL12-CXCR4, prolonged exposure of Jurkat cells to AMD3100 would increase intracellular cAMP, activate CREB and increase CXCR4 genomic expression.

To test this hypothesis, we first investigated intracellular cAMP concentrations using a direct cAMP ELISA in Jurkat cells treated with AMD3100 every 12 hours. This assay provides a highly sensitive, high throughput colorimetric assay for the quantitative determination of intracellular cAMP by competition for antibody binding between cAMP in samples with enzyme-linked cAMP standards. Treatment with forskolin, which stimulates adenylate cyclase to generate cAMP, led to a subtle increase in intracellular cAMP concentrations when compared to those of vehicle-treated cells (figure 11) [168, 169]. However, treatment with AMD3100 for 72 hours did not significantly affect intracellular cAMP concentrations (figure 11). While there was a trend for increasing cAMP over time, this was not significant except for at the 48-hour time point.

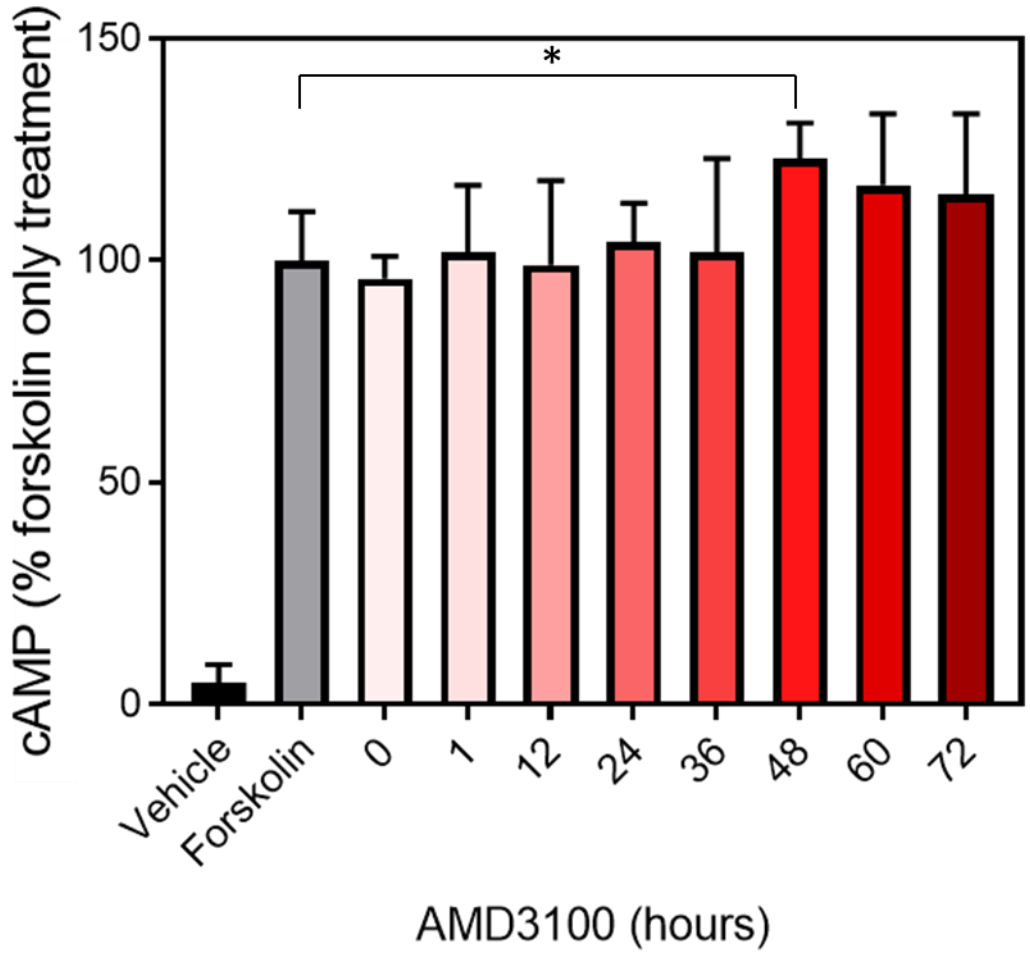

Figure 11: AMD3100 prolonged exposure increases intracellular cAMP after 36 hours.

(A) Elevated intracellular concentrations of cAMP in Jurkat cells were detected by ELISA after treatment with the potent adenylate cyclase agonist Forskolin, and 1 μM AMD3100 for up to 72 hours. cAMP levels peaked at 48 hours. (*p = 0.05 by ANOVA, n = 3 replicates per condition, data shown are mean ± SD).

To investigate if this correlated with the activation of CREB, we performed immunoblotting for total CREB and phosphorylation of CREB at serine 133. CREB is a basic leucine zipper transcription factor that regulates gene expression by binding to cAMP response elements (CRE) in the promoters of its target genes, upon phosphorylation at serine 133 by kinases e.g. PKA [170, 171]. Treatment with 30 nM CXCL12, which reduces cAMP through activation of Gαi, paradoxically increased serine 133 phosphorylation (figure 12). However, this can be explained by CXCL12 activation of PKC and ERK, which can in turn activate CREB downstream of CXCR4 [172]. Initial treatment with AMD3100 resulted in a decrease in the activation of CREB up to 36 hours that was not in agreement with cAMP ELISA data (figure 11). This suggests that these affects are cAMP independent. However, after 36 hours, phosphorylation of serine 133 rises until a significant increase is seen after 72 hours of treatment (figure 12). This suggests that after prolonged exposure to AMD3100, CREB activation may increase and upregulate the expression of CXCR4.

To investigate if the increase in CREB activation altered CXCR4 gene expression, we performed polymerase chain reaction (RT-qPCR) to measure CXCR4 gene expression in Jurkat cells treated with vehicle or AMD3100 every 12 hours for 72 hours. We observed that there was no significant change in CXCR4 expression over the 72 hours treatment with AMD3100, but there was an increasing trend over time, similar to that seen for CREB phosphorylation (figure 13). Taken together, this data suggests that other mechanisms, such as increased stability of CXCR4 mRNA, may contribute to the increased expression of CXCR4 at the plasma membrane during the development of antagonist tolerance, but inhibition of endocytosis by AMD3100 is a significant contributor.

One other mechanism for the increased levels of CXCR4 in AMD3100-treated cells may be related to decreased degradation of the receptor. Upon CXCL12-mediated endocytosis, CXCR4 is rapidly degraded and rarely recycled to the membrane [102, 104]. To address the possibility that

tolerance develops in response to changes in CXCR4 degradation, we treated Jurkat cells with different concentrations of the proteasome inhibitor Bortezomib and measured CXCR4 on the cell surface by flow cytometry. Bortezomib inhibits the catalytic activity of the 26S proteasome and is currently in clinical trials in combination with AMD3100 for treatment of relapsed/refractory multiple myeloma [173, 174]. We observed that Bortezomib treatment at multiple doses for 6 hours did not increase CXCR4 on the surface of Jurkat cells (figure 14a) and did not alter the ability of AMD3100 to inhibit CXCL12-mediated chemotaxis (figure 14b).

We also investigated whether simply overexpression of CXCR4 could induce tolerance to AMD3100 in Jurkat cells. We hypothesised that increasing the expression of CXCR4 in Jurkat cells via transient transfections would enhance the ability of the cells to overcome the effect of AMD3100. We electroporated Jurkat cells with 2 µg of pcDNA3.1 empty vector or pcDNA3.1-Ha-CXCR4, waited for 36 hours for peak expression of the receptor, then performed a chemotaxis assay to assess the IC50 of AMD3100. In cells electroporated with Ha-CXCR4, we saw an overall increase in the number of cells undergoing chemotaxis. However, the change in the IC_{50} of AMD3100 was not of the same magnitude as for cells that had been treated with AMD3100 for 72 hours (Appendix A, figure 1). This suggested that either the receptor was not overexpressed to the same extend as it is after AMD3100 treatment, or there is a ligand-induced effect that cannot be replicated solely by overexpression of the receptor.

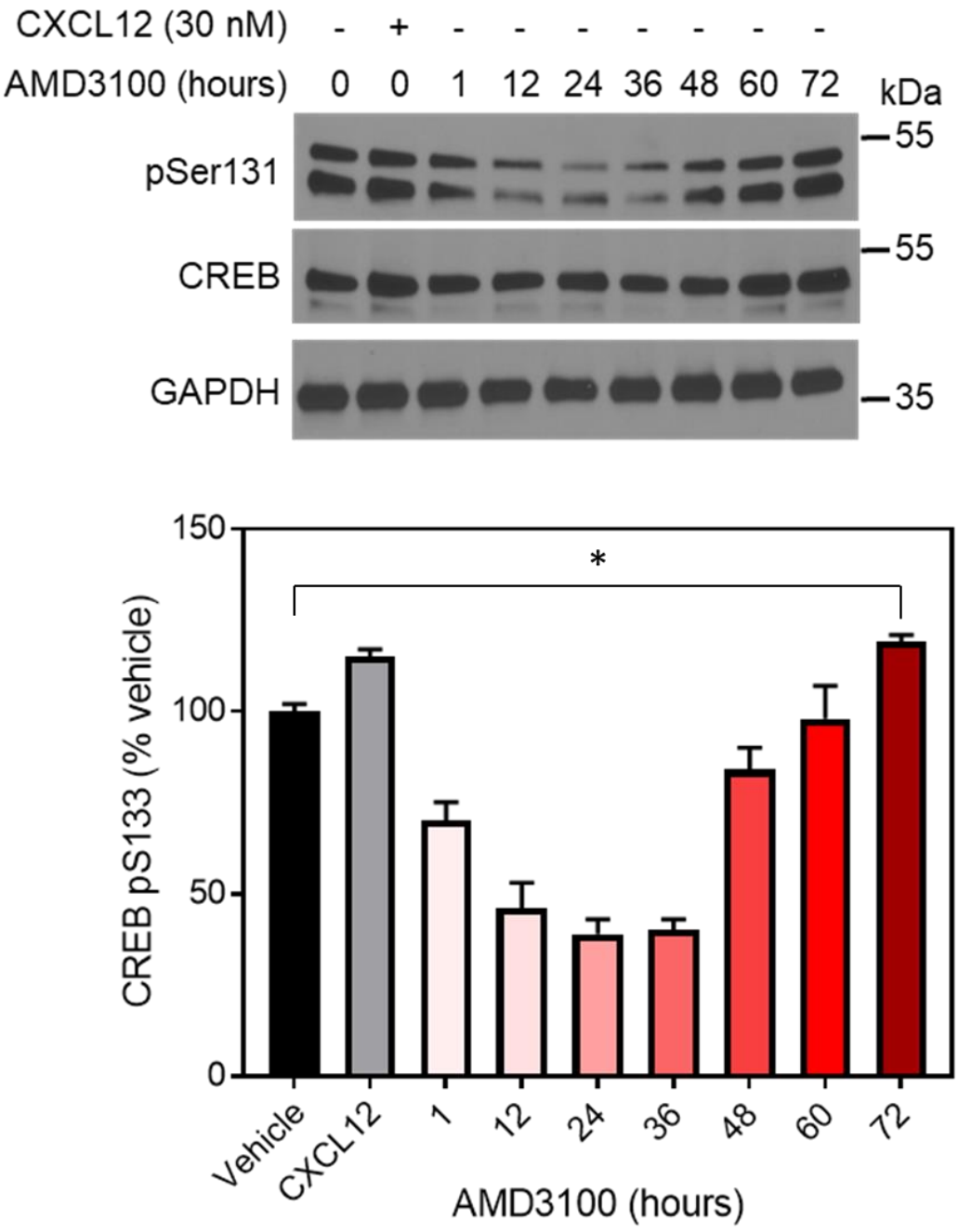

Figure 12: AMD3100 causes an increase in phosphorylation of CREB serine 133 after 48 hours.

Time-dependent fluctuation in phosphorylation of CREB at S131 was assessed by western blot in Jurkat cells treated with 1 μM AMD3100 for up to 72 hours. Quantification was performed using ImageJ and normalized to vehicle only. Western blot is representative of 3 independent experiments (*P = 0.05 by ANOVA, n = 3 independent experiments, data shown are means ± SD).

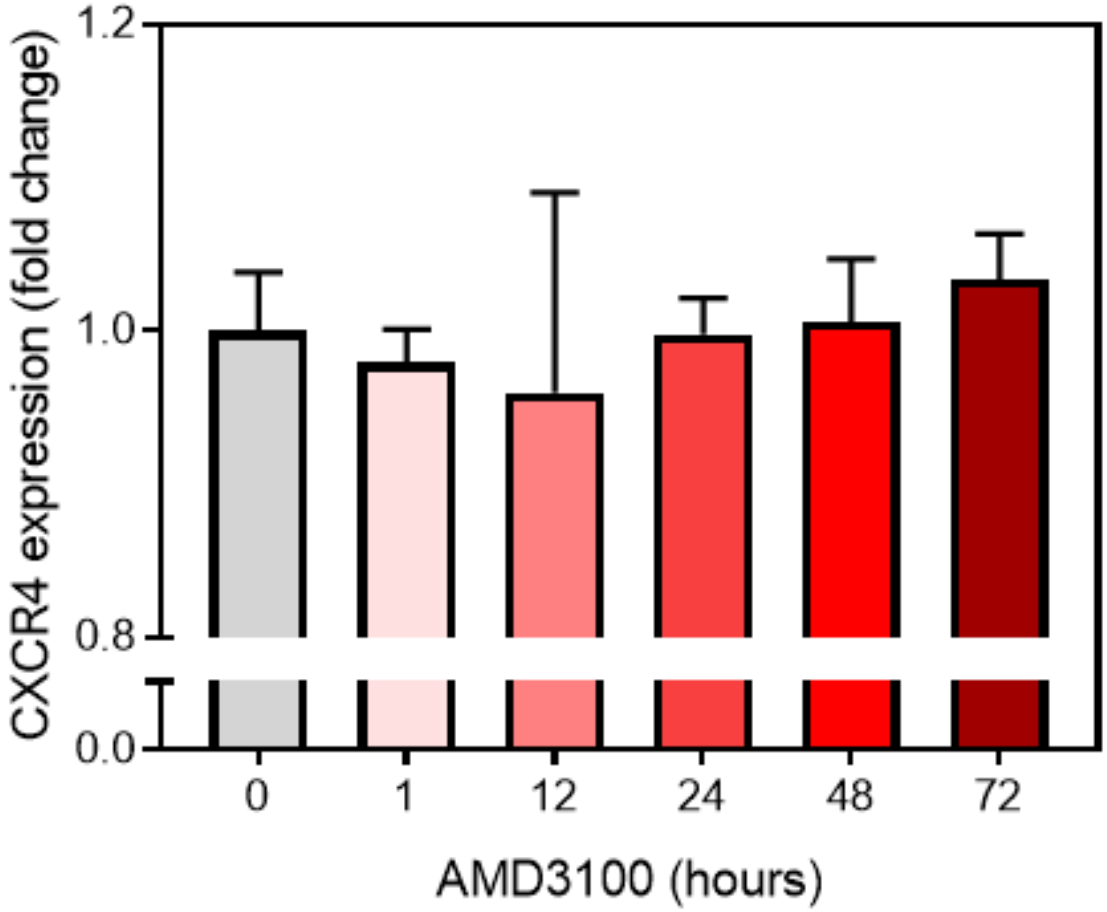

Figure 13: Treatment with AMD3100 for 72 hours treatment does not significantly increase CXCR4 gene expression.

Time dependent change in CXCR4 expression was detected by RT-qPCR after prolonged exposure of Jurkat cells to 1 μM AMD3100 for up to 72 hours. N = 3 replicates per condition.

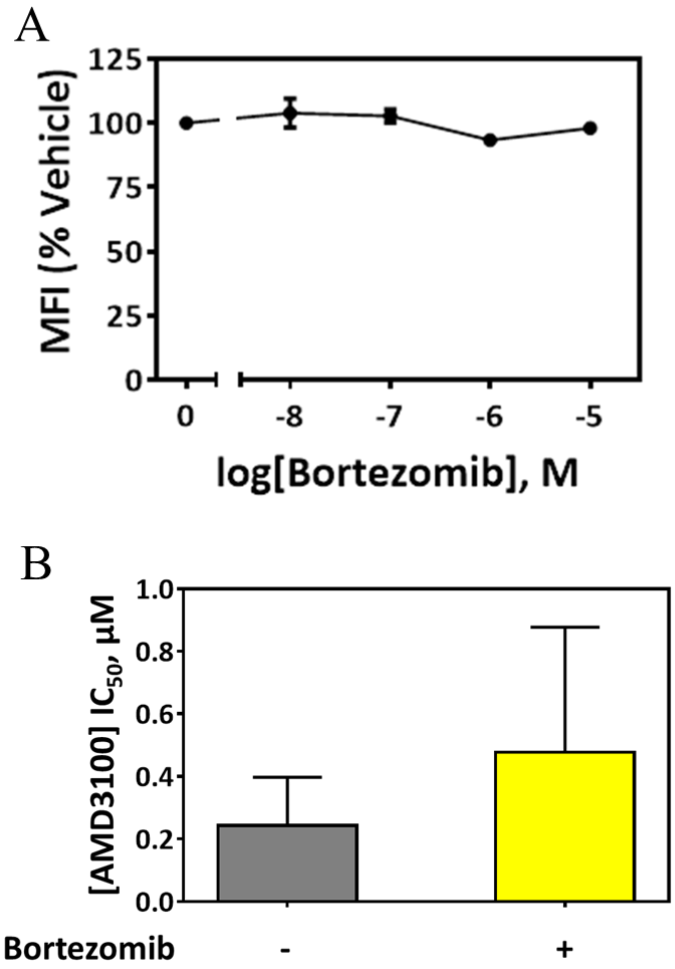

Figure 14: Proteasome inhibition does not increase CXCR4 cell surface expression.

(A) Jurkat cells were treated with increasing concentrations of Bortezomib and CXCR4 cell surface expression examined by flow cytometry using the anti-cxcr4 monoclonal antibody 12G5 (at each data point n = 3, one experiment). (B) Jurkat Cells were treated with 500 nM Bortezomib for one hour before being stimulated to chemotax towards 30 nM CXCL12 in the presence of increasing concentrations of AMD3100. IC_{50} values for AMD3100 before and after treatment with bortezomib was not significantly altered (n = 3, one experiment).

3.3 Inhibition of Endocytosis Leads to CXCR4 Accumulation and Antagonist Tolerance

3.3.1 Inhibition of endocytosis leads to tolerance to AMD3100.

Our findings suggested that inhibition of endocytosis by AMD3100 is a major contributing factor to increasing CXCR4 cell surface expression and leading to the development of tolerance. We tested this hypothesis by treating Jurkat cells with the endocytosis inhibitor Dynasore and investigating the ability of cells to overcome AMD3100 inhibition of chemotaxis. Dynasore is an inhibitor of the GTPase activity of dynamin-1 and dynamin-2 which blocks clathrin-mediated receptor endocytosis, the principal mechanism of CXCR4 internalization [91, 175]. Treatment with Dynasore for 1 hour increased CXCR4 cell surface expression as measured by flow cytometry (figure 15a). The increased amount of CXCR4 on the cell surface correlated with the reduced potency of AMD3100 to inhibit chemotaxis to CXCL12 (figure 15c). This observation correlates the inhibition of endocytosis by either AMD3100 or Dynasore with receptor accumulation on the cell surface and the subsequent development of antagonist tolerance. The ability of cells exposed to Dynasore to overcome the effects of AMD3100 in a chemotaxis assay was increased in a small but statistically significant manner (figure 15b). This might be explained by the relatively small increase in cell surface expression caused by Dynasore treatment. Treatments with Dynasore for prolonged periods of time may be required to see larger differences in IC_{50} values, although under these conditions the effects of Dynasore on reducing plasma membrane cholesterol can indirectly affect CXCR4 in a manner independent of its effects on endocytosis [175]. Additionally, treatment with Dynasore is unlikely to induce ligand dependent affects e.g. ligand-dependent conformational changes, that binding of AMD3100 to CXCR4 may induce because Dynasore is not a ligand for CXCR4.

The expression level of CXCR4 at the plasma membrane is linearly correlated with increase in receptor function [161]. To investigate if overexpression of CXCR4 at the cell surface is sufficient to induce tolerance to AMD3100, we electroporated Jurkat cells with increasing concentrations of

pcDNA3.1 containing CXCR4. We then performed chemotaxis assays with 30 nM CXCL12 to calculate IC_{50} values. We hypothesized that as CXCR4 expression increased, so would the ability of cells to overcome inhibition by AMD3100. While the cells that overexpressed CXCR4 were more chemotactic, i.e. more cells migrated towards CXCL12, the IC_{50} value for AMD3100 inhibition of CXCL12-mediated chemotaxis was only slightly increased, and not as significantly as observed after 72 hours exposure to the antagonist. Taken together with the Dynasore experiments, these data suggest that a combination of endocytosis inhibition and receptor overexpression underlie the development of tolerance to AMD3100 in Jurkat cells.

While CXCR4 is a fidelitous receptor in that it only binds a single chemokine ligand, CXCL12 can bind to other receptors such as CXCR7, also known as atypical chemokine receptor 3 (ACKR3) [176]. ACKR3 does not signal through G proteins but does bind BAs and undergo endocytosis [177]. ACKR3 is considered a decoy receptor that functions as a "sponge" for CXCL12 to tailor CXCR4 signalling [176]. ACKR3 also binds to AMD3100 [178]. We hypothesised that an alternative mechanism for the development of tolerance could be upregulation of decoy receptors that would bind CXCR4 ligands e.g. AMD3100 and reduce the effective concentrations in the local environment. We investigated if ACKR3 expression was upregulated in tolerant Jurkat cells after 72 hours of exposure to AMD3100. We also investigated the expression of CXCR3 as CXCR4, ACKR3 and CXCR3 can all regulate one another and provide crosstalk in signalling pathways [179]. We measured cell surface expression of these receptors by flow cytometry. As expected, AMD3100 treatment over 72 hours increased CXCR4 cell surface expression (Appendix A, figure 2a, d). However, we did not observe any changes in AKCR3 or CXCR3 expression (Appendix A, figure 2b, c, d).

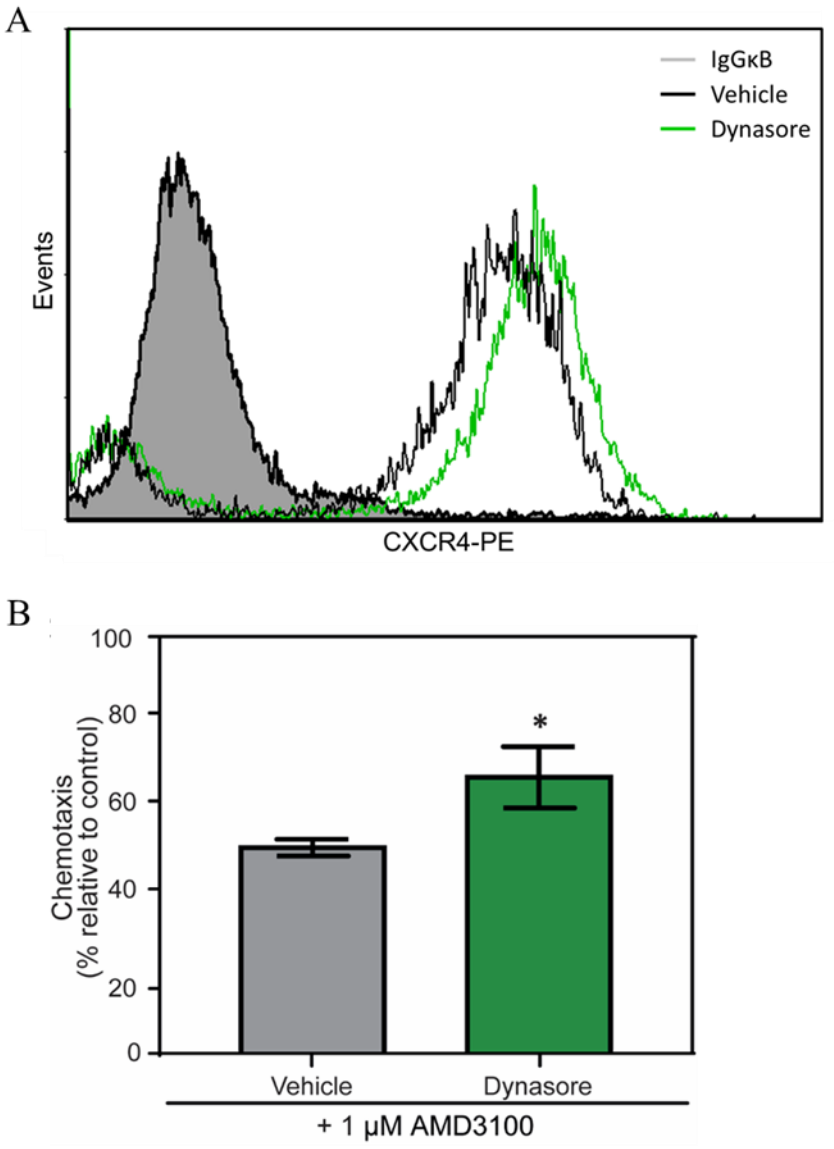

Figure 15: Inhibition of endocytosis increases CXCR4 cell surface expression and leads to tolerance to AMD3100.

Jurkat cells were treated with 80 μM dynamin inhibitor Dynasore for 1 hour of treatment. (A) Flow cytometry analysis of CXCR4 cell surface expression was investigated using and the anti-CXCR4 antibody 12G5 before and after treatment with Dynasore. (B) Transwell migration assay of Jurkat cell chemotaxis toward CXCL12 after treatment with the indicated concentration of AMD3100 with or without Dynasore for 1 hour. Chemotaxis is plotted relative to chemotaxis in the presence of CXCL12 alone. ($p = 0.04$ by Students t test, $n = 3$ independent experiments, data are means ± SD).

3.3.2 Oligomerization of CXCR4 occurs upon prolonged exposure to AMD3100

Higher levels of CXCR4 expression are also correlated with CXCR4 oligomerization and multiple studies have suggested that oligomeric CXCR4 is more active than monomeric receptor [159, 180, 181]. We hypothesized that the increased activity of CXCR4 in antagonist tolerant Jurkat cells was, at least in part, due to increased receptor expression leading to receptor oligomerisation. To first investigate the effect of AMD3100 on CXCR4 oligomerization, Jurkat cells were treated with vehicle or 1 μM AMD3100 for 1 or 72 hours and receptor oligomerization assessed by immuno-electron microscopy (EM). AMD3100 or vehicle was replaced every 12 hours to prevent potential degradation of the drug. Cells were then smeared onto coverslips and stained for CXCR4 using the monoclonal antibody 2B11 that recognizes an epitope in the N-terminus of the receptor, and protein A conjugated to 10 nm gold particles. In all Jurkat cells, CXCR4 was observed in both monomeric and dimeric states (figure 16). Receptor clusters (three or more receptors) appeared only in cells treated for 72 hours with AMD3100 (figure 16c, d, e). This result suggests that in Jurkat cells CXCR4 exists primarily as monomers and dimers, and that the development of tolerance to AMD3100 might be linked to receptor oligomerization.

To independently confirm that prolonged exposure to AMD3100 causes CXCR4 oligomerization or clustering, we performed a Bioluminescence Resonance Energy Transfer (BRET) experiment. BRET allows for the study of protein-protein interactions in cells and relies on Forster resonance energy transfer from a bioluminescent donor to an acceptor in the presence of a substrate. Here, we fused CXCR4 to either Renilla luciferase (Rluc) to act as a BRET donor and to YFP for the BRET acceptor. Given the close proximity of a Rluc tagged receptor and a YFP-tagged CXCR4, then addition of the Rluc substrate coelenterazine will result in the emission of light at 395 nm, which excites YFP. The excitation of YFP causes emission of a yellow-green fluorescence that can be measured at approximately 520 nm. We used HEK293T cells transfected

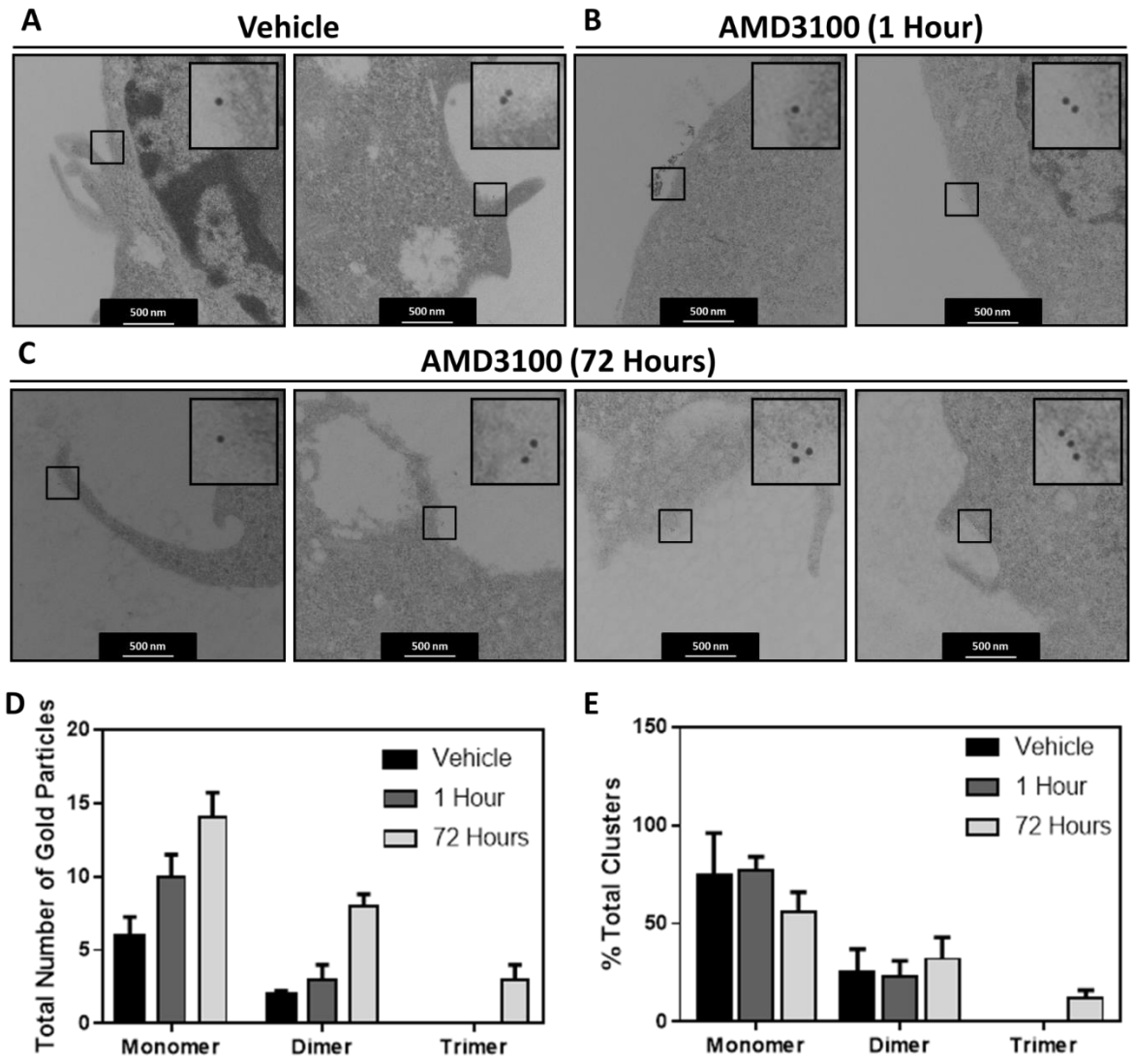

Figure 16: Immunogold labelling of CXCR4 detects receptor oligomerisation in Jurkat cells treated with AMD3100 for 72 hours.

Jurkat cells were treated with (A) vehicle or 1 µM AMD3100 for (B) 1 or (C) 72 hours. Samples were stained for CXCR4 using a CXCR4 monoclonal antibody and single 11 nM gold particles were detected by EM. We imaged a minimum of 3 cells per condition and (D) quantified the total number of gold particles in any cluster and (E) the percent of all clusters that contained one (monomer), two (dimer), or three (trimer) gold particles. Inserts show zoomed in areas in boxes.

with 50 ng CXCR4-hRluc pcDNA3.1 BRET donor, and titrated increasing amounts of pcDNA3.1 encoding either CXCR4-YFP BRET acceptor. The cells were then exposed to vehicle or 1 μM AMD3100 for 30 minutes or 72 hours before measuring luminescence. In all samples, luminescence surges as CXCR4-YFP expression increases, indicating receptor homo-oligomerization (figure 17). In cells treated with AMD3100 for 30 minutes, the $BRET_{50}$ and $BRET_{max}$ signals ($BRET_{50}$ = 0.04 ± 0.01, $BRET_{MAX}$ = 1.57 ± 0.02) are not significantly different from vehicle treated cells ($BRET_{50}$ = 0.04 ± 0.01, $BRET_{MAX}$ = 1.58 ± 0.01) (figure 17a). However, cells treated with AMD3100 for 72 hours have both a lower $BRET_{50}$ and higher $BRET_{max}$ ($BRET_{50}$ = 0.03 ± 0.01, $BRET_{MAX}$ = 1.64 ± 0.01) than vehicle treated counterparts (figure 17b). The lower $BRET_{50}$ suggests that saturation of the fluorescent signal occurs more rapidly in cells treated with AMD3100 for 72 hours, inferring that prolonged exposure to the antagonist increases receptor affinity for other receptors. However, the higher $BRET_{max}$ signal, which is dependent on the distance between donor and acceptor fluorophores, infers that a conformational change occurs when receptors oligomerize after prolonged exposure to AMD3100 [182].

Any conformational change in a GPCR can shift the conformational equilibrium of the receptor such that GPCR function is altered [32, 36]. A change in the conformational equilibrium can significantly impact the binding of GPCR ligands and effectors. Our BRET data suggesting that CXCR4 undergoes a conformational change after prolonged exposure to AMD3100 led us to hypothesise that AMD3100 may interact differently with tolerant CXCR4 as compared to the regular receptor. In order to understand the conformational changes that may have occurred upon receptor oligomerisation and the development of antagonist tolerance, we examined the published crystal structures of CXCR4 [183]. The X-ray structures of CXCR4 dimer and higher-order oligomer (trimer) were solved in complex with a low molecular weight antagonist IT1t. In both cases, IT1t was used to stabilize the receptor by binding the extracellular loop 2 (ECL2). The dimer structure of CXCR4 (PDB ID: 3ODU) described the dimer interface involving helices V

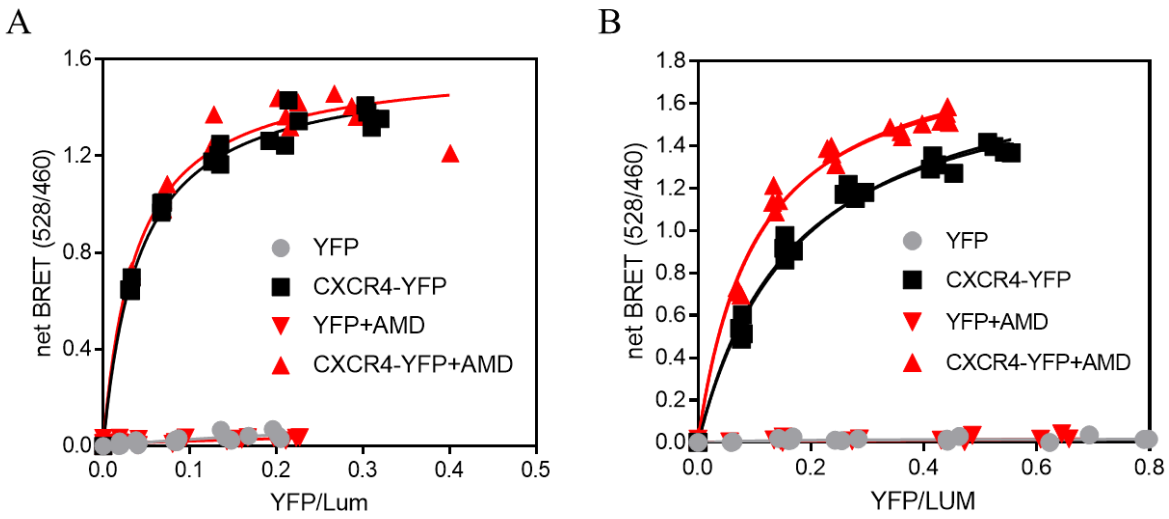

Figure 17: BRET experiments suggest CXCR4 physically interact within clusters.

Bioluminescence Resonance Transfer (BRET) between YFP-CXCR4 and Rluc-CXCR4 in HEK293 cells treated with AMD3100 or vehicle for (A) 30 minutes or (B) 72 hours. These results are representative of three independent experiments.

and VI, as well as intracellular ends of helices III and IV and intracellular loop 2 (figure 18a). In addition to the structure of the dimeric receptor, in a different crystal, CXCR4 formed a trimer in the crystallographic asymmetric unit. This structure was solved using molecular replacement and refined to 3.1 Å resolution (PDB ID: 3OE8). The reported dimer interface is preserved in trimeric CXCR4 (figure 18b). The third receptor molecule interacts with dimeric CXCR4 primarily through helices I, II, V, and VI. The specific contacts are $I47^{1.41}$-$L253^{6.49}$ and $I39^{1.34}$-$I261^{6.57}$ in monomer 1 and monomer 2, respectively. Additionally, $V62^{1.54}$ contacts $I223^{5.62}$, $V99^{2.65}$ interacts with $I261^{6.57}$, and $Q66^{1.60}$ forms a hydrogen bond with $S224^{5.63}$ in monomer 1 and monomer 2, respectively. Despite a highly similar topology, the monomeric subunits of CXCR4 in the dimer and trimer are not identical, with a root mean square deviation of 1.1 Å for all equivalent Cα atoms. In the trimeric receptor, the region proximal to the extracellular surface of helix VI moves away from helix VII towards helix V. This movement significantly alters the conformation of the ECL2 (figure 18c). This relocation results in a change in the distance between the Hδ1 proton of Ile185 in ECL2 and one of the two cyclohexane rings in IT1t from 3.5 Å in CXCR4 dimer (figure 18c) to 5.4 Å in the trimeric receptor (figure 18d). It also alters the region of the receptor containing known residues for AMD3100 binding (figure 19a) [148, 149, 184]. Within the trimeric CXCR4 assembly, the movement of helices IV and VI that contain antagonist binding residues $Asp171^{4.60}$ and $Asp262^{6.58}$ may alter the ability of AMD3100 to bind (figure 19b). In the dimer, the distance between $Asp262^{6.58}$ and $Gln200^{5.39}$ is 8.6 Å (figure 19c). In the trimer $Asp262^{6.58}$ moves toward $Gln200^{5.39}$ by 3.8 Å (figure 19d), and although within the crystal structure the 5 Å distance is still too large for a hydrogen bond to form, it is possible that the distance is less than this inside of the cell. This potentially sequesters a crucial residue for AMD3100 binding and could explain the reduced affinity of the tolerant, trimeric receptor.

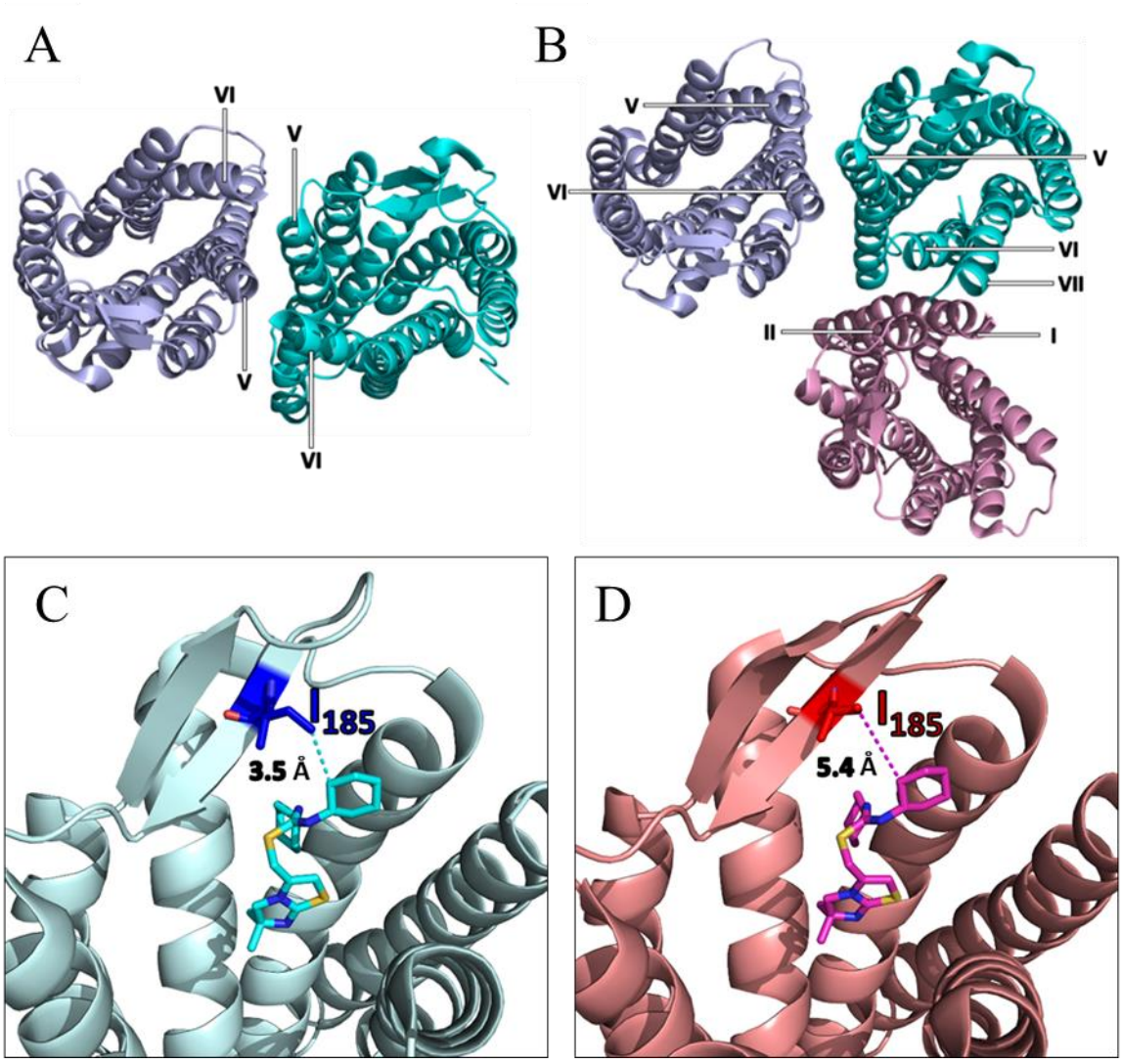

Figure 18: CXCR4 dimer and timer interact differently with IT1t.

(A) CXCR4 dimer (3ODU) and (B) CXCR4 trimer (3OE8) crystal structures were solved bound to IT1t. The dimer interface is present in both dimer and trimer, but an additional interface is present in the trimeric receptor. The distance of Ile185 in CXCR4-ECL2 with one of the two cyclohexane rings in IT1t is (C) 3.5 Å in CXCR4 dimer and (D) 5.4 Å in the CXCR4 trimer.

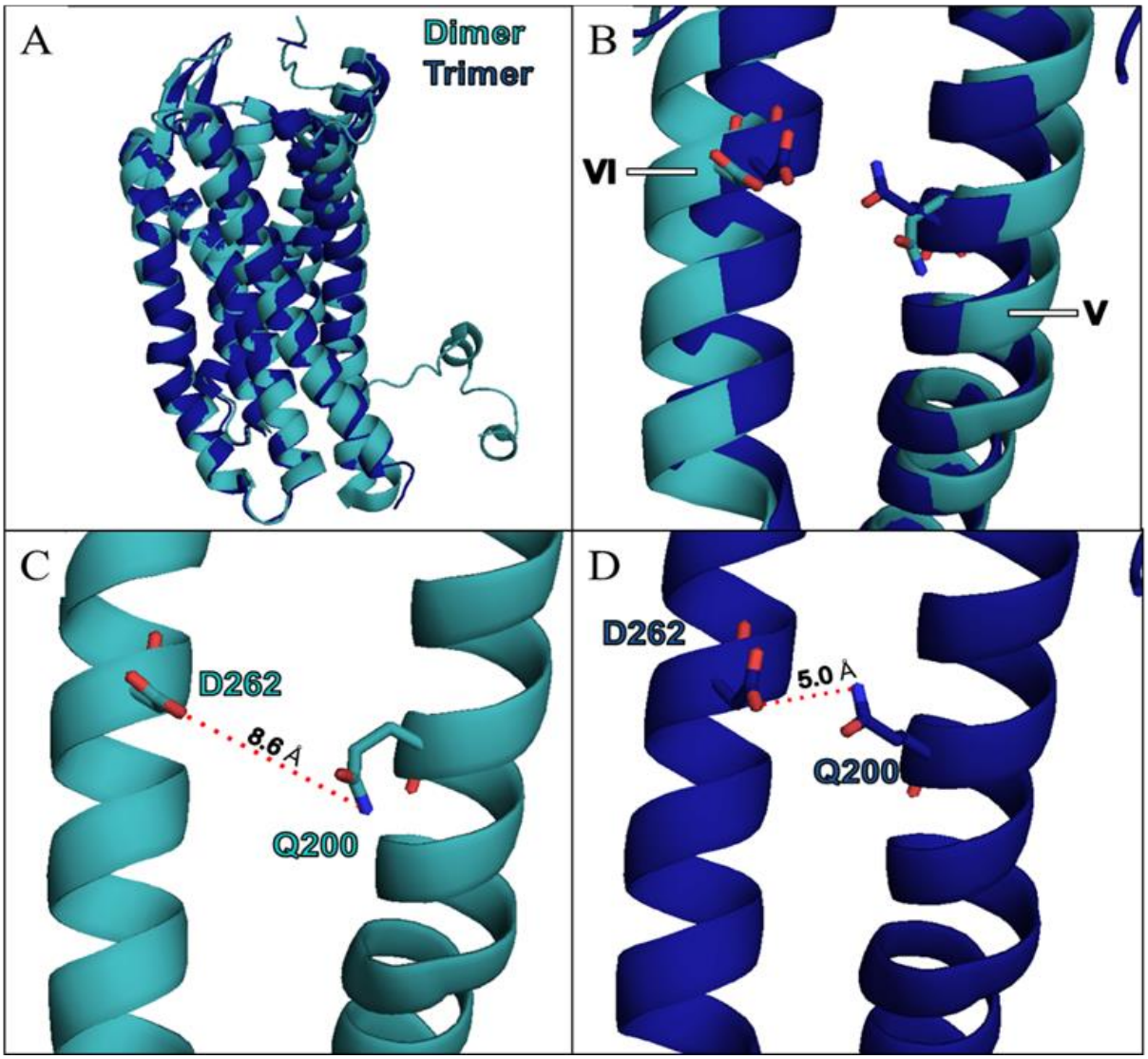

Figure 19: Differences in the AMD3100 binding site between dimeric and trimeric CXCR4. (A) Overlay of monomers from CXCR4 dimer and CXCR4 trimer. (B) Helix 5 and 6 are moved closer to one another in the CXCR4 trimer as compared to the trimer. (C) In the CXCR4 dimer, D262 and Q200 are 8.6 Å apart. (D) In the trimer D262 moves toward Q200 by 3.8 Å and are 5.0 Å apart.

The difference in the binding mode of IT1t between the two receptor forms allowed us to use this small molecule as a structural probe for CXCR4 conformations in the native plasma membrane. We utilized saturation transfer difference (STD) NMR to detect the binding modes of the antagonist. This method relies on magnetization transfer from the protein of interest to the small molecule due to the distance-dependent Nuclear Overhauser effect (NOE). This transfer is very efficient when the interacting portions of the small molecule are within 2-3 Å from the target protein. In this case, a high intensity signal is detected in the STD spectrum. A 1-2 Å change in the distance between the small molecule and the protein has a dramatic effect on NOE and results in a reduction of the STD signal, allowing conformational changes to be detected with high precision.

The 1H 1D spectrum of IT1t showed 5 signals at 6.2, 3.1, 2.5, 1.8, and 1.4 ppm (figure 20a). We performed STD experiments on an 800 MHz spectrometer on 125 μM IT1t in the presence of CXCR4 in the plasma membrane fractions from Jurkat cells treated with vehicle or AMD3100 for 72 hours. No STD transfer was observed for the antagonist alone (figure 20). STD revealed that the cyclohexane signal of IT1t in the presence of membranes with low CXCR4 expression is found at 1.4 ppm (figure 20c). The membranes from cells overexpressing the receptor caused a reduction in the cyclohexane signal intensity by 25%, as compared to the low CXCR4 expression control. In contrast, the 6.2 ppm signal corresponding to the ring structure of IT1t did not exhibit a significant change in intensity (figure 20b). This can be predicted by the crystal structure of trimeric CXCR4 that shows a dislocation of the cyclohexane group from its position in the receptor dimer, while the position of the ring structure remains unchanged (figure 18c, d). These experiments suggest that small molecules can detect conformational changes in GPCRs in mammalian cell membrane preparations. This is a useful tool because it allows receptors to be in their native environment with complete and proper modifications.

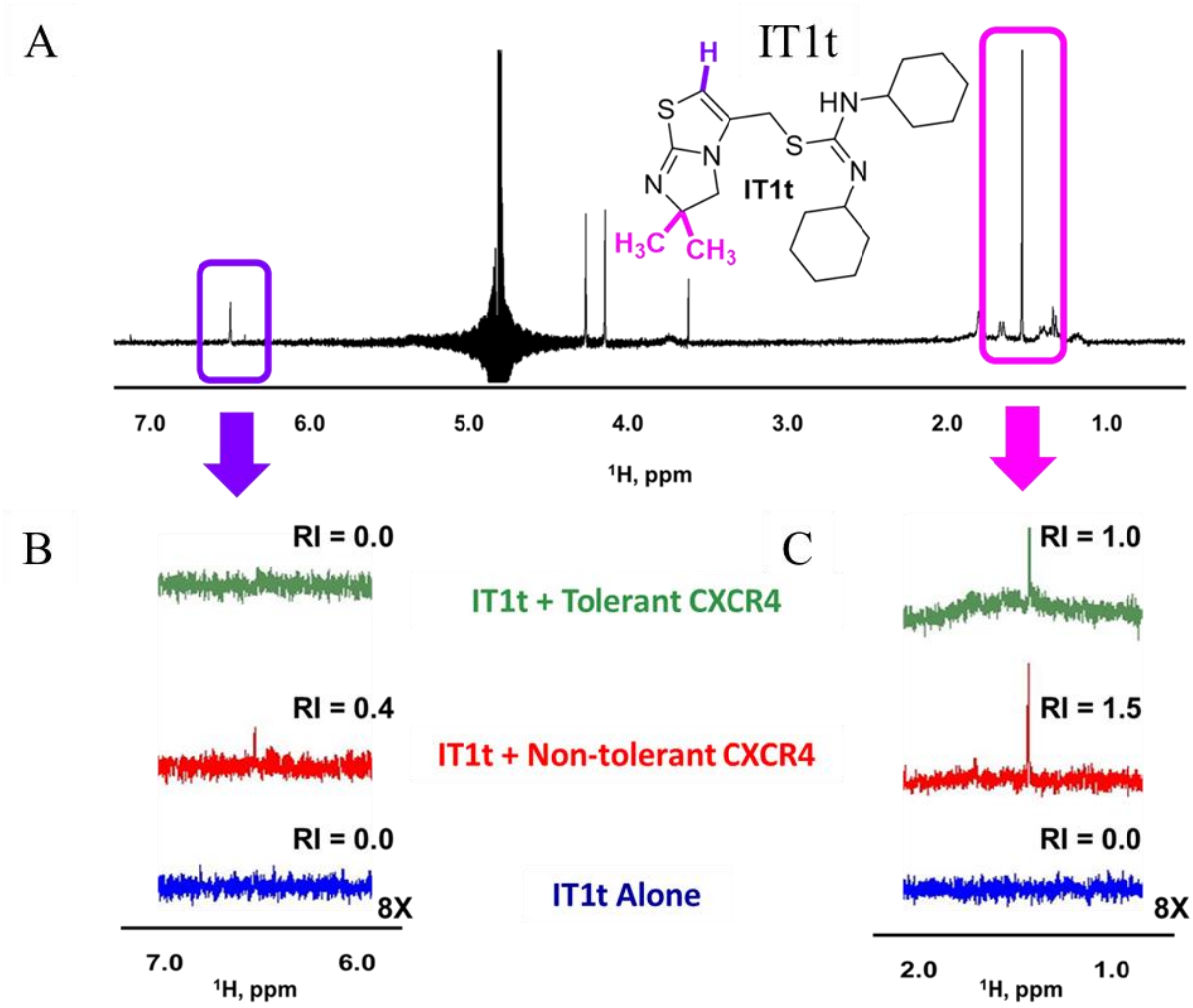

Figure 20: STD-NMR shows that IT1t interacts differently with tolerant and non-tolerant CXCR4.

(A) 1D-NMR spectrum of 125 µM IT1t. STD spectra of IT1t alone (blue), IT1t plus membrane preps Jurkat cells treated with vehicle for 72 hours (red) or IT1t plus membrane preps Jurkat cells treated with AMD3100 for 72 hours. RI stands for relative intensity.

We hypothesized that we could use this technique to investigate if AMD3100 employs different binding modes to interact with CXCR4 from tolerant and non-tolerant cells, and that we could detect these differences using NMR. To address this hypothesis, we performed 1D 1H NMR and STD-NMR experiments using 100 μM AMD3100 in the presence of plasma membranes purified from antagonist-tolerant or non-tolerant Jurkat cells.

The signals of the protons in the bicyclam rings of AMD3100, which are primarily responsible for binding CXCR4, agreed with the previously published spectra of the drug (figure 21a) [184, 185]. In the presence of CXCR4 in the plasma membrane from non-tolerant Jurkat cells, the 1H signals experienced line-broadening and chemical shift changes consistent with binding (figure 21b). In the presence of CXCR4 in the plasma membrane from antagonist-tolerant cells, the bicyclam signals exhibited less broadening and chemical shift changes than in the presence of membranes from non-tolerant cells. This suggested that AMD3100 changes its mode of binding and affinity for CXCR4 in antagonist-tolerant cells. We also performed STD-NMR with membranes from tolerant and non-tolerant Jurkat cells. We observed signals from the aromatic 1,4-xylyl spacer of AMD3100 around 7.8 ppm (figure 21a). This portion of the molecule is thought to interact with Phe172 and Phe174 in TM-IV and Phe199 and Phe210 in ECL2 [186]. The intensity of these signals was significantly greater in the presence of membrane from tolerant cells compared to non-tolerant cells (figure 21c).

To demonstrate that these NMR signals were specific to CXCR4-AMD3100 interaction we performed STD-SMR with AMD3100 in membranes prepared from non-tolerant Jurkat cells and blocked AMD3100 binding with the anti-CXCR4 monoclonal antibody 12G5. In the presence of the 12G5 antibody, the signal from the 1,4-xylyl spacer protons was no longer observed, indicating AMD3100 no longer bound (figure 21d). This showed that the signals came from AMD3100 binding to CXCR4 and not from non-specific binding or binding to other receptors e.g. ACKR3.

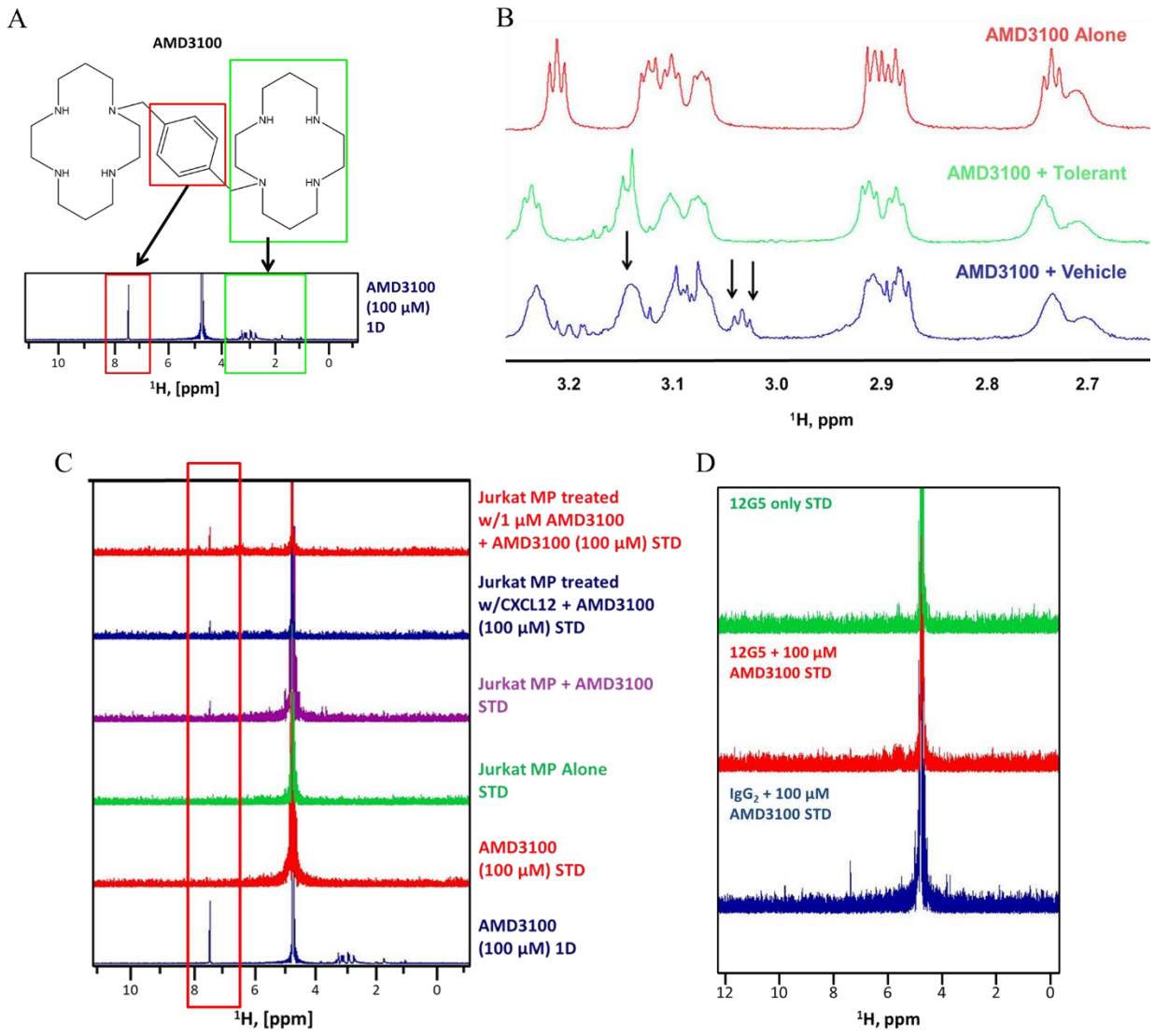

Figure 21: Interaction of AMD3100 with CXCR4 is altered in antagonist tolerant cells.

(A) 1D-1H NMR of 100 µM AMD3100 alone. (B) 1D-1H NMR of 100µM AMD3100 plus vehicle (blue), membranes from AMD3100 tolerant Jurkat cells (green) and membranes from non-tolerant cells (red). Arrows indicated differences in line broadening. (C) STD-NMR of (bottom to top) AMD3100 alone (1D), AMD3100 alone (STD), Jurkat membrane prep alone, Jurkat membrane prep plus AMD3100, membrane preps from Jurkat cells pretreated with CXLC12, and Jurkat membrane prep from tolerant cells plus AMD3100. (D) STD-NMR from Jurkat membrane peps treated with anti-CXCR4 monoclonal antibody 12G5 (green), Jurkat membrane peps treated with anti-CXCR4 monoclonal antibody 12G5 plus 100 µM AMD3100, and Jurkat membrane peps treated with IgG antibody control plus 100 µM AMD3100 (blue).

We subsequently performed computational docking of AMD3100 into the structure of dimeric and trimeric CXCR4 using AutoDock Vina software [137]. AutoDock is an automated docking tool that uses a set of grids to predict how small molecules bind to a receptor with a known structure. Our computational docking of AMD3100 into the structure of trimeric CXCR4 predicts interactions between one cyclam ring of the drug and Asp171$^{4.60}$ in CXCR4, while the interactions with Asp262$^{6.58}$ and E288$^{7.39}$ observed for AMD3100 docked into the structure of CXCR4 dimer are diminished (figure 23a, b). While this predictive model provides insight into the potential the altered binding mode of AMD3100 with tolerant CXCR4, it is a model based on a static crystal structure and other mechanisms may be involved in changing the way AMD3100 binds. However, the model correlates with our NMR data suggesting the interaction modes of AMD3100 with regular and tolerant receptors are different. These data also suggest a change in affinity for AMD3100 between the dimeric and trimeric receptors due to the reduced contacts with the drug in the trimeric CXCR4.

To measure the affinity of antagonist tolerant and non-tolerant CXCR4 for AMD3100, we treated Jurkat cells with vehicle or 1 μM AMD3100 for 72 hours before fractionating the cells on a sucrose gradient and collecting the plasma membrane. These fractions were used for surface plasmon resonance (SPR) studies of receptor affinity for AMD3100 by immobilizing the membranes onto C1 sensor chips via coupling to wheat germ agglutinin (WGA). WGA captures membranes because as an agglutinin, it binds carbohydrates such as N-acetyl-D-glucosamine and sialic acid that are common carbohydrate modifications of proteins [187]. AMD3100 was flowed over the captured membranes, allowing us to determine a K_D of 3.2 ± 0.6 nM for non-tolerant CXCR4 (figure 23a) and 490 ± 54 nM for the tolerant receptor (figure 23b). This data suggests that tolerance to AMD3100 is associated with a reduced affinity of CXCR4 for AMD3100, due to conformational changes associated with receptor oligomerisation.

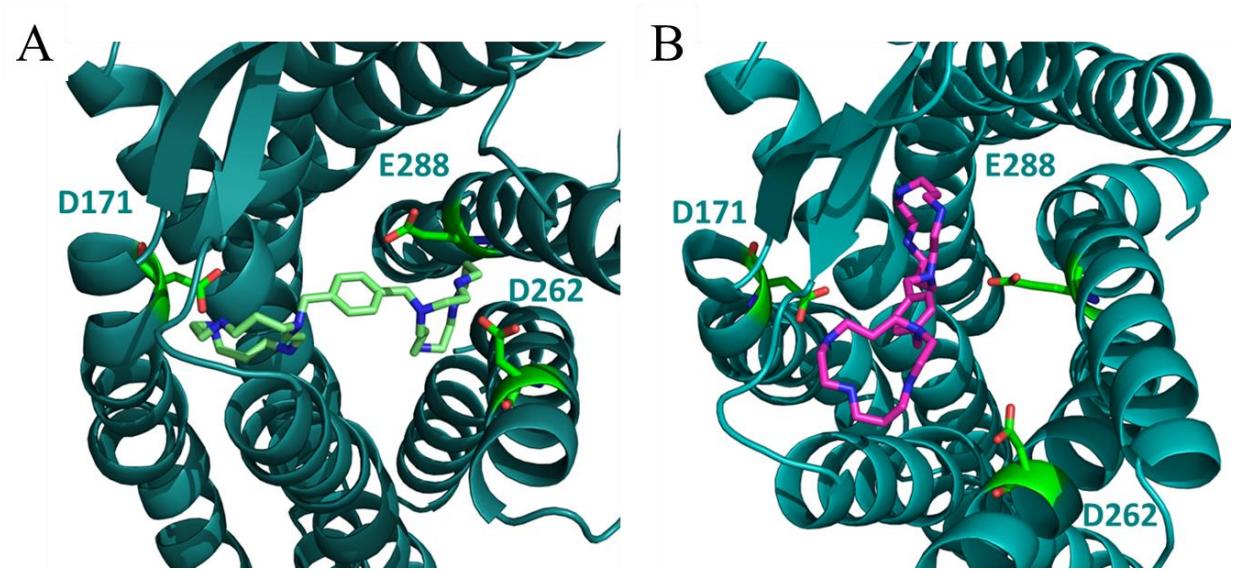

Figure 22: Docking of AMD3100 into Structures of CXCR4 Suggests Altered Binding Mode.

When docked into the (A) CXCR4 dimer structure, AMD3100 makes contact with CXCR4 residues that are known binding determinants. When docked into the (B) CXCR4 trimer, it does not make the same contacts. Docking performed using AutoDock Vina.

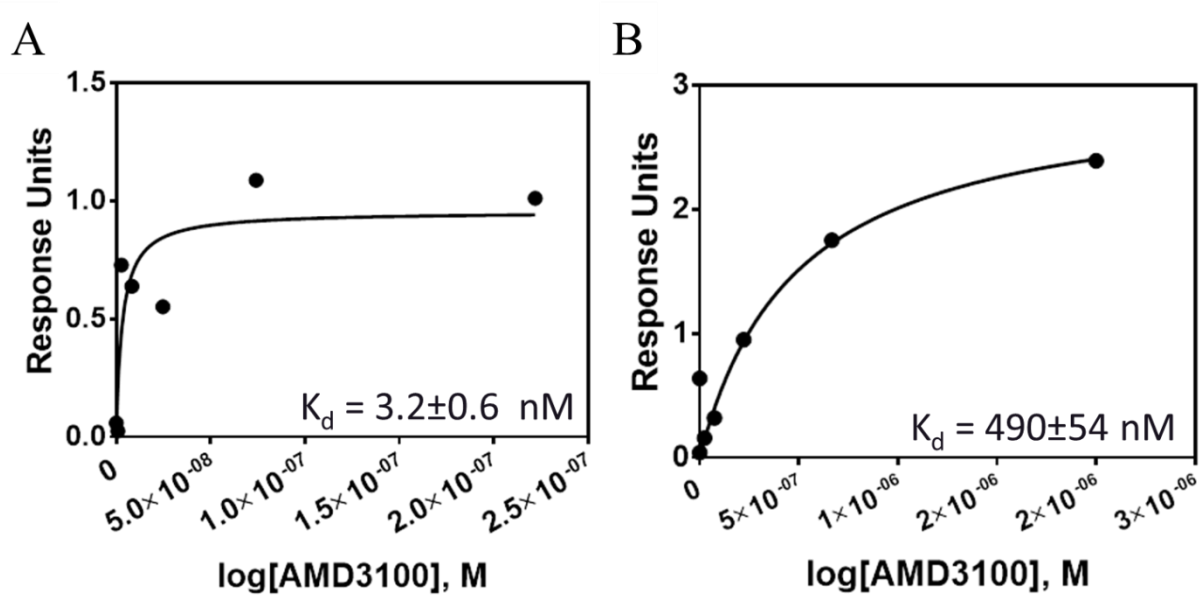

Figure 23: SPR shows that AMD3100 has a reduced affinity for CXCR4 in the plasma membrane from AMD3100-tolerant cells in comparison to CXCR4 in the membrane from non-tolerant cells.

Jurkat cells with (A) vehicle or (B) 1 μM AMD3100 for 72 hours before fractionating the cells and collecting cell membranes. These fractions were used for SPR studies of receptor affinity for AMD3100 by immobilising the membranes onto a C1 sensor chip using wheat germ aglutinin. AMD3100 was then flowed over the membranes, allowing us to calculate (A) the kD of non-tolerant CXCR4 for AMD3100 as 3.2±0.6 nM. (B) This increased to 490±54 nM for the tolerant receptor.

To test the hypothesis that receptor oligomerisation underlies the development of tolerance to AMD3100, we aimed to design mutants of CXCR4 that would not oligomerize. Previous studies have shown that three simultaneous mutations in the intracellular portion of TM6 inhibit the formation of CXCR4 oligomers [188]. We generated the triple mutant (K239E, V242A, L264A) and an I261A mutant of CXCR4. Ile261$^{6.57}$ is the only residue that forms two intermolecular contacts across the trimer interface in the crystal structure, with residues Ile39$^{1.34}$ and Gln66$^{1.60}$ and we hypothesised that this minimal mutation would disrupt trimer formation. To assess the effects of these mutations on oligomerisation, we transfected Chinese Hamster Ovary (CHO) cells with 0.5, 1, or 2 µg for WT or I261A pcDNA3.1-HA-CXCR4. CHO cells do not endogenously express CXCR4. To assess CXCR4 clustering, we performed immunogold EM as previously described in this thesis. However, staining was unsuccessful with very few receptors observed in each sample. The process of fixing cells for immuno-EM is a harsh one and includes aggressive fixation with glutaraldehyde that reacts indiscriminately with amines, potentially disrupting protein structure and epitopes. This may result in insufficient receptor epitopes present in the samples. Whilst troubleshooting these experiments, we decided to investigate oligomerisation of Ile261Ala-CXCR4 by BRET. We performed a BRET titration experiment in HEK293T cells, using 50 ng WT CXCR4-hRluc pcDNA3.1 with increasing amounts of pcDNA3.1 encoding either WT or I261A CXCR4-YFP. Although $BRET_{50}$ values were similar for WT and I261A CXCR4, $BRET_{Max}$ was significantly lower for the titration with I261A CXCR4 in comparison with WT receptor (figure 24). This similar $BRET_{50}$ suggests that the affinity for CXCR4 self-association was minimally affected by the I261A mutation, but the lower $BRET_{Max}$ is consistent with a reduction in the number of protomers within each CXCR4 cluster and/or a mutation-induced conformational change in the receptor.

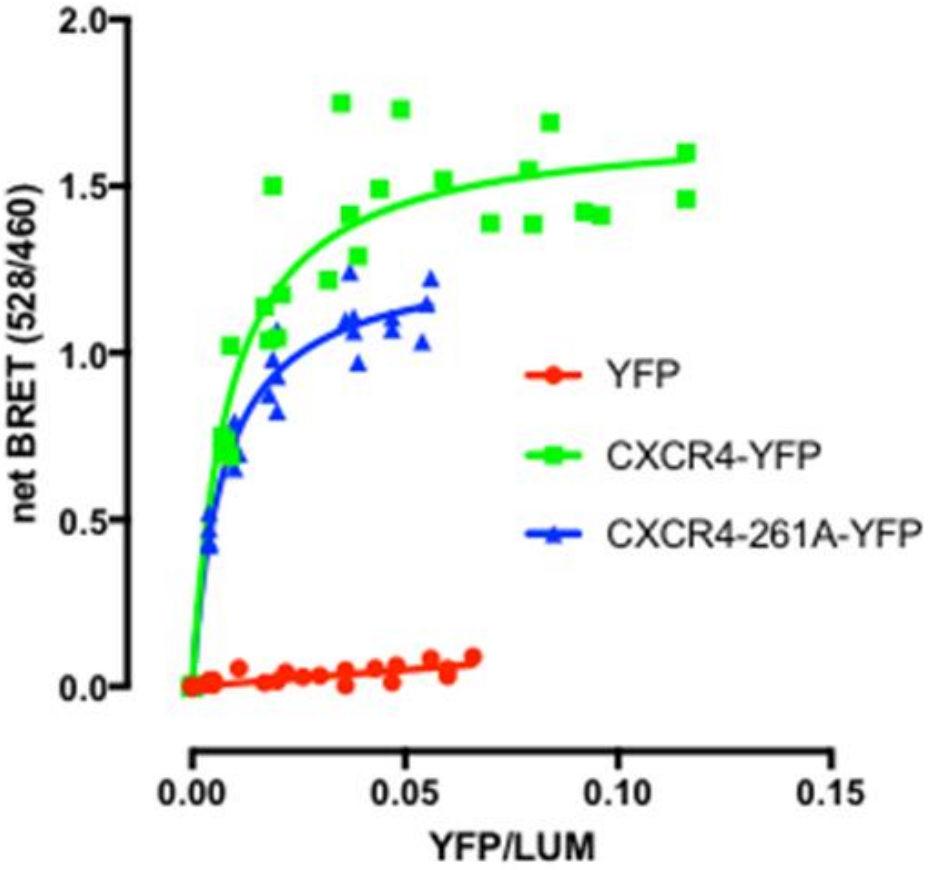

Figure 24: I261A-CXCR4 forms smaller oligomers than WT-CXCR4.

Bioluminescence Resonance Transfer (BRET) between Rluc-CXCR4 and increasing concentrations of WT-CXCR4-YFP (green) and I261A-CXCR4-YFP (blue) in HEK293 cells.

To further confirm this potential oligomerization-induced conformational change in CXCR4, we used the conformational CXCR4 monoclonal antibody 12G5 that specifically recognizes an epitope spanning the N-terminus and ECL2 of this receptor [158, 189]. CHO cells transfected with 0.5, 1, and 2 µg of pcDNA3.1 encoding either WT or I261A HA-CXCR4. The differences in receptor expression levels were confirmed by flow cytometry with the anti-HA antibody and found to be identical for WT and I261A HA-CXCR4 transfectants (figure 25a). However, the 12G5 antibody detected I261A HA-CXCR4 with a higher efficiency than the WT receptor in transfections with 1 and 2 µg of CXCR4-bearing plasmids, while the detected levels were identical for WT and I261A HA-CXCR4 in the 0.5 µg transfection (figure 25b). This result suggests that the conformation of ECL2 in CXCR4 is affected by the receptor expression levels.

To examine if the binding mode of AMD3100 to I261A CXCR4 was altered as seen with the tolerant receptor or remained the same as the non-tolerant receptor, we prepared membrane fractions from CHO cells expressing these CXCR4 constructs at high concentrations and performed NMR. We hypothesised that I261A-CXCR4 would form fewer higher order oligomers than WT CXCR4 and their interaction with AMD3100 would be different. We based this hypothesis on BRET data suggesting this mutant has a lower $BRET_{Max}$ than WT receptor. We also generated D171N-CXCR4 as a control for these experiments. The D171N mutation generates a form of CXCR4 that has reduced binding to AMD3100 due to removal of a ligand in the small molecule binding site [148, 184]. We hypothesized that the signals generated from AMD3100 in the presence of I261A-CXCR4 would resemble those generated by AMD3100 in the presence of non-tolerant WT-CXCR4. We also hypothesised that membranes containing D171N-CXCR4 would function as a negative control as the AMD3100 binding site is mutated in this receptor.

Membrane from cells expressing WT or D171N CXCR4 induced similar, weak line broadening effects, while AMD3100 in the presences of I261A membrane showed significant

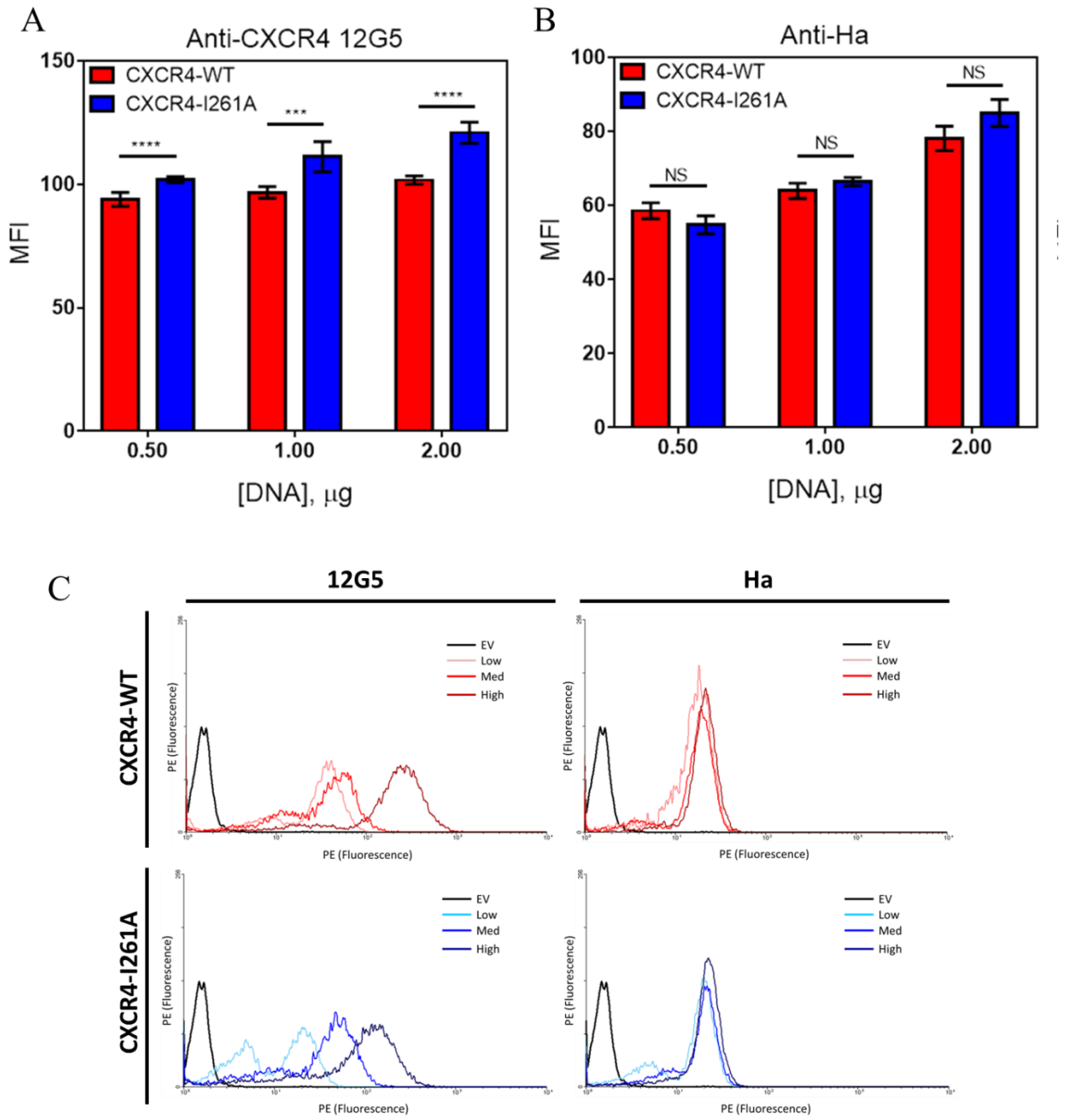

Figure 25: Flow cytometry analysis of transient transfections of CXCR4 WT and I261A suggest different conformations.

(A) Quantified MFI for CHO cells transfected with WT (red) or I261A (blue) CXCR4, stained with anti-CXCR4 12G5 antibody (***p < 0.01, ****p < 0.005, by one way ANOVA, n = 3 replicated per sample, data are means ± SD). (B) Quantified MFI for CHO cells transfected with WT (red) or I261A (blue) CXCR4, stained with anti-HA antibody (NS = not significant as assessed by one way ANOVA). (C) Histograms showing raw data.

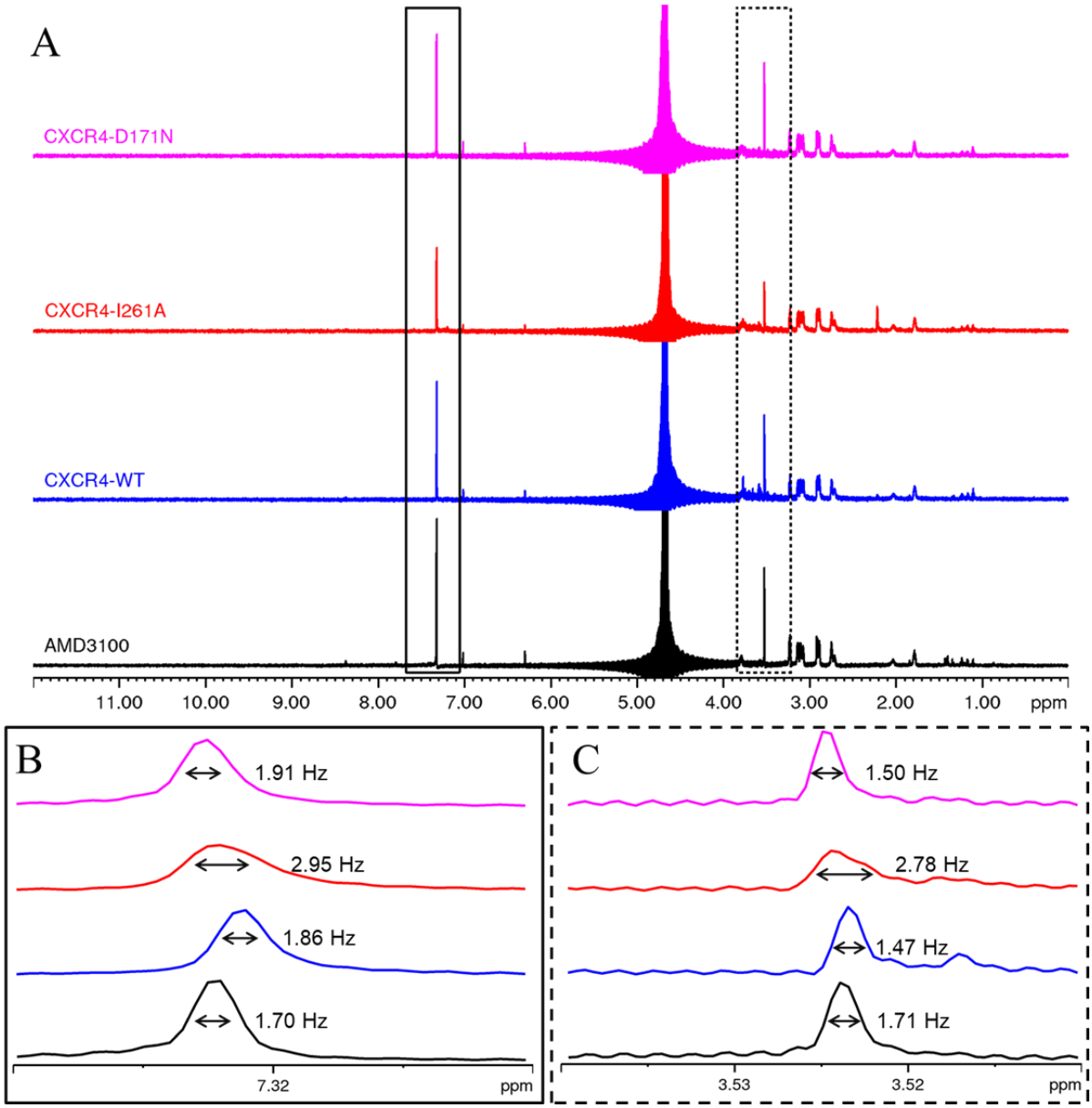

Figure 26: 1D-NMR shows that AMD3100 interacts differently with overexpressed WT and I261A-CXCR4.

(A) 1D-NMR spectrum of 100 µM AMD3100 alone (black), or 100 µM AMD3100 plus membrane preps containing WT-CXCR4 (blue), membrane preps containing I261A-CXCR4 (red) or membrane preps containing D171N-CXCR4 (magenta). (B) and (C) are linewidth analysis for different regions of AMD3100.

line broadening (figure 26). This was the case for both the signals at 7.3 ppm and 3.5 ppm (figure 26 b, c). This data suggests that when highly expressed in CHO cells, CXCR4 forms oligomers, becomes tolerant and does not efficiently bind AMD3100, much like D171N-CXCR4 [149]. I261A however, even when expressed at high levels in CHO cells, still binds CXCR4. Oligomerisation needs to be confirmed in these cells lines as discussed previously.

2.3.3 Why does tolerance persist?

If the altered binding mode for AMD3100 within oligomeric CXCR4 reduces the affinity of the drug for the receptor, it could logically be expected that antagonist tolerance would eventually be alleviated because inhibition of receptor endocytosis would reduce with time and the receptor would be cleared from the cell surface. Yet our experiments suggest cells start to become tolerant to AMD3100 in chemotaxis assays after just 12 hours of exposure and continue to become tolerant up to 72 hours. This suggests that while CXCR4 affinity for AMD3100 reduces, the interaction of CXCL12/AMD3100 and the tolerant receptor is also altered. To address this possibility, we measured IC_{50} values for AMD3100's inhibition of chemotaxis of Jurkat cells to CXCL12 and for inhibition of receptor endocytosis before and after the development of antagonist tolerance. As expected, with no pre-exposure to the antagonist, before the cells become tolerant, AMD3100 acts in an unbiased fashion, with similar IC50s for CXCL12-induced chemotaxis and CXCR4 endocytosis of 0.7 ± 0.2 µM and 0.7 ± 0.1 µM, respectively (figure 27a). After pre-exposure to 1 µM AMD3100 for 72 hours, the IC50s for CXCL12-induced chemotaxis and receptor endocytosis are 3.2 ± 1.9 µM and 0.5 ± 0.1 µM, respectively (figure 27b). Thus, in antagonist tolerance, AMD3100 becomes a weaker inhibitor of chemotaxis but retains its potency against receptor endocytosis. This acquired bias of AMD3100 might contribute to persistence of antagonist tolerance. This is in agreement with previous studies that suggest AMD3100 inhibits CXCL12 by blocking only the extreme N-terminus of the chemokine from interacting with CXCR4 [151]. To

study the effect of prolonged exposure to AMD3100 on chemokine binding, we treated Jurkat T-lymphocytes either with vehicle, 1 μM, or 10 μM drug for 72 hours and compared the efficiency of CXCL12-induced endocytosis of CXCR4 and chemotaxis. Prior to performing the assays, the drug was removed by rinsing the cells with fresh media. We found that the EC50s for CXCR4 endocytosis (4 nM) and chemotaxis (13 nM) in vehicle-treated Jurkat cells were affected significantly by the 72-hour treatment with 1 μM or 10 μM AMD3100 (figure 28). CXCL12 was significantly less efficient at inducing endocytosis of tolerant CXCR4, as reflected by the EC50s of 12.0 ± 4.3 nM and 60.0 ± 12.6 nM for 1 μM or 10 μM AMD3100 treatments, respectively (figure 27c, d). At the same time, prolonged exposure to the drug resulted in a slight decrease in CXCL12's EC50s for chemotaxis of 8.0 ± 3.1 nM and 5.0 ± 1.9 nM for cells treated with 1 μM or 10 μM AMD3100, respectively. This result suggests that, being a more potent inducer of chemotaxis than endocytosis, CXCL12 becomes a biased agonist in the context of antagonist-tolerant CXCR4.

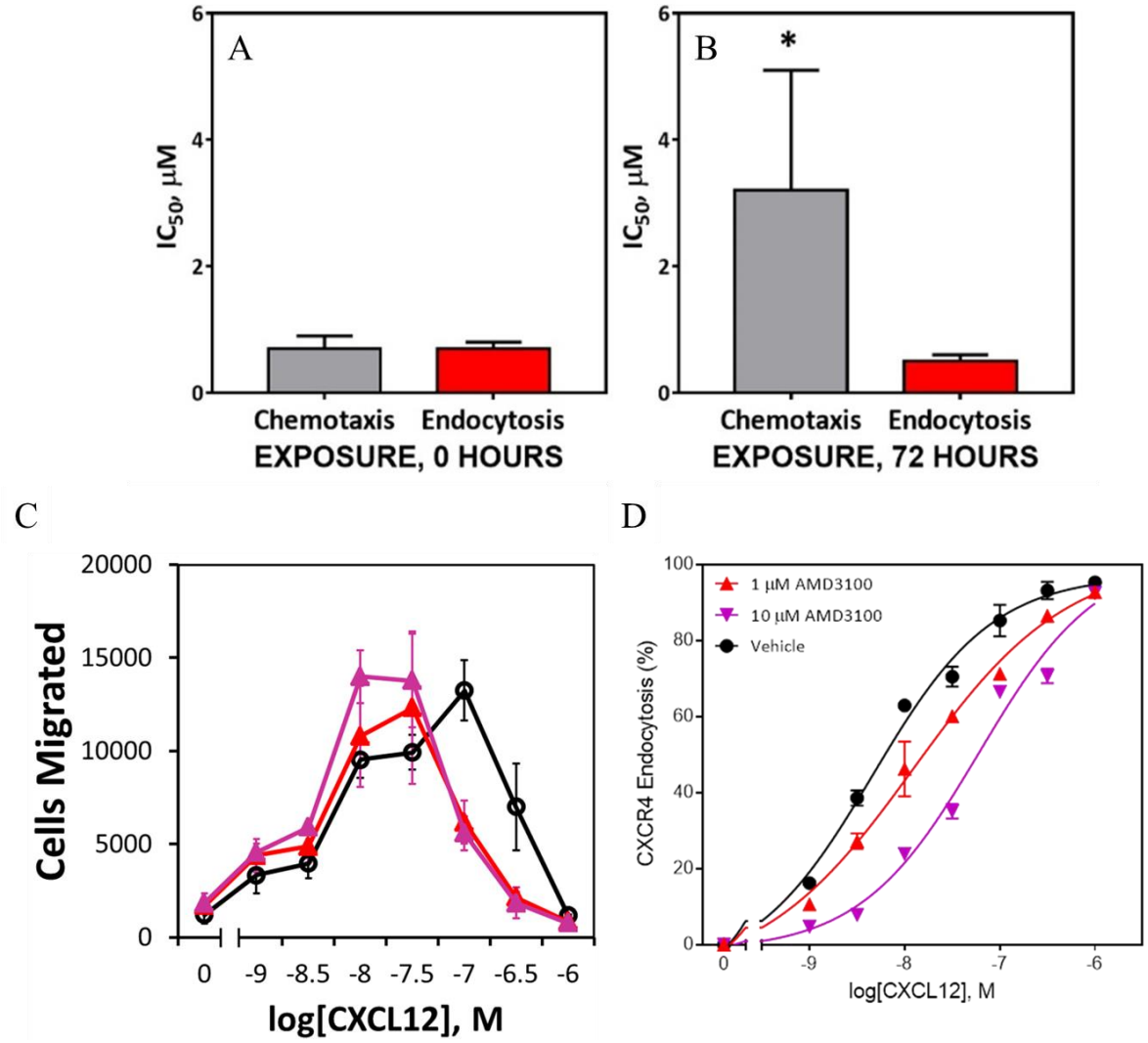

Figure 27: AMD3100 and CXCL12 acquire bias in the tolerant CXCR4.

We measured AMD3100 IC_{50} values for chemotaxis and endocytosis (a) before and (b) after exposure (*$p < 0.01$ by Students t test, $n = 3$ independent experiments, data are means ± SD). We measured CXCL12 EC_{50} values for (C) chemotaxis and (D) endocytosis before and after exposure to 1 and 10 µM AMD3100.

We have performed ^{15}N HSQC experiments on ^{15}N-labelled CXCL12 with CXCR4 in membranes from non-tolerant and AMD3100-tolerant Jurkat T lymphocytes. The addition of membranes prepared from non-tolerant cells caused attenuation of signals primarily in the N-terminus of CXCL12 (S4, L5, Y7-C9, R12, E15, S16) (figure 28a). This signal attenuation is likely due to intermediate exchange between free and receptor-bound CXCL12. Addition of AMD3100-tolerant membranes did not alter signal attenuation for S4 in the extreme N-terminus of the chemokine, responsible for activation of G proteins and chemotaxis, but decreased signal attenuation for Y7 and R8 and gave rise to chemical shift perturbations (CSPs) indicative of fast exchange in the portion of CXCL12 responsible for activation of receptor endocytosis (figure 28b). Deletion mutations in the N-terminus of CXCL12 have determined that residues 3-14 are important for CXCR4 endocytosis [75, 151, 183, 190-194]. Residue R8 in the 3-14 region of CXCL12 is predicted to interact with Asp262 of dimeric CXCR4[190-194]. Because, in CXCR4 trimer, Asp262 potentially forms a hydrogen-bond with Gln200 we propose that R8 of CXCL12 is less involved in the binding interface with the trimeric receptor with the consequence being a reduced ability of the chemokine to induce recruitment of BA to the receptor, a necessary event for endocytosis.

Since tolerance is a phenomenon that develops against many GPCR drugs, we investigated if tolerance develops to other chemokine receptor antagonists, specifically the CCR5 inhibitor Maraviroc. The CCR5 receptor is expressed on various cell types and is an important receptor for directing cell migration in inflammatory response [195]. Compared to CXCR4, CCR5 is a promiscuous receptor with multiple ligands including the macrophage inflammatory protein 1 alpha (MIP1-α) and regulated upon activation, normal T-cell expressed, and secreted (RANTES, CCL5) [196, 197]. CCR5 is a coreceptor during HIV cellular entry, for which Maraviroc is an FDA approved inhibitor [195]. To assess if tolerance develops to Maraviroc, we first established the optimal concentration of CCL5 for chemotaxis of Jurkat and THP-1 cells. Jurkat cells were

not chemotactic to CCL5, showing no increase in cell migration toward the chemokine compared to basal activity (figure 29a). THP-1 cells displayed a small amount of chemotaxis when stimulated with 3 nM CCL5 (figure 29b). We subsequently investigated the IC_{50} values of Maraviroc for chemotaxis toward 3 nM CCL5, before and after 72 hours exposure to the drug. We were not able to calculate accurate IC_{50} values, likely due incomplete inhibition of chemotaxis (figure 29c). However, both before and after 72 hours treatment with the drug, there appears to be little change in the ability of Maraviroc to inhibit chemotaxis. It may also be important to note that analysis may be skewed by the very small number of cells migrating towards CCL5. In the same cell lines, a more robust induction of chemotaxis is observed for CXCL12. Additionally, to date, inhibition of chemotaxis has not previously been observed for Maraviroc. It may be useful to study tolerance in other chemokine antagonists that do inhibit chemotaxis.

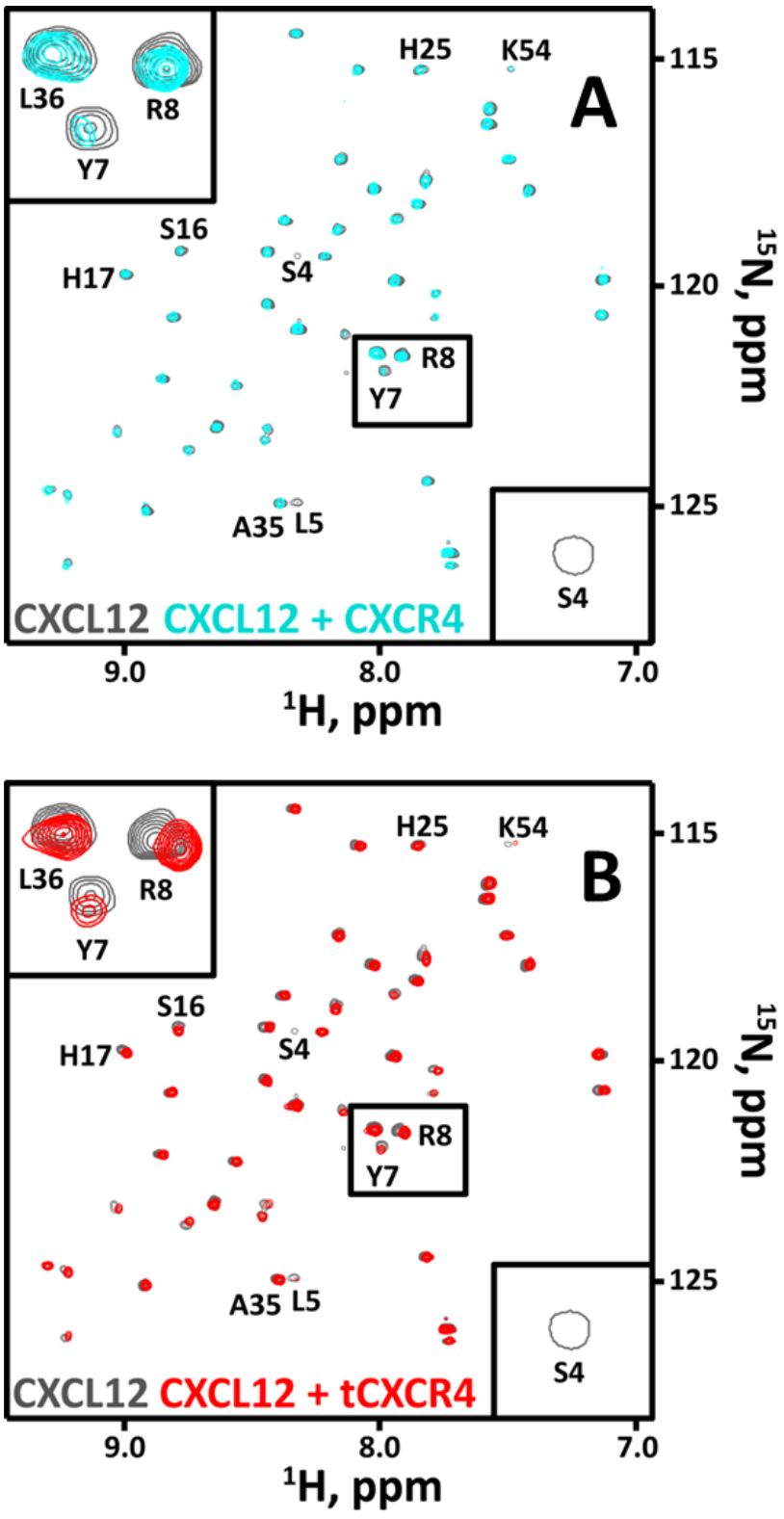

Figure 28: CXCL12 interacts differently with CXCR4 in AMD3100-tolerant versus non-tolerant cells.

Overlays of ^{15}N HSQC spectra of CXCL12 alone (grey) with CXCL12 in the presence of membranes prepared from (a) non-tolerant Jurkat cells and (B) tolerant Jurkat cells.

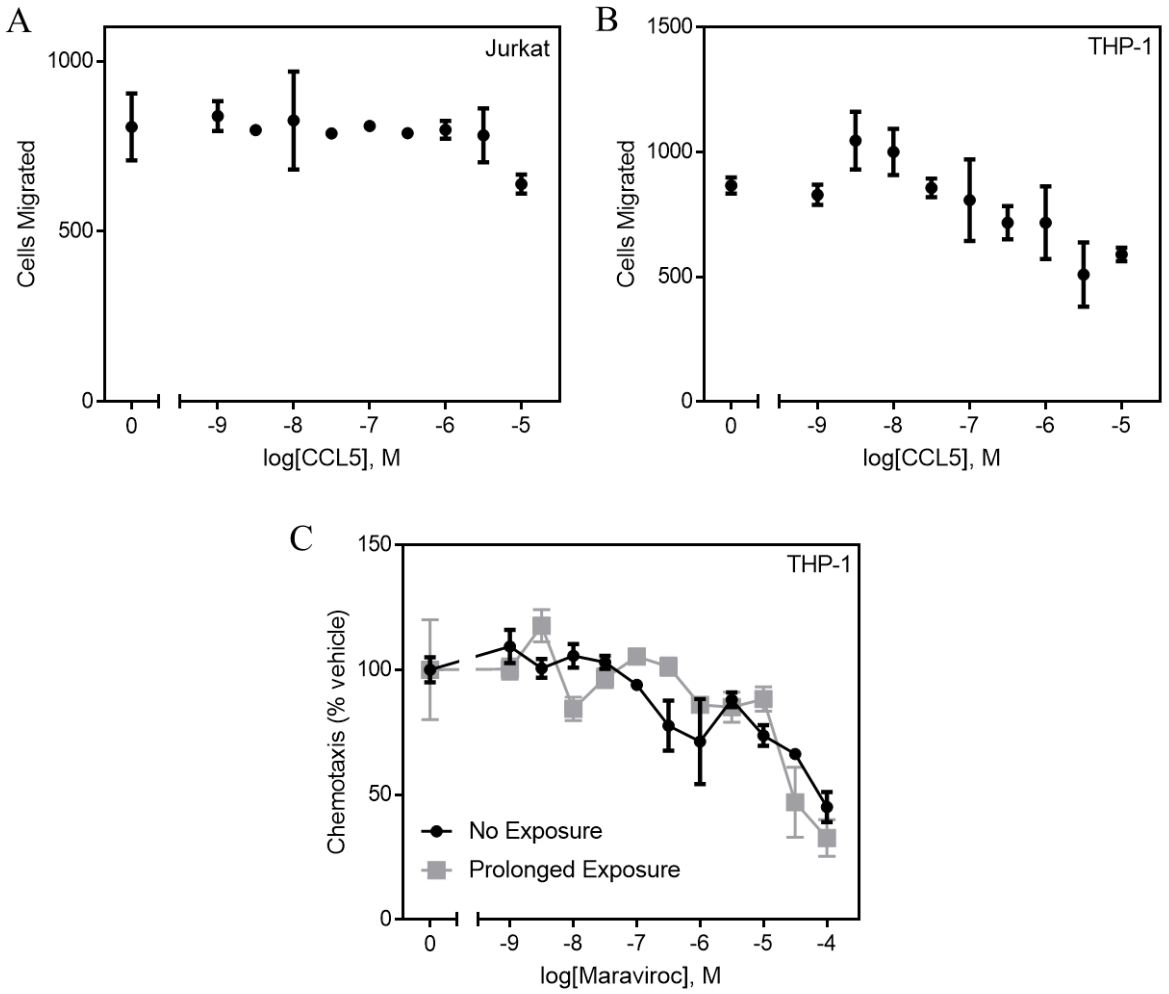

Figure 29: Tolerance to the CCR5 inhibitor Maraviroc is not observed in Jurkat or THP-1 cells.

(A) Optimisation of Jurkat cell chemotaxis to CCL5. (B) Optimisation of THP-1 cell chemotaxis to CCL5 (C) Ability of Maraviroc to inhibit CCL5-mediated chemotaxis before and after 72 hours of THP-1 cell exposure to Maraviroc.

IV. CHARACTERISATION OF CXCR4 BIASED ANTAGONISTS AND HOW THEY AVOID TOLERANCE

4.1 A transmembrane peptide derived from CXCR4 is a biased antagonist that avoids tolerance.

4.1.1 Tolerance does not develop to the CXCR4 peptide antagonist X4-2-6.

GPCRs are formed of a single polypeptide chain that forms a protein with a core made of 7 transmembrane alpha helices. As discussed previously, they are the target of more than 30% of all FDA approved drugs, the majority of which are small molecules [15]. However, in 1996, Hebert *et al.*, demonstrated that peptides derived from GPCR transmembrane helicies could acts as antagonists of receptor function [198]. This built on work from the 1980's and 1990's that showed expressing "portions" of GPCRs resulted in the formation of receptor-like units with partial function [198-207]. Studies by Jakubik & Weis showed that receptor fragments could directly associate with each other when coexpressed in cells [200]. Work on the muscarinic receptor demonstrated that the function of truncated GPCRs containing transmembrane domains I through V could be rescued with polypeptides derived from the extracellular or the intracellular loops of the receptor [203, 207]. Taken together these works led to the hypothesis that peptides derived from TM helicies acted as antagonists of GPCR by disrupting the receptor structure and thus inhibiting function.

In 1999, Tarasova *et al.*, showed that peptides derived from the TMs of CXCR4 and CCR5 could potently and specifically inhibit receptor signalling and HIV-1 cellular entry at concentrations as low as 200 nM [208]. By far the most efficacious of the CXCR4 inhibitors was a peptide derived from TM2 and ECL1 of the receptor. In an effort to develop nanoparticles that selectively delivery of therapeutic molecules to cells, further work on this peptide revealed it formed nanoparticles when modified with PEG [209]. The modified TM2-ECL1 peptide, called X4-2-6, could self-assemble into uniform nanoparticles and inhibit CXCR4 function *in vitro* and CXCR4-dependent tumour metastasis *in vivo* [209, 210].

Interestingly, while both AMD3100 and X4-2-6 abated metastasis and reduced tumour burden in mice, X4-2-6 prolonged survival, while AMD3100 did not [209, 211]. Additionally, upon treatment of both HeLa and A549 cells with rhodamine-labelled X4-2-6, the peptide was seen in the cytoplasm of cells by confocal microscopy, despite the peptide inhibiting CXCR4 mediated G protein processes [208, 209]. We hypothesized that while the potency of AMD3100 decreases over time, while X4-2-6 maintains its inhibitory activity by acting through a unique mechanism. We tested this hypothesis by comparing the potency of AMD3100 and X4-2-6 against CXCR4-mediated chemotaxis of Jurkat cells with no pre-treatment or pre-treated with the antagonists for 72 hours. We showed in cells with no pre-exposure to the drug, AMD3100 inhibited chemotaxis with an IC50 of 0.7 ± 0.2 μM. In agreement with previous results, cells pre-exposed to 1 μM AMD3100 for 72 hours became tolerant to the antagonist, resulting in a higher IC50 value of 3.2 ± 1.9 μM (figure 30a). More severe tolerance developed after escalating the dose of AMD3100 to 10 μM, raising the IC50 value to 4.7 ± 1.4 μM. Prolonged treatment with X4-2-6 did not lead to antagonist tolerance, exhibiting IC_{50}s of 1.0 ± 0.7 μM and 0.9 ± 0.8 μM after no pre-exposure or pre-exposure for 72 hours, respectively (figure 30a). Thus, prolonged exposure of cells to AMD3100 decreased the potency of the drug, consistent with antagonist tolerance, while no tolerance was observed with X4-2-6.

Previous reports correlated antagonist tolerance with elevated cell surface expression of the target receptor [50, 212]. We showed that inhibition of endocytosis resulted in the development of tolerance to AMD3100. Given that Tarasov *et al.* found rhodamine-labelled peptide in the cytoplasm of cells, and we did not see tolerance develop in cell treated with X4-2-6, we hypothesised that the peptide was a weak inhibitor of endocytosis. To test this hypothesis, we treated Jurkat cells with 30 nM CXCL12 in the presence of vehicle, 1 μM AMD3100 or 10 μM X4-2-6 and tracked CXCR4 endocytosis over 60 minutes by flow cytometry using the CXCR4 antibody 4G10. We observed over 50% reduction in CXCR4 surface staining after 5 minutes of

treatment with CXCL12 and vehicle (figure 30b). After 60 minutes, this increased to approximately 82%. As expected, treatment with AMD3100 completely inhibited CXCL12-mediated endocytosis and thus CXCR4 cell surface staining remained at 100% through 60 minutes (figure 30b). Conversely, cells treated with CXCL12 and X4-2-6 lost CXCR4 cell surface expression as a similar rate to CXCL12 and vehicle treated cells, suggesting X4-2-6 did not inhibit CXCR4 endocytosis (figure 30b). In agreement with these findings, treatment of cells with 1 μM AMD3100 for 72 hours increased cell surface CXCR4 but treatment 10 μM X4-2-6 for 72 hours had no effect on receptor cell surface expression (figure 30b). We subsequently determined that while AMD3100 inhibited CXCL12-mediated receptor internalization with an IC_{50} of 0.7 ± 0.1 μM, X4-2-6 neither efficiently inhibited (IC_{50} > 300 μM) nor promoted this process (figure 30c). Subsequently, when Jurkat cells were treated with 10 μM X4-2-6 for 72 hours, we saw no increase in CXCR4 cell surface expression as compared to AMD3100 (figure 30d).

4.1.2 X4-2-6 does not inhibit β-arrestin1/2 downstream of CXCR4

CXCR4 endocytosis is largely regulated by BA1/2 that are recruited to the receptor upon stimulation by CXCL12 [97, 213]. In Jurkat cells at rest, confocal microscopy showed that CXCR4 populated both the cell membrane and internal compartments, while BA2 was abundant in the cytoplasm (figure 31). Co-localization of CXCR4 and BA2 in intracellular punctate structures was observed in CXCL12-stimulated cells with M1 and M2 Manders co-localization coefficients of 0.96 and 0.95, respectively. X4-2-6 did not affect CXCL12-mediated CXCR4 co-localization with BA2 (M1 and M2 were 0.90 and 0.99, respectively) or receptor internalization. AMD3100 inhibited both CXCR4 endocytosis and co-localisation with BA2 (M1 and M2 were 0.11 and 0.26, respectively) (figure 31). Additionally, the effects of the antagonists on recruitment of BA2 to CXCR4 were monitored in a PRESTO-Tango assay where GAL4-VP16

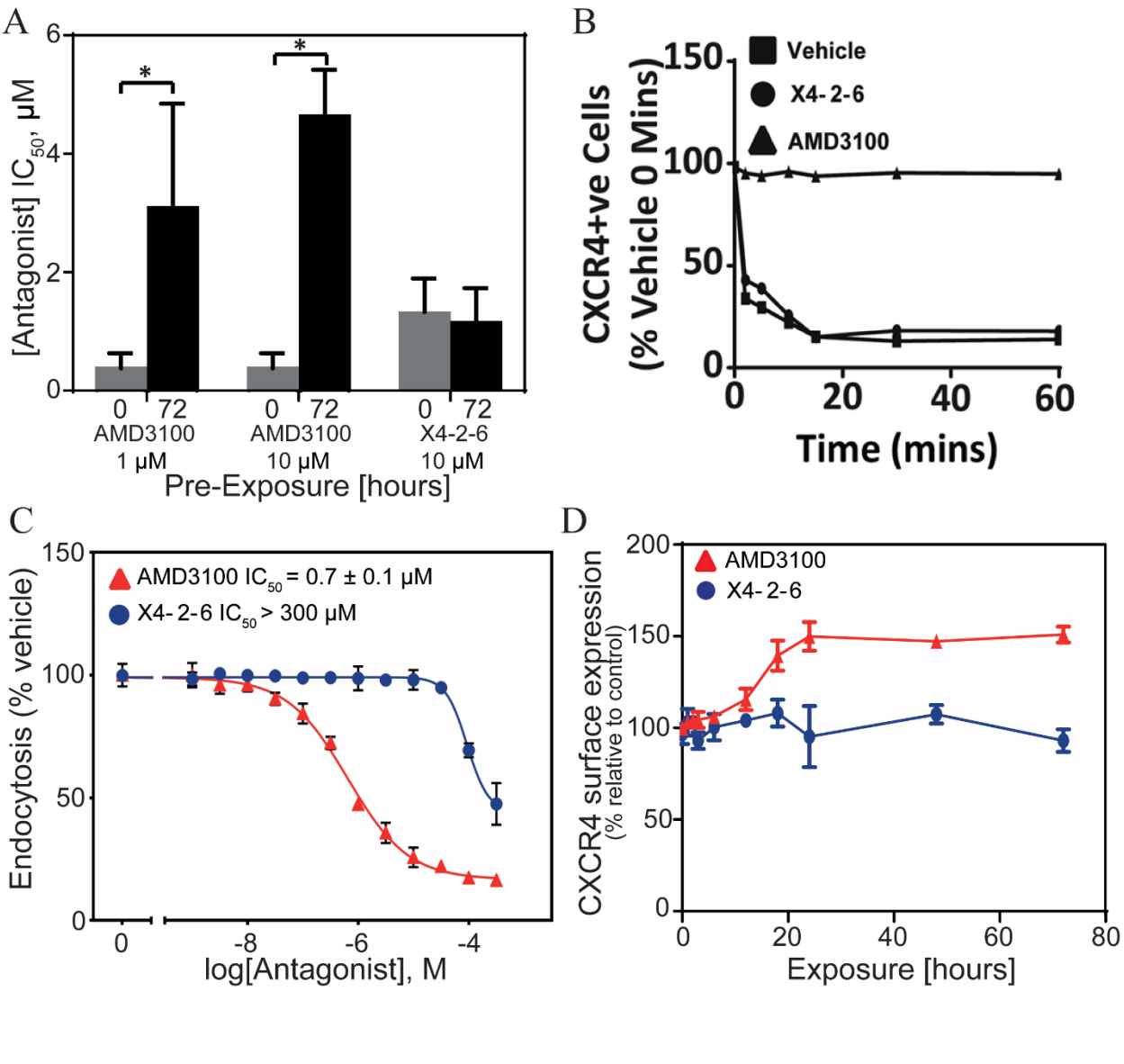

Figure 30: X4-2-6 does not inhibit endocytosis and does not develop tolerance

(A) IC50 values of CXCR4 antagonists in a CXCL12-stimulated chemotaxis assay using Jurkat cells before and after pre-exposure to 1 µM and 10 µM AMD3100 or 10 µM X4-2-6 for 72 hours (*$p < 0.001$ by Student's t test, n = 3 independent experiments, data are means ± SD). (B) Flow cytometry to determine CXCR4 cell surface expression in Jurkat cells treated with 1 µM AMD3100 (□) or 10 µM X4-2-6 (□) in the presence of 30 nM CXLC12 over 60 minutes. (C) IC_{50} values of AMD3100 and X4-2-6 for CXCL12-mediated endocytosis. (D) Flow cytometry to determine CXCR4 cell surface expression in Jurkat cells treated with 1 µM AMD3100 (□) or 10 µM X4-2-6 (□) over 72 hours (data are means ± SD, n = 3 replicates per data point).

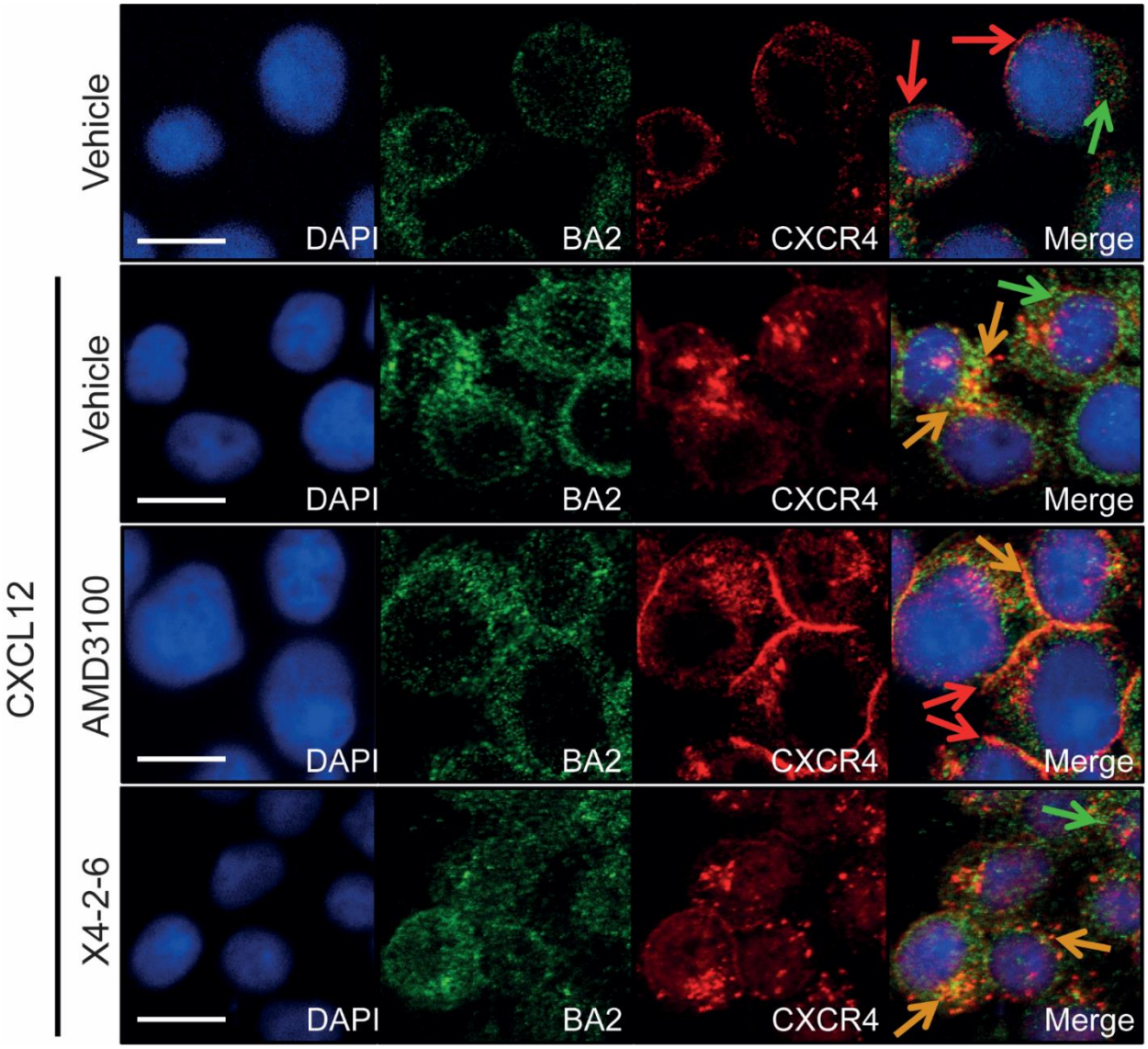

Figure 31: β-arrestin2 recruitment to CXCR4 is not significantly affected by X4-2-6.

Immunostaining for CXCR4 and BA2 in untreated (top row) or CXCL12-stimulated (100 nM, 30 minutes) Jurkat cells pretreated with vehicle (second row), 1 µM AMD3100 (third row) or 10 µM X4-2-6 (bottom row) for observation of co-localisation by confocal microscopy. Scale bar = 20 µm.

attached to the receptor is released by the recruited BA2-TEV protease fusion and activates transcription of the β-lactamase reporter gene [140]. CXCL12 activated BA2 recruitment with an EC50 of 1.4 ± 0.9 nM (figure 32a). This was unaffected by X4-2-6, while AMD3100 increased the EC50 to 5037 ± 2123 nM (figure 32a). Bioluminescence resonance energy transfer (BRET) between CXCR4 and BA2 corroborated that X4-2-6 did not inhibit BA2 recruitment (figure 32b).

To enhance BA1/2 recruitment and receptor endocytosis, serine residues in the CXCR4 C-terminus are phosphorylated by several kinases, such as GRKs, Protein kinase C (PKC) and proviral integration site Moloney murine leukaemia virus-1 kinase (PIM1) [91, 214]. To investigate the effects of AMD3100 and X4-2-6 on CXCL12-mediated CXCR4 phosphorylation, we immunoblotted for phosphorylation of serine residues 324/325 and 339 in the C-terminus of CXCR4 [215]. X4-2-6 did not reduce phosphorylation of Ser324/325 or Ser339, while AMD3100 inhibited it (figure 33). Thus, X4-2-6 was distinct from AMD3100 in its inability to affect receptor phosphorylation, BA2 recruitment, endocytosis of CXCR4, and its level on the plasma membrane, a requirement for avoiding antagonist tolerance.

4.1.3 X4-2-6 inhibits ERK1/2 activation downstream of CXCR4

Inefficient inhibition of BA1/2 may suggest poor activity of X4-2-6 against CXCR4, although it has previously been shown to bind and inhibit this receptor [192, 208, 216]. We therefore investigated the effects of X4-2-6 on ERK1/2 phosphorylation (pERK1/2) at threonine residue 202 and tyrosine residue 204, a process that involves both G protein signalling and BA1/2 regulation [97, 217, 218]. As described previously, pERK1/2 peaked at five minutes of treatment with the CXCL12 (figure 34) [94]. Phosphorylation of ERK1/2 continued for up to thirty minutes after the initial treatment with CXCL12. Knockdown of BA1/2 in Jurkat cells increased both early and late pERK1/2 compared to Jurkat cells electroporated with scrambled

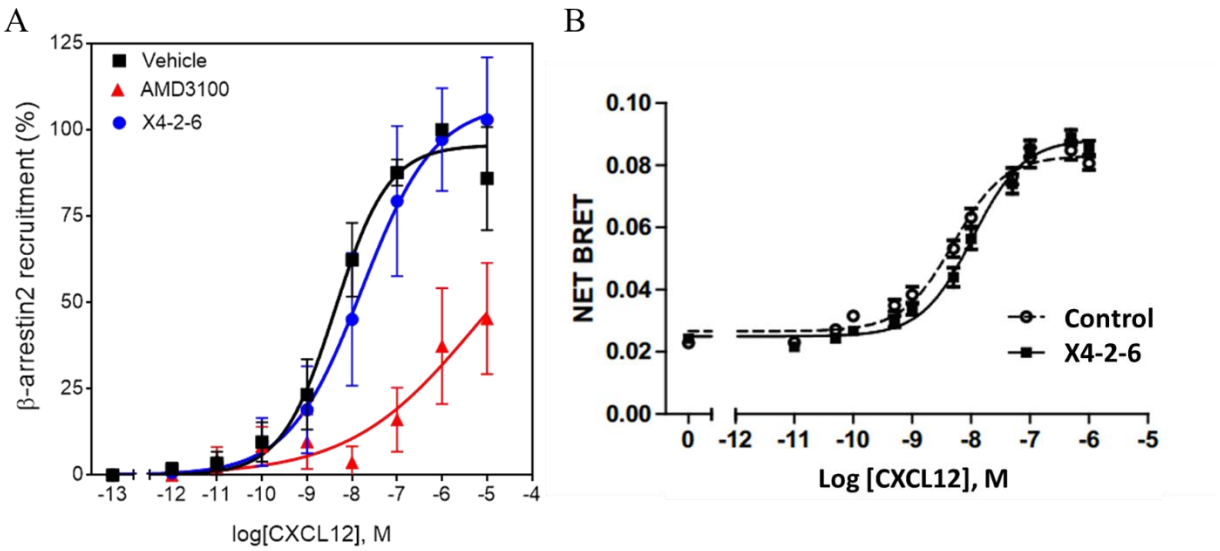

Figure 32: X4-2-6 does not inhibit β-arrestin2 recruitment to CXCR4.

(A) Recruitment of BA1/2 to CXCR4 after treatment with increasing concentrations of CXCL12 in the presence of vehicle (■), 1 µM AMD3100 (▲) or 10 µM X4-2-6 (●) was measured by PRESTO-Tango assay (data are means ± SD, n = 6 replicates per data point). (B) **.** HEK293E cells transiently coexpressing BA2-GFP10 and CXCR4-RlucIII were incubated with indicated concentrations of ligand with or without 10 µM X4-2-6 and resulting BRET measured after 10 min at room temperature. Data are mean of three independent experiments performed in triplicate ± S.E.M. CXCL12 plus vehicle control (○); CXCL12 + 10 µM X4-2-6 (■).

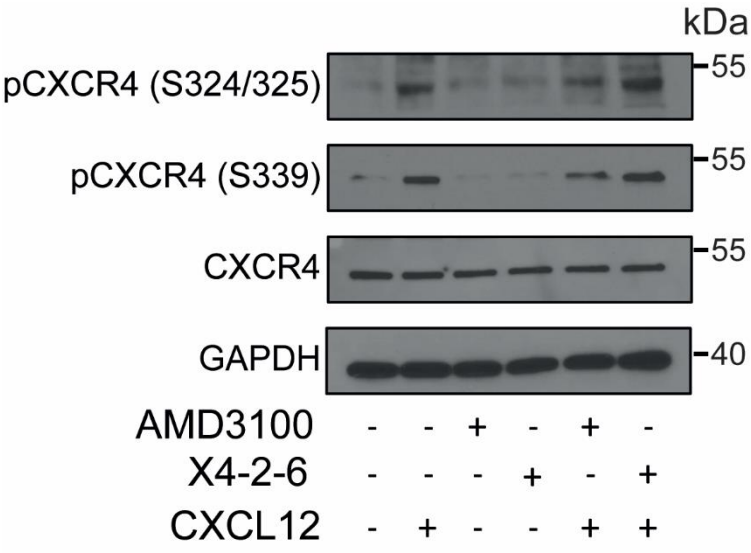

Figure 33: X4-2-6 does not inhibit CXCR4 phosphorylation.

Western blotting analysis of CXCL12-induced (30 nM) phosphorylation of CXCR4 Ser324/325 and Ser339 in Jurkat cells in the presence of vehicle, 1 µM AMD3100 or 10 µM X4-2-6.

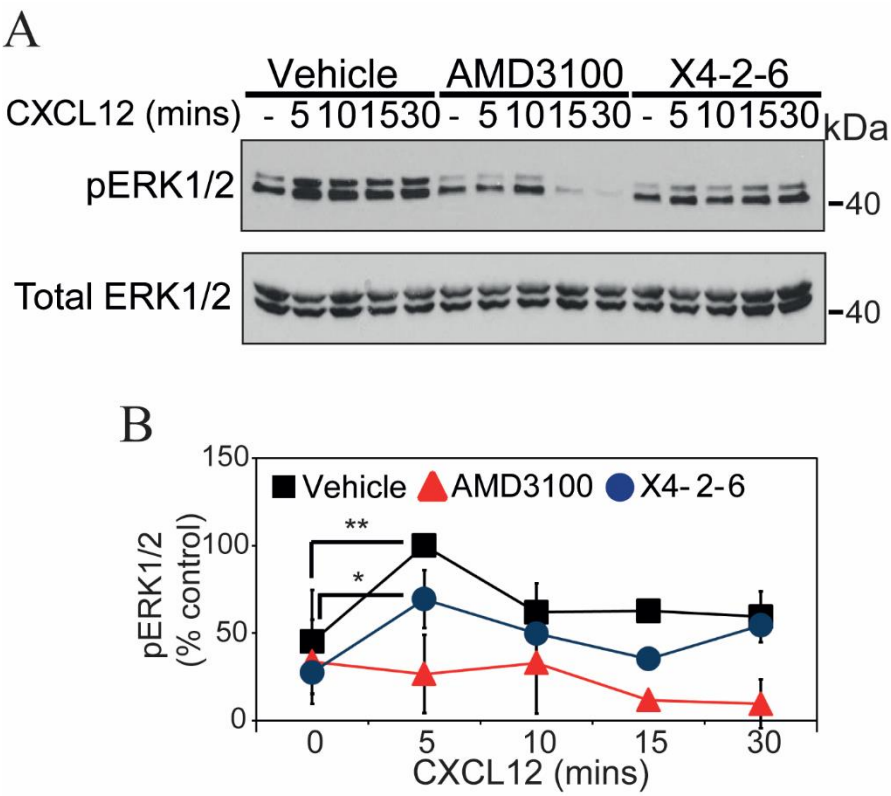

Figure 34: X4-2-6 inhibits Erk1/2 phosphorylation downstream of CXCR4.

(A) Western blotting analysis of CXCL12-induced (30 nM) phosphorylation of ERK1/2 at Thr^{202}/Tyr^{204} in Jurkat cells treated with vehicle, 1 µM AMD3100 or 10 µM X4-2-6. (B) Quantification of the relative abundance of pERK1/2 normalized to that of total ERK1/2 (*P < 0.05 and **P < 0.01 by ANOVA with post hoc Tukey test, data are means ± SD from 3 independent experiments).

siRNA controls (figure 35a, b). The inhibitor of BA1/2 binding to the β-adaptin subunit of AP2, Barbadin also increased early and late pERK1/2 versus vehicle treated cells (figure 35) [219]. A similar result was observed in mouse embryonic fibroblast (MEF) cells lacking BA1/2 expression but not in wild-type MEFs (figure 35c) [220]. This suggested that phosphorylation of ERK1/2 downstream of CXCR4 was due to G protein signalling while BA1/2 played a role in desensitization and attenuation of G protein mediated signalling. While X4-2-6 attenuated early pERK1/2, regulation of pERK1/2 was sustained, with a reduction in the pERK1/2 band intensity at 30 minutes compared to the five-minute time point, in a manner consistent with the vehicle control (figure 35). AMD3100 inhibited both early and late pERK1/2 in Jurkat cells stimulated with CXCL12 (figure 35). Thus, X4-2-6 inhibited G protein-mediated pERK1/2.

4.1.3 X4-2-6 is a biased antagonist that specifically inhibits G protein activation downstream of CXCR4

Because X4-2-6 inhibited chemotaxis, a process associated with G protein signalling, but did not affect BA1/2 recruitment, we reasoned that X4-2-6 might act as a biased antagonist of CXCR4. Amplification of signalling leading to pERK1/2 can potentially obscure the analysis of bias in X4-2-6. To study the direct effect of the antagonist on G proteins, Gαi-GTP was immunoprecipitated and analyzed by immunoblotting in lysates of Jurkat cells treated with CXCL12 in the presence of either vehicle, 1 μM AMD3100 or 1 μM X4-2-6. CXCL12 in the presence of vehicle increased Gαi-GTP by 58 ± 21% over the unstimulated control (figure 36a, b). AMD3100 and X4-2-6 reduced Gαi-GTP in CXCL12-treated cells by 80 ± 8% and 83 ± 12%, respectively (figure 36a, b). To assess the effect of the antagonists on the function of Gαi-GTP, we measured cAMP in CXCL12-stimulated Jurkat cells in the presence or absence of either AMD3100 or X4-2-6. Forskolin, an adenylate cyclase agonist [169], increased intracellular cAMP over the vehicle control. Treatment with CXCL12 attenuated this increase, albeit only slightly (figure 36c). Both

AMD3100 and X4-2-6 returned cAMP to the levels observed in forskolin only treated cells (figure 36c). Taken together with data showing X4-2-6 inhibited CXCL12-mediated chemotaxis, X4-2-6 like AMD3100 inhibited activation and function of Gαi downstream of CXCR4. We showed that the IC_{50} of X4-2-6 as approximately 1 μM for inhibition of CXCL12 chemotaxis (figure 36d), confirming that while AMD3100 is an unbiased antagonist of CXCR4, X4-2-6 is a biased antagonist, inhibiting G protein signalling but not BA1/2 recruitment and receptor endocytosis.

To confirm that biased antagonism is due to specific activity of X4-2-6, we compared the effects of the peptide against CXCR4 and CCR2-mediated Ca^{2+} flux, initiated by G proteins through phospholipase C [221]. CXCR4 and CCR2 chemokine receptors share high sequence identity of 63% in the region corresponding to X4-2-6. X4-2-6 inhibited Ca^{2+} flux induced by CXCL12 (figure 36e) but not by CCL2 (figure 36f) in THP-1 human monocytic leukaemia cells, which express both CXCR4 and CCR2, demonstrating specificity of the peptide for CXCR4. X4-2-6 also inhibited CXCL12-chemotaxis in the same cell line [222]. We also tested the ability of another TM2 peptide derived from the CCR3, named R3-2-1, receptor to inhibit CXCL12 mediated chemotaxis [223]. We found that R3-2-1 no effect on chemotaxis up to concentrations exceeding 10 μM, although very high concentrations did begin to inhibit cell migration (figure 37). This data suggests that TM peptides can specifically inhibit the receptor from which they are derived.

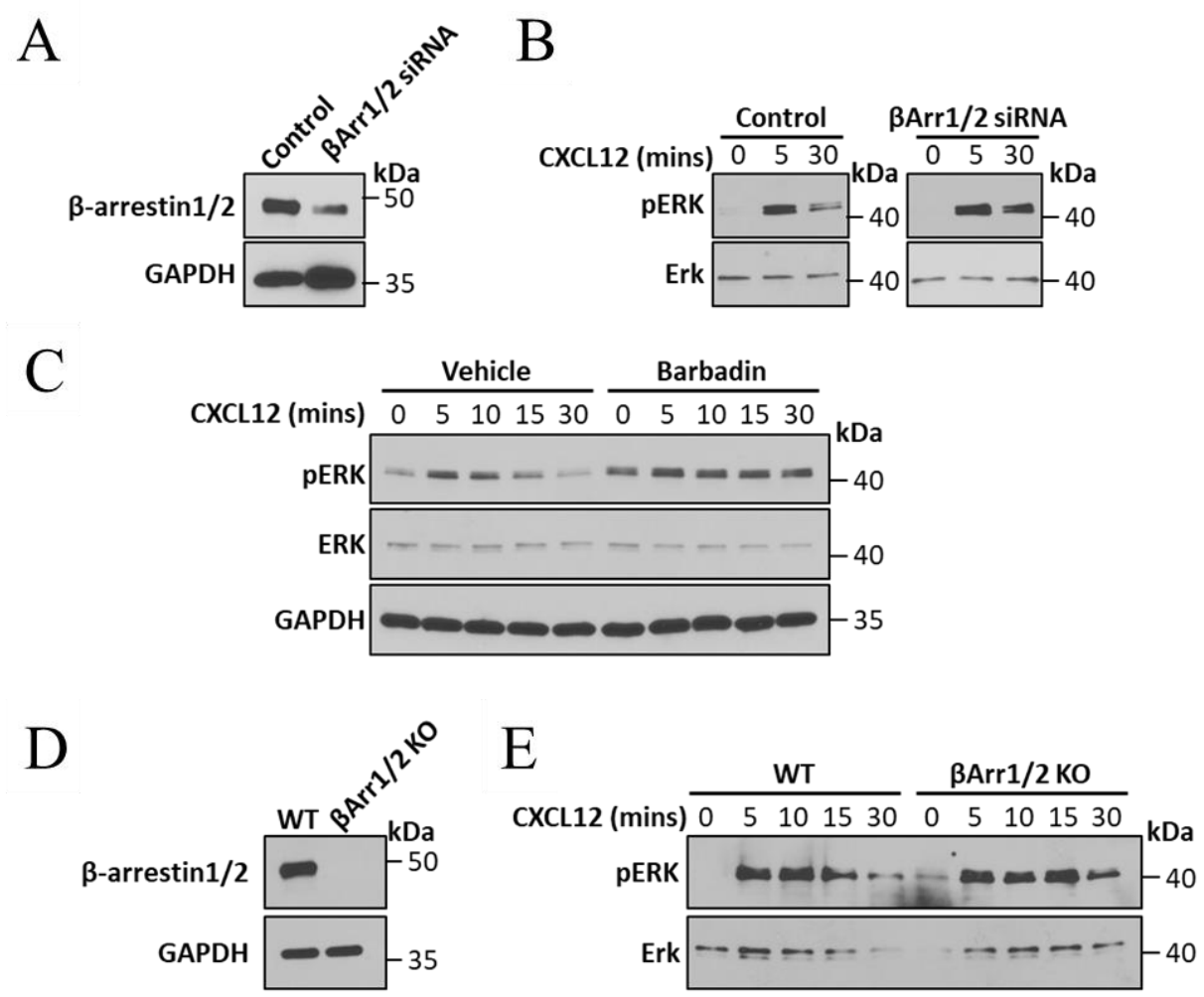

Figure 35: β-arrestin1/2 regulate ERK phosphorylation downstream of CXCR4.

(A) Expression of BA1/2 in Jurkat cells electroporated with control or BA1 and 2 siRNA. The monoclonal antibody D24H9 preferentially recognizes BA1, leading to the appearance of a single band for BA1/2 (B) ERK1/2 phosphorylation in Jurkat cells electroporated with BA1 and 2 siRNA was enhanced compared to those containing control siRNA, in response to 30 nM CXCL12 treatment over 30 minutes. (C) Inhibition of BA1/2 in Jurkat cells with 30 μM Barbadin resulted in enhanced CXCL12-mediated ERK1/2 phosphorylation over 30 minutes compared to vehicle treated cells. (D) Expression of BA1 and 2 in WT and BA1/2 knocked-out MEF cells. (E) ERK1/2 phosphorylation in BA1/2 knocked-out MEF cells was enhanced compared to WT-MEFs, in response to 30 nM CXCL12 treatment over 30 minutes. In B, C, and E, two bands for ERK1/2 are visible but not clearly resolved due to low resolution of the gels.

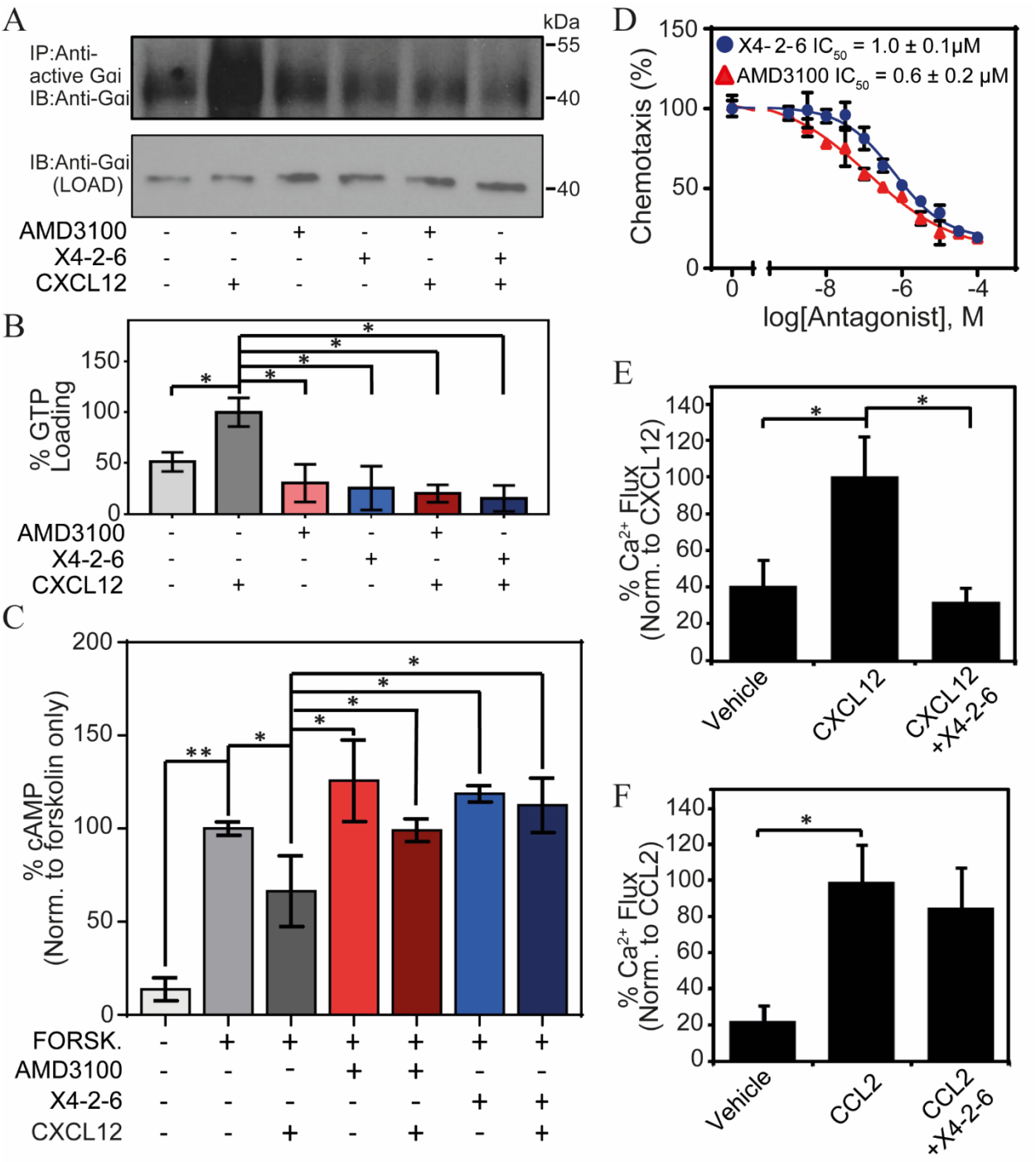

Figure 36: X4-2-6 specifically inhibits G protein activation downstream of CXCR4.

(A) Western blotting analysis for GTP-loading of Gαi in Jurkat cells stimulated with 30 nM CXCL12 and pretreated with either vehicle, AMD3100 (1 μM) or X4-2-6 (10 μM). Blots are representative of 3 independent experiments. (B) Densitometric analysis of 3 independent experiments described in A (*$p < 0.01$ by one way ANOVA, data are means ± SD, n = 3 independent experiments). (C) ELSIA analysis of intracellular concentrations of cAMP in Jurkat

cells treated as indicated (*$p < 0.05$, **$p < 0.005$, by one way ANOVA, data are means ± SD, n = 6 replicates per condition). (D) Inhibition of CXCL12-mediated (30 nM) Jurkat cell chemotaxis by AMD3100 or X4-2-6 (data are means ± SD, n = 3 replicates at each data point). (E) Measurement of CXCL12-mediated Ca^{2+} flux in THP-1 cells and treated with vehicle or X4-2-6 (50 μM) (*$p \leq 5 \times 10^{-8}$ by one way ANOVA, n = 12, data are mean ± SD). (F) Measurement of CCL2-mediated Ca^{2+} flux in THP-1 cells and treated with vehicle or X4-2-6 (50 μM) (*$p \leq 5 \times 10^{-8}$ by one way ANOVA, n = 12, data are means ± SD). Data in (A) through (D) representative of at least 3 independent experiments.

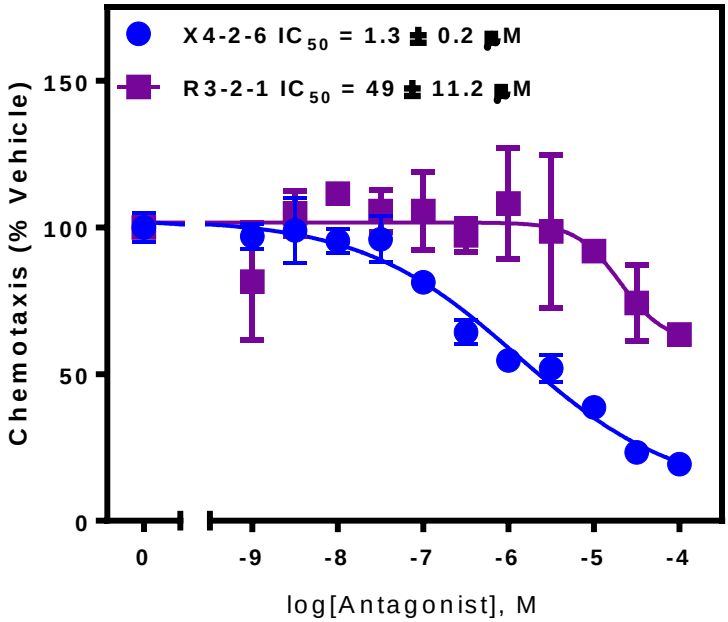

Figure 37: A CCR3 derived peptide does not inhibit CXCL12-mediated chemotaxis.

Dose response curve for Jurkat cells stimulated to migrate towards 30 nM CXCL12 in the presence of X4-2-6 or R3-2-1.

4.1.4 Neither X4-2-6 nor AMD3100 are cytotoxic at their chemotaxis IC50 concentrations over 72 hours.

One mechanism by which X4-2-6 may appear to avoid tolerance while AMD3100 does not, may be through differences in the cytotoxicity of the antagonists. If X4-2-6 were more cytotoxic than AMD3100, this could obscure the development of tolerance observed by counting cells in chemotaxis assays. To test the cytotoxic effects of X4-2-6 and AMD3100 we performed MTT assays to assess the dose-dependent cytotoxicity of both antagonists, and to assess the inhibition of Jurkat cell growth by the drugs when cells are treated every 72 hours. We found that neither X4-2-6 nor AMD3100 were cytotoxic up to 10 µM (figure 38a). We also found that neither antagonist significantly affected cell growth in cells dosed with each drug every 12 hours for 72 hours (figure 38b).

4.1.5 X4-2-6 is not a competitive antagonist of CXCR4.

As previously described, competitive inhibitor is one that increases the K_m of a substrate without affecting the V_{max} [153]. To investigate the mechanism by which X4-2-6 inhibits CXCR4, we performed various functional assay in Jurkat cells, using increasing concentrations of CXCL12 to try to outcompete the inhibitory activity of a fixed concentration (10 µM) of X4-2-6. We first investigated the ability of X4-2-6 to inhibit activation of Gαi after stimulation of Jurkat cells with increasing concentrations of CXCL12. To do this, we performed immunoblotting using an antibody that recognises the GTP-loaded form of Gαi. In the presence of vehicle, CXCL12 induced an increase in activation of Gαi, peaking at a CXCL12 concentration of 1 nM (figure 39). Cells treated with X4-2-6 showed a total reduction in Gαi activity (figure 39a).

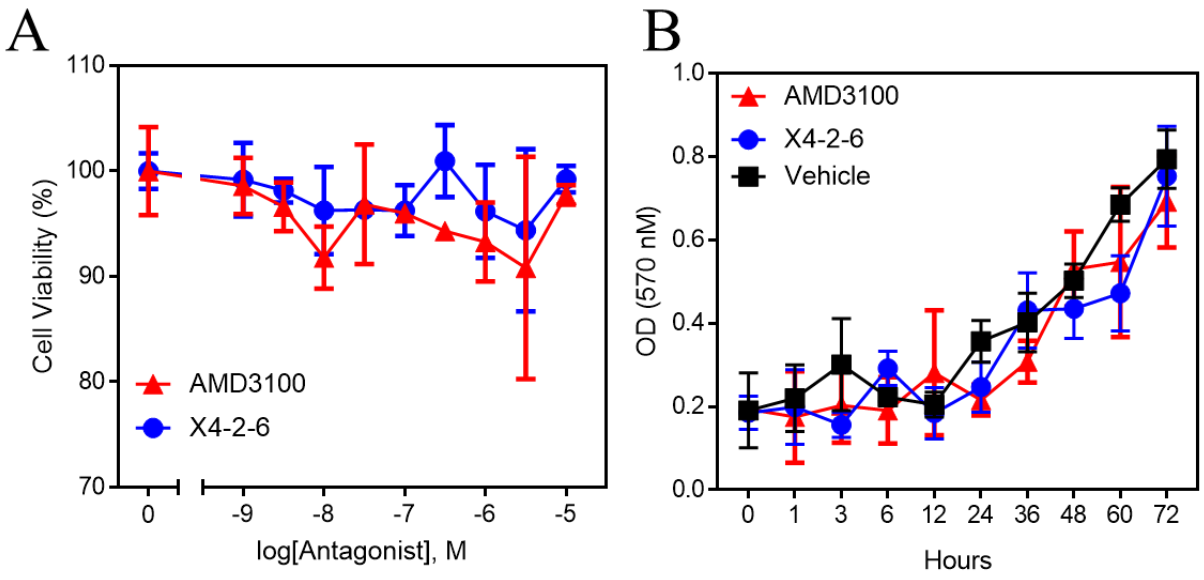

Figure 38: Neither X4-2-6 nor AMD3100 are cytotoxic above IC50 concentrations.

MTT assays of Jurkat cells treated with (A) increasing concentrations of AMD3100 or X4-2-6 and (B) treated with vehicle, 1 µM AMD3100 or 10 µM X4-2-6 every 12 hours for 72 hours.

Next, we investigated whether increasing the concentration of CXCL12 could outcompete X4-2-6 in a functional, chemotaxis assay. To test this, we performed a chemotaxis assay with increasing concentrations of CXCL12 and a single concentration (10 μM) of X4-2-6. The maximum chemotactic response of Jurkat cells occurred at approximately 30 nM CXLC12 (figure 39b). Unlike chemotaxis in the presence of 1 μM AMD3100 where similar numbers of cells migrated but the maximum response of cells shifted to ~100 nM, treatment with X4-2-6 reduced the maximum number of cells migrating but did not shift the maximum concentration of chemokine. This suggests that increasing concentrations of CXCL12 could not outcompete the inhibitory effects of X4-2-6 and that the peptide is not a competitive inhibitor.

Previous studies showed that the peptide binds directly to CXCR4 [224]. To elucidate where the peptide binds, we mutated Asn 119 in the CXCR4 TM3 to serine to generate a constitutively active receptor [147]. Mutation of asparagine Asn119$^{3.35}$ to Ser creates a constitutively active CXCR4 because N119 is a key residue in which mutations have been shown to alter GPCR activity as a function of the size of the amino acid side chain [167, 225, 226]. The constitutively active CXCR4 adopts the active conformation. We hypothesised that an antagonist that binds to the orthosteric site would have no effect on the activity of the constitutively active receptor, because the binding of a ligand is not required for activity of this receptor. However, an allosteric antagonist or an inverse agonist would still elicit its effects on the active receptor. To test where X4-2-6 binds, we transfected HEK293T cells with pcDNA3.1 containing WT-CXCR4 or N119S-CXCR4 and assessed the ability of AMD3100 and X4-2-6 to inhibit GTP-loading. HEK239 cells transfected with WT-CXCR4 increased Gαi-GTP loading in response to CXCL12 treatment. Cells transfected with N119S-CXCR4 all increased Gαi-GTP loading, while treatment with AMD3100 inhibited this but X4-2-6 did not (figure 40). This suggested that X4-2-6 does not bind to the orthosteric site of the receptor.

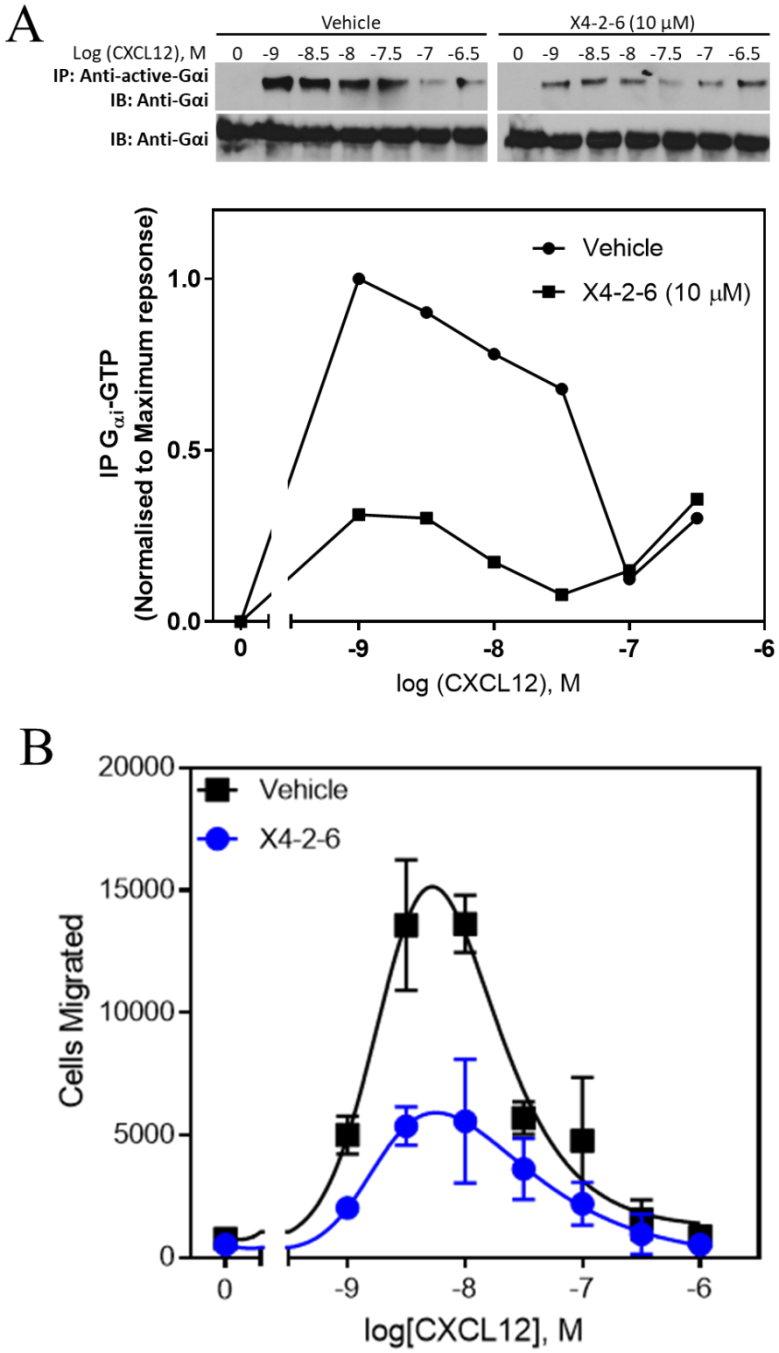

Figure 39: X4-2-6 is not a competitive inhibitor of CXCR4.

(A) Western blotting analysis for GTP-loading of Gαi in Jurkat cells stimulated with increasing amounts of CXCL12 and either vehicle or X4-2-6 (10 µM). Densitometric analysis shown below. (B) Chemotaxis assay in Jurkat cells stimulated with increasing concentrations of CXCL12 and either vehicle or 10 µM X4-2-6.

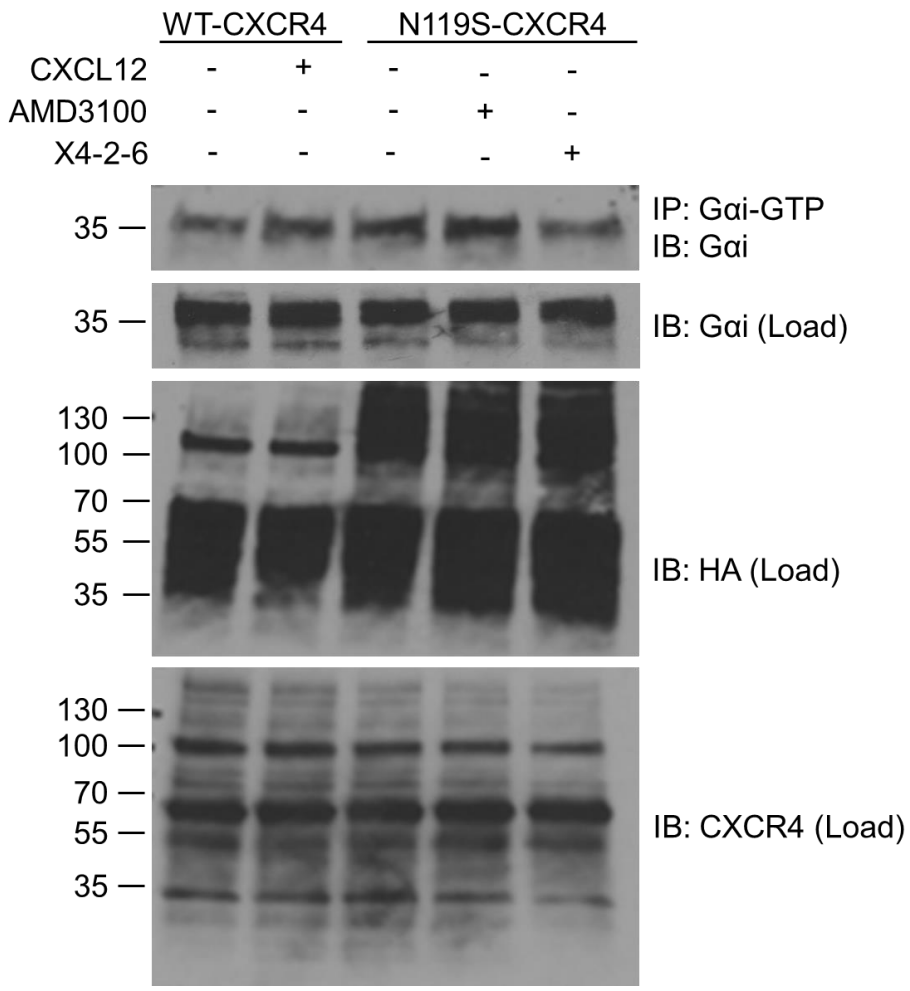

Figure 40: X4-2-6 can inhibit Gαi activation downstream of a constitutively active mutant of CXCR4.

Western blotting analysis for GTP-loading of Gαi in HEK293 cells transfected with WT or N119S HA-CXCR4 and stimulated with CXCL12, 1 µM AMD3100 or 10 µM X4-2-6.

To further investigate the peptide binding site, we performed a flow cytometry experiment to determine the ability of X4-2-6 to inhibit the binding of two CXCR4 antibodies with distinct epitope. The CXCR4 antibody 12G5 is a conformational antibody that binds to the ECL2 of CXCR4, while 4G10 binds to the receptor N-terminus [158, 189]. AMD3100 inhibited the binding of the 12G5 antibody as previously reported but had no effect on the binding of 4G10 (figure 41). X4-2-6 did not affect the binding of either antibody. This may be explained by the peptide having a binding site distinct from the antibodies, or the antibodies having a greater affinity for the receptor than the peptide. However, taken together with the previous data, this suggested that X4-2-6 acts as an allosteric antagonist of CXCR4.

4.1.5 X4-2-6 forms a ternary complex with CXCR4 and CXCL12 to mediated biased antagonism.

Because X4-2-6 is derived from CXCR4, the specificity and biased antagonism might arise from the interaction of X4-2-6 with CXCL12. The tertiary structure of CXCL12 is similar to other chemokines with a flexible N-terminus and an extended N-loop consisting of residues up to Arg20 [139]. This is connected via a 310 helix to the "globular portion" of the chemokine, which consists of a three-stranded β-sheet. The CXCL12 N-terminus is crucial for binding to and activation of CXCR4, while the globular portion of the chemokine interacts with the receptor N-terminus [75, 151, 183, 190-194]. We observed significant signal attenuation in HSQC NMR spectra of 15N-labeled CXCL12 in the presence of X4-2-6 for residues Phe 14, Ser 16 and His 17 in the N-loop of the chemokine. This indicated intermediate exchange between the bound and free N-loop of the chemokine and X4-2-6 (figure 42a, b, c). This finding was further corroborated by tryptophan fluorescence experiments showing a significant change in tryptophan fluorescence maximum and intensity upon X4-2-6 binding to CXCL12 [222]. Since the CXCL12 N-terminus is crucial for binding to and activation of CXCR4 [75, 151, 183, 190-192], signals corresponding to the N-

terminal residues of CXCL12 (e.g. Ser 4 and Leu 5) were attenuated upon addition of CXCR4 expressing cell membranes (figure 42d, e, f). Residues in the globular domain of the chemokine (Ala 35, Asn 46 and Lys 54) were also affected, suggesting a larger interaction interface between the chemokine and the receptor compared to CXCL12 and X4-2-6. CXCR4-containing membranes, together with X4-2-6, induced significant signal attenuation of residues within the β1 and β2 strands of CXCL12 (figure 42g, h, i). Addition of CXCR4 membranes together with X4-2-6 did not recapitulate the chemokine spectra with CXCR4 or peptide alone, suggesting that both the receptor and the peptide bind the chemokine simultaneously. While Leu^5 of CXCL12 was undetectable with CXCR4 alone, a weak signal was observed with the combination of the membrane and peptide. This suggests that, by forming a ternary complex with the chemokine and receptor, X4-2-6 partially liberated the extreme N-terminal portion of CXCL12. In contrast, AMD3100 decreased the affinity of the entire N-terminus of CXCL12 for CXCR4, as evidenced by fast exchange between the free and bound species for N-terminal Ser 4, Ser 6-Arg 8, Arg 12, Ser 16, and His 17, as well as Lys 27, Val 39, Lys 56, and Leu 66 in the globular portion of the chemokine (Appendix A, figure 4), as previously reported [151]. Our results agreed with the notion that the extreme N-terminal region of the chemokine is more critical for chemotaxis than for receptor endocytosis [74] and provided a previously unknown mechanism of biased antagonism. Moreover, our findings explained how specificity of transmembrane peptides for their targets can be enhanced by additional interactions with receptor ligands.

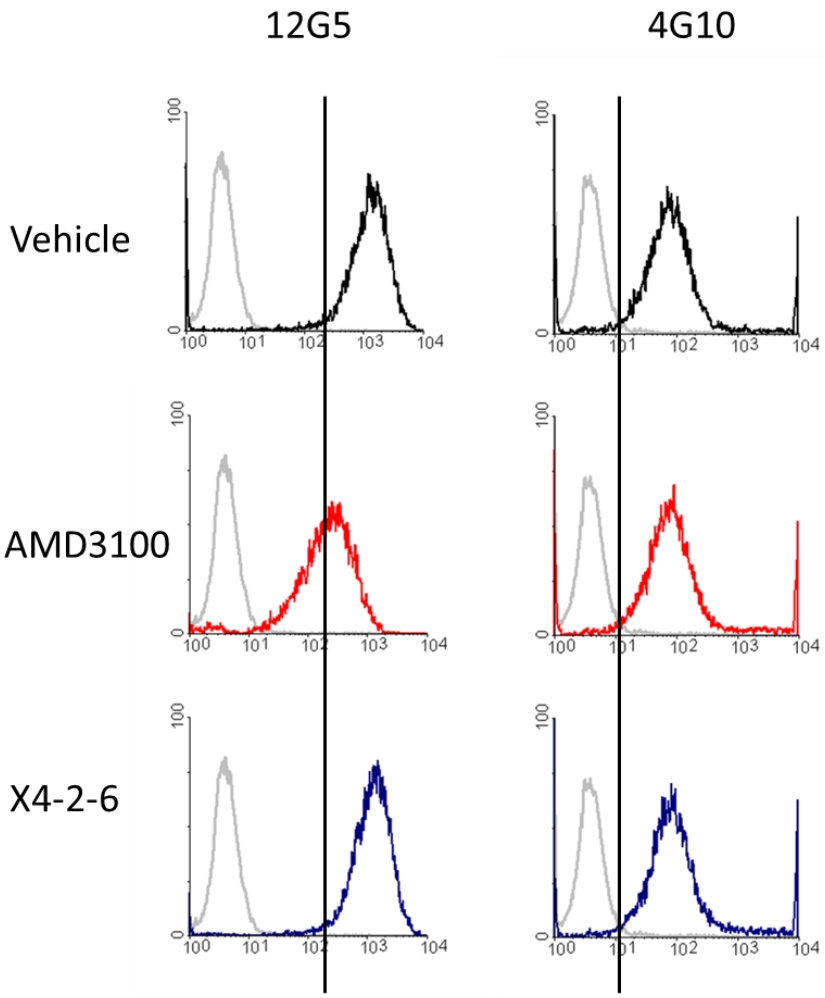

Figure 41: AMD3100 but not X4-2-6, inhibits binding of two CXCR4 monoclonal antibodies.

Jurkat cells were stained for CXCR4 using either 12G5 (ECL2 epitope) or 4G10 (N-terminal epitope) CXCR4 monoclonal antibodies in the presence of vehicle, 1 µM AMD3100 or 10 µM X4-2-6.

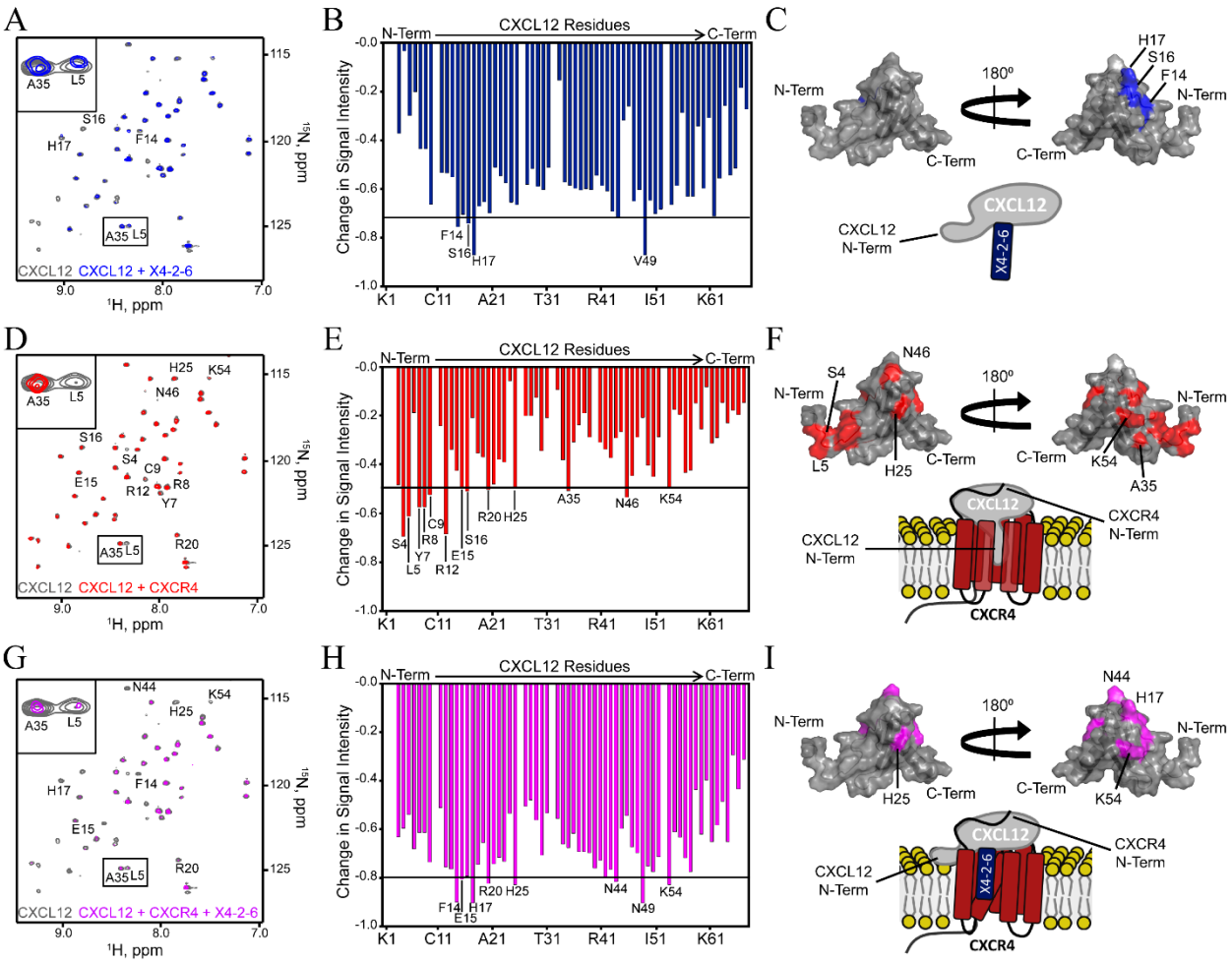

Figure 42: X4-2-6 forms a ternary complex with CXCL12 and CXCR4 to function as a biased antagonist.

(A) Superimposition of ^{1}H-^{15}N HSQC NMR spectra of 50 µM CXCL12 (grey) and 50 µM CXCL12 in the presence of 10 µM X4-2-6 (blue). (B) Changes in CXCL12 HSQC signal intensity caused by the addition of X4-2-6 are graphed and significant changes annotated. (C) These residues are mapped onto the NMR structure of CXCL12 (PBD ID: 2KEE). A cartoon describes the model of the interaction mechanism between the N-loop of CXCL12 and X4-2-6. (D) Superimposition of ^{1}H-^{15}N HSQC NMR spectra of 50 µM CXCL12 (grey) and 50 µM CXCL12 plus 20 µg of membrane preparations containing CXCR4 (red). (E) Changes in signal intensity of CXCL12 residues caused by the addition of CXCR4 are graphed and significant changes annotated. (F) These residues are mapped onto the structure of CXCL12. A cartoon describes the model of the interaction mechanism, involving insertion of the chemokine N-terminus into the

receptor transmembrane helical bundle. (G) Superimposition of ^{1}H-^{15}N HSQC NMR spectra of 50 µM CXCL12 (grey) and 50 µM CXCL12 plus 20 µg CXCR4 membrane preparation and 10 µM X4-2-6 (magenta). (H) Changes in CXCL12 signal intensity caused by the addition of CXCR4 plus X4-2-6 are graphed and significant changes annotated. (I) The most significant changes are mapped onto the NMR structure of CXCL12. We propose a model where X4-2-6 binds CXCR4 and CXCL12 to partially inhibit the binding of the extreme N-terminus of the chemokine to the receptor.

4.2 A small molecule biased antagonist of CXCR4 also avoids the development of tolerance.

We investigated if the avoidance of antagonist tolerance is a unique property of X4-2-6 or if tolerance can be generally evaded by biased antagonists. A small molecule biased antagonist of CXCR4, SEN071, unrelated to X4-2-6 was previously described [227]. Here, we showed that SEN071 inhibited chemotaxis of Jurkat cells to CXCL12 with an IC_{50} of 4.4 ± 0.3 μM, while permitting CXCR4 endocytosis at the same concentration (figure 43a). Like X4-2-6, SEN071 exhibited similar IC_{50}s for CXCL12-induced chemotaxis with no pre-exposure or after 72 hours of pre-exposure to the compound (figure 43b) and did not increase CXCR4 on the cell surface (figure 43a). Thus, both peptide and small molecule biased antagonists avoided accumulation of the receptor on the cell surface and antagonist tolerance after prolonged exposure.

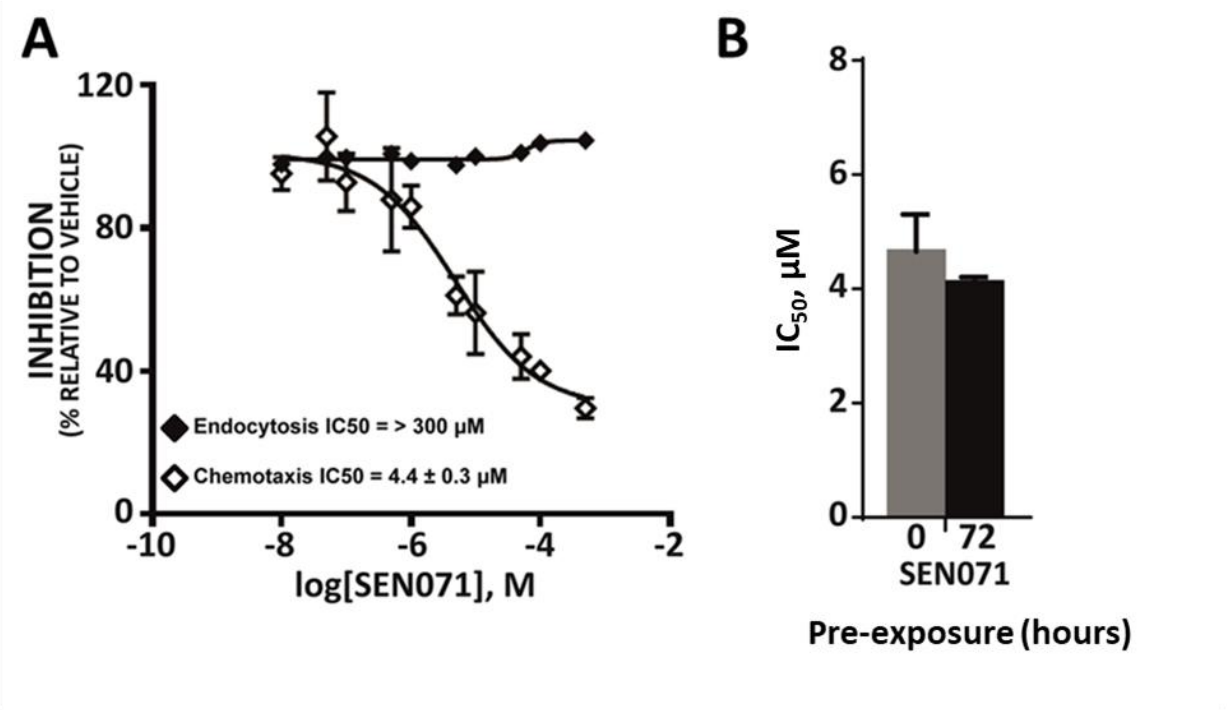

Figure 43: A small molecule SEN071 is a CXCR4 biased antagonist that avoids antagonist tolerance.

(A) The small molecule SEN071, a CXCR4 biased antagonist [227], inhibits CXCL12-induced chemotaxis with an IC_{50} of 4.4 ± 0.3 µM (◇) but not CXCL12-induced endocytosis, measured by flow cytometry (◆). (B) Pre-exposure of Jurkat cells to 4 µM SEN071 for 72 hours did not significantly change the IC_{50} for CXCL12-induced chemotaxis of the biased antagonist (no pre-exposure IC_{50} = 4.8 ± 1.0 µM, 72 hours pre-exposure IC_{50} = 4.1 ± 0.2 µM).

DISCUSSION AND CONCLUSIONS

GPCRs are the target of most FDA approved drugs [14, 15]. Understanding their pharmacology has provided plentiful opportunities for the design of novel therapeutic compound that influence the function of receptors in unique ways. However, tolerance to GPCR drugs is becoming a more common occurrence and strategies to avoid tolerance are needed. The exact molecular events leading to antagonist tolerance and the ways to avoid it remain obscure. Multiple studies have shown that antagonist tolerance correlates with accumulation of the target receptor on the cell surface [45, 50, 155, 156, 228]. Some examples include overexpression of β adrenergic receptors in response to prolonged treatment with their antagonists propranolol and nadolol [229, 230], up-regulation of α1A and α1D adrenergic receptors after prolonged exposure to their inhibitors prazosin and terazosin [46, 228], and elevated expression of dopamine D2 receptor, following chronic treatment with antipsychotic antagonists haloperidol and perphenazine [45]. Accelerated trafficking to the plasma membrane and increased expression of the receptor have been suggested as potential mechanisms for its accumulation after repeated dosing with antagonists [230]. Our results showing that prolonged exposure of cells to AMD3100 leads to increased expression of its primary target and antagonist tolerance are in line with previous observations on CXCR4 [50, 51] and other GPCRs [46, 212, 229].

CXCR4 in T lymphocytes undergoes slow constitutive internalization, approximately 1% of surface receptor per minute [92]. AMD3100 inhibits this process and leads to accumulation of the receptor on the cell surface. Our experiments with the inhibitor of endocytosis dynasore suggest that blocking receptor endocytosis is sufficient to induce tolerance to the drug (figure 15). Expedited trafficking of CXCR4 to the plasma membrane, its accelerated expression or reduced degradation in response to AMD3100 might contribute to increased concentration of the receptor on the plasma membrane and antagonist tolerance. The experiment with dynasore provides justification for the use of biased antagonists that inhibit G protein signalling but not receptor endocytosis to avoid antagonist

tolerance. We have also investigated if overexpression of CXCR4 in Jurkat cells is sufficient to induce tolerance, with mixed results so far. This suggests ligand induced effects may play a role in the development of tolerance. We have also investigated if tolerance is associated with a switch in G protein coupling of CXCR4. Ordinarily, CXCR4 couples to the PTX sensitive Gαi G protein, but can also couple to other G proteins e.g. Gαq [231]. We hypothesised that AMD3100 may inhibit different G proteins with different potencies, and that in tolerance CXCR4 switches to signalling via G proteins less sensitive to AMD3100. While we did see that tolerant cells come overcome the inhibitory effects of PTX, more experiments need to be performed to investigate if AMD3100 has different potencies or efficacies for different G proteins.

Ligand induced effects may include forcing receptors to adopt conformations more favourable to dimerization. Our BRET data suggests that AMD3100 can induce conformational changes in CXCR4. Our immune EM data suggests that a consequence of AMD3100 treatment if the formation of CXCR4 trimers, and it is though that oligomers of CXCR4 are more active than monomeric receptor [180, 181]. It is worth noting that while our data shows CXCR4 trimers as the highest order oligomer, others have observed upward of 9 receptors clustering in response cell stimulation [232]. We have also performed structured illumination microscopy (SIM) and observed an increase in CXCR4 particle size after treatment with AMD3100 (Appendix A, figure 3), but further investigations with higher resolution may be necessary. Indeed, the use of the oligomeric-deficient mutants that we have generated in the lab will be increasingly important for these studies.

While these pharmacological studies are important, there are many other studies and trials investigating the dosing regimen of AMD3100 [232-234]. It may be that one way to overcome the development of tolerance is through intermittent or low dosing. But this does not detract from the usefulness of compounds that avoid these complications in the first place.

While we established that unbiased antagonists develop tolerance, our investigations revealed that X4-2-6, a peptide analog of the TM2 and ECL1 of CXCR4 [209], acts as a biased antagonist. These peptides have been well studied over the past few decades, but recent advances showing GPCR derived peptides can be biased agonists or antagonists is potentially useful step forward in the field [218]. In our case, unlike AMD3100, the peptide at its IC_{50} does not prevent C-terminal phosphorylation of CXCR4 (figure 33), subsequent recruitment of BA1/2 (figure 32), and receptor endocytosis (figure 30) in response to stimulation with CXCL12. At the same time, X4-2-6 acts similarly to AMD3100, blocking GTP-loading of Gαi (figure 36), inhibiting CXCL12-modulation of cAMP production (figure 36), downregulating early pERK1/2 (figure 34), reducing Ca^{2+} flux (figure 36), and inhibiting chemotaxis to CXCL12 (figure 36). Inhibition of Ca^{2+} flux by X4-2-6 is expected to reduce the activity of PKC, a kinase that phosphorylates the Ser324/325 site in CXCR4 [215]. However, in addition to PKC, these residues can also be phosphorylated in Jurkat cells by PIM1 [235]. Phosphorylation of Ser324/325 in CXCR4 by GRK2 and GRK6 has been reported in HEK293 cells [91, 215]. In Jurkat T lymphocytes, 50% of GRK2 is degraded one hour after stimulation with CXCL12 [236]. Expression of GRK6 in Jurkat cells has been confirmed [237]. Thus, while X4-2-6 might prevent PKC from phosphorylating CXCR4, other kinases potentially substitute via non-G protein mediated mechanisms.

Phosphorylation of ERK1/2 in response to CXCL12 stimulation is reportedly due to the activity of G proteins downstream of CXCR4 [238]. Late pERK1/2, 30 minutes after stimulation with the chemokine, is either due to G protein activation of the Ras-Raf pathway or due to the scaffolding function of BA1/2 [97, 238, 239]. Relative contributions of G proteins and BA1/2 to late pERK1/2 vary in different GPCRs [240]. For example, in the context of the angiotensin AT1a receptor BA1/2 promotes pERK1/2 [241], while G protein signalling is responsible for activation of ERK1/2 downstream of the M3 muscarinic receptor [242] where BA1/2 play a regulatory role [243]. Our experiments in BA1/2 knocked-out MEFs suggest that the function of BA1/2 is to

promote receptor desensitization and to prevent excessive phosphorylation of ERK1/2 downstream of CXCR4. The fact that Barbadin, an inhibitor of arrestin association with the β-adaptin subunit of AP2, also increases pERK1/2 in CXCL12-stimulated cells suggests that these kinases are regulated by receptor internalization rather than recruitment of BA1/2. Our results are in agreement with the previous report that BA1/2 knockdown in HeLa cells increases pERK1/2 in response to CXCL12 [94] and is similar to the reported attenuation of pERK1/2 downstream of the chemokine receptor CXCR2 in BA1/2 knocked-out MEFs [244]. Moreover, our findings agree with a recent study that used CRISPR/Cas9 to delete multiple Gα proteins and BA1/2 to demonstrate that a broad set of GPCRs engage G proteins but not arrestins to initiate ERK signalling [245]. However, our results contrast the observation that BA1/2 are required for CXCR4-dependent pERK1/2 in HEK293 cells [97, 246], suggesting BA1/2 might have a cell type specific role in CXCR4 signalling. X4-2-6 decreases early pERK1/2 in Jurkat cells by inhibiting G proteins but allows BA1/2 recruitment to the receptor and subsequent regulation of phosphorylation of both isoforms of this kinase. In contrast, AMD3100 potently suppresses early as well as late pERK1/2. As ERK1/2 signalling in T lymphocytes is considered pro-survival, X4-2-6 and AMD3100 might differentially affect cell viability [247].

The differences in the mechanisms of inhibition between AMD3100 and X4-2-6 are likely due to distinct interactions of the antagonists with the receptor and the chemokine (figure 44A-C). X4-2-6 interacts with both CXCL12 and CXCR4 simultaneously, forming a ternary complex. Within the ternary complex the interaction between the receptor and the peptide causes the extreme N-terminus of the chemokine to be expelled from CXCR4 (figure 44B). This portion of CXCL12 has been implicated in inducing the conformation of the receptor that promotes GTP-loading of Gαi [74]. Thus, X4-2-6 can prevent CXCR4 conformational transitions leading to activation of G proteins but allow phosphorylation of the receptor C-terminus and recruitment of BA1/2. This contrasts with AMD3100 that interacts with the receptor and reduces CXCL12 binding by

displacing its entire N-terminus from CXCR4 (Appendix A, figure 4). The residual weak binding of CXCL12 to the receptor-AMD3100 complex is likely mediated by the globular domain of the chemokine, which is less affected by the drug [151]. At high concentrations AMD3100 can become a partial agonist of CXCR4 [147], while X4-2-6 does not exhibit similar activity. This further highlights the differences between AMD3100 and X4-2-6 in binding modes and the mechanisms of action.

Binding of X4-2-6 to CXCL12 involves the N-loop of the chemokine. This binding site cannot be predicted based on the amino acid sequence of the peptide corresponding to TM2 and ECL1 of CXCR4. The current model of CXCL12 interaction with CXCR4 suggests that Lys^{25} in the N-terminus of the receptor binds the N-loop region of the chemokine [191]. The amino acid sequence of X4-2-6 does not have lysine residues [209]. However, X4-2-6 contains two, non-native to CXCR4 C-terminal aspartates and amidated polyethylene glycol (PEG) that can create or modify a binding site for the chemokine within the peptide. In addition, the tertiary structure of X4-2-6 is different from the structure of the corresponding region in CXCR4 and this might expose a novel site for interaction with CXCL12 [209].

Our proposed mechanism for biased antagonism differs from the previously reported model for the cholecystokinin (CKK) receptor [136]. This model suggested the existence of different conformational states of receptors, with antagonists that selectively interact with G protein activating conformers but not BA1/2 activating conformers [136]. However, X4-2-6 has previously been shown to interact with receptors on the cell surface and those that have undergone endocytosis, suggesting X4-2-6 can bind these receptor conformations [209]. Thus, multiple mechanisms of biased antagonism are possible.

Future pharmaceutical development will likely benefit from a diversity of agents that can avoid the development of tolerance. The fact that a small molecule biased antagonist can act similarly to a peptide biased antagonist by avoiding tolerance suggests that flexibility in the design of such

agents is possible. Currently, very few biased antagonists have been characterized and the advantages of this flexibility and of biased antagonists in general remains an unexplored avenue for drug discovery [135, 136, 227, 248]. Our study suggests that biased antagonists can potentially provide therapeutic options to patients who develop tolerance to unbiased antagonists.

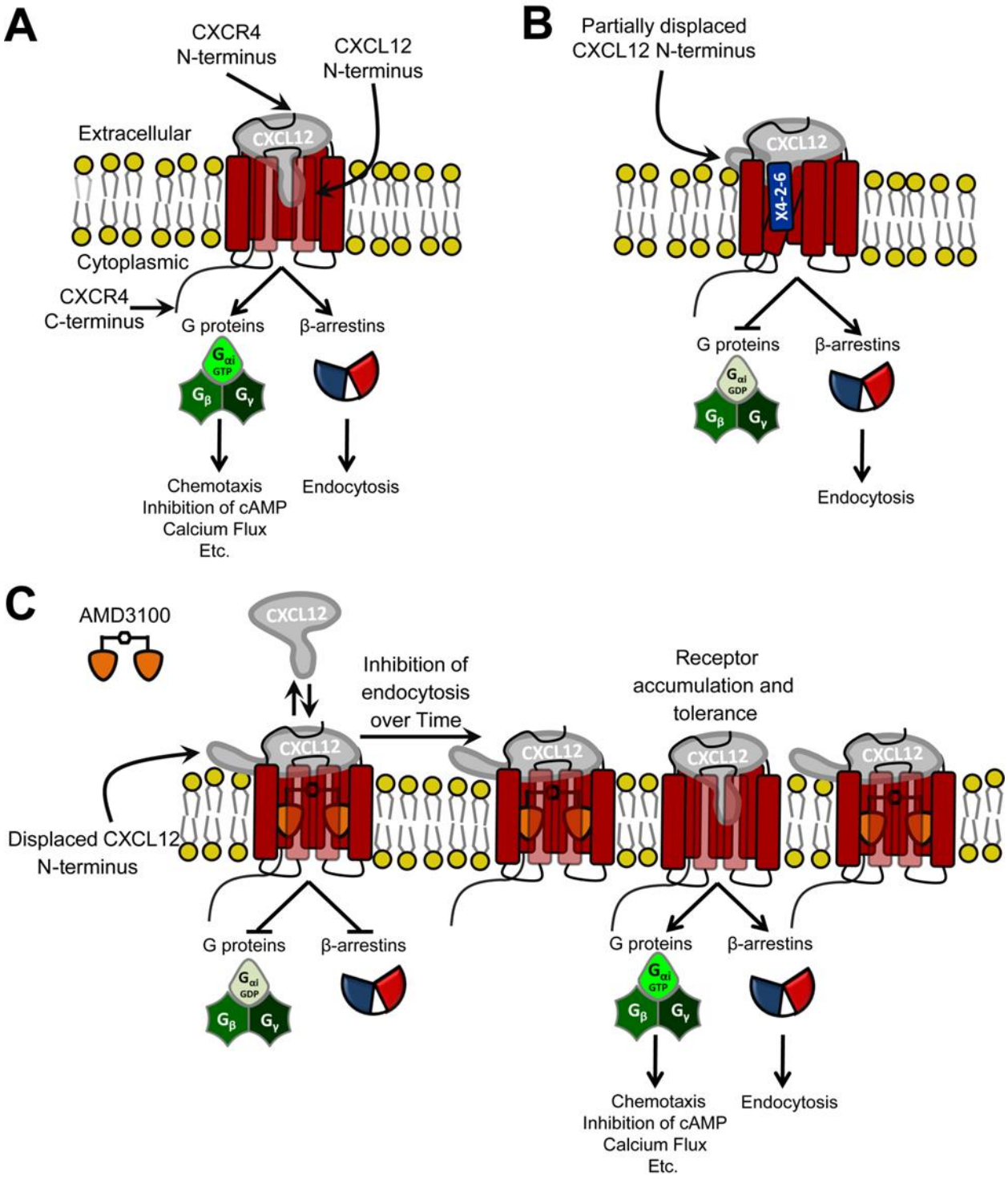

Figure 44: Proposed model for the mechanism of biased antagonism and development of tolerance to unbiased antagonists.

(A) Cartoon depiction of the current paradigm of CXCL12 mediated-CXCR4 signalling. The CXCL12 N-terminus and N-loop insert into the CXCR4 transmembrane helical bundle, while the receptor N-terminus binds the globular domain of the chemokine. This leads to activation of CXCR4 and subsequent G protein signalling, BA1/2 recruitment, and receptor endocytosis. (B)

X4-2-6 binds to CXCL12 and CXCR4 to form a ternary complex and displaces the extreme N-terminal portion of CXCL12 away from the CXCR4 transmembrane helical bundle to inhibit G protein signalling but not BA1/2 recruitment to function as a biased antagonist. (C) AMD3100 displaces the entire CXCL12 N-terminus to inhibit all CXCR4 signalling. Over time, the inhibition of BA1/2 and subsequent endocytosis results in accumulation of CXCR4 on the cell surface, CXCL12 binding to the receptor and the development of tolerance to AMD3100.

CITED LITERATURE

1. Kinch, M.S., et al., *An overview of FDA-approved new molecular entities: 1827-2013.* Drug Discov Today, 2014. **19**(8): p. 1033-9.
2. DiMasi, J.A., H.G. Grabowski, and R.W. Hansen, *Innovation in the pharmaceutical industry: New estimates of R&D costs.* J Health Econ, 2016. **47**: p. 20-33.
3. Wong, C.H., K.W. Siah, and A.W. Lo, *Estimation of clinical trial success rates and related parameters.* Biostatistics, 2018.
4. Davies, J. and D. Davies, *Origins and evolution of antibiotic resistance.* Microbiol Mol Biol Rev, 2010. **74**(3): p. 417-33.
5. Lynch, S.S. *Tolerance and Resistance to Drugs*. Factors Affecting Response to Drugs 2017; Available from: https://www.merckmanuals.com/home/drugs/factors-affecting-response-to-drugs/tolerance-and-resistance-to-drugs.
6. Chin, J.H. and D.B. Goldstein, *Drug tolerance in biomembranes: a spin label study of the effects of ethanol.* Science, 1977. **196**(4290): p. 684-5.
7. Crabbe, J.C., et al., *Rapid development of tolerance to the hypothermic effect of ethanol in mice.* J Pharmacol Exp Ther, 1979. **208**(1): p. 128-33.
8. Gahwiler, B.H., *Development of acute tolerance during exposure of hippocampal explants to an opioid peptide.* Brain Res, 1981. **217**(1): p. 196-200.
9. Leblanc, A.E., R.J. Gibbins, and H. Kalant, *Generalization of behaviorally augmented tolerance to ethanol, and its relation to physical dependence.* Psychopharmacologia, 1975. **44**(3): p. 241-6.
10. Loh, H.H., P.L. Tao, and A.P. Smith, *Role of receptor regulation in opioid tolerance mechanisms.* Synapse, 1988. **2**(4): p. 457-62.
11. McRorie, J.W., J.A. Kirby, and P.B. Miner, *Histamine2-receptor antagonists: Rapid development of tachyphylaxis with repeat dosing.* World J Gastrointest Pharmacol Ther, 2014. **5**(2): p. 57-62.
12. Sharma, S.V., et al., *A chromatin-mediated reversible drug-tolerant state in cancer cell subpopulations.* Cell, 2010. **141**(1): p. 69-80.
13. Bespalov, A., et al., *Drug Tolerance: A Known Unknown in Translational Neuroscience.* Trends Pharmacol Sci, 2016. **37**(5): p. 364-378.
14. Santos, R., et al., *A comprehensive map of molecular drug targets.* Nat Rev Drug Discov, 2017. **16**(1): p. 19-34.
15. Sriram, K. and P.A. Insel, *G Protein-Coupled Receptors as Targets for Approved Drugs: How Many Targets and How Many Drugs?* Mol Pharmacol, 2018. **93**(4): p. 251-258.
16. Alexander, S.P., et al., *The Concise Guide to PHARMACOLOGY 2015/16: G protein-coupled receptors.* Br J Pharmacol, 2015. **172**(24): p. 5744-869.
17. Venter, J.C., et al., *The sequence of the human genome.* Science, 2001. **291**(5507): p. 1304-51.
18. Fredriksson, R., et al., *The G-protein-coupled receptors in the human genome form five main families. Phylogenetic analysis, paralogon groups, and fingerprints.* Mol Pharmacol, 2003. **63**(6): p. 1256-72.
19. Shimada, I., et al., *GPCR drug discovery: integrating solution NMR data with crystal and cryo-EM structures.* Nat Rev Drug Discov, 2018.
20. Allen, J.A. and B.L. Roth, *Strategies to discover unexpected targets for drugs active at G protein-coupled receptors.* Annu Rev Pharmacol Toxicol, 2011. **51**: p. 117-44.
21. Roth, B.L. and W.K. Kroeze, *Integrated Approaches for Genome-wide Interrogation of the Druggable Non-olfactory G Protein-coupled Receptor Superfamily.* J Biol Chem, 2015. **290**(32): p. 19471-7.

22. Wacker, D., R.C. Stevens, and B.L. Roth, *How Ligands Illuminate GPCR Molecular Pharmacology.* Cell, 2017. **170**(3): p. 414-427.
23. Gilman, A.G., *G proteins: transducers of receptor-generated signals.* Annu Rev Biochem, 1987. **56**: p. 615-49.
24. De Lean, A., J.M. Stadel, and R.J. Lefkowitz, *A ternary complex model explains the agonist-specific binding properties of the adenylate cyclase-coupled beta-adrenergic receptor.* J Biol Chem, 1980. **255**(15): p. 7108-17.
25. Maguire, M.E., P.M. Van Arsdale, and A.G. Gilman, *An agonist-specific effect of guanine nucleotides on binding to the beta adrenergic receptor.* Mol Pharmacol, 1976. **12**(2): p. 335-9.
26. DeGraff, J.L., et al., *Role of arrestins in endocytosis and signaling of alpha2-adrenergic receptor subtypes.* J Biol Chem, 1999. **274**(16): p. 11253-9.
27. Luttrell, L.M., et al., *Beta-arrestin-dependent formation of beta2 adrenergic receptor-Src protein kinase complexes.* Science, 1999. **283**(5402): p. 655-61.
28. Violin, J.D., et al., *Biased ligands at G-protein-coupled receptors: promise and progress.* Trends Pharmacol Sci, 2014. **35**(7): p. 308-16.
29. Ferrand, A., et al., *A novel mechanism for JAK2 activation by a G protein-coupled receptor, the CCK2R: implication of this signaling pathway in pancreatic tumor models.* J Biol Chem, 2005. **280**(11): p. 10710-5.
30. Cerione, R.A., et al., *The mammalian beta 2-adrenergic receptor: reconstitution of functional interactions between pure receptor and pure stimulatory nucleotide binding protein of the adenylate cyclase system.* Biochemistry, 1984. **23**(20): p. 4519-25.
31. Koski, G., R.A. Streaty, and W.A. Klee, *Modulation of sodium-sensitive GTPase by partial opiate agonists. An explanation for the dual requirement for Na+ and GTP in inhibitory regulation of adenylate cyclase.* J Biol Chem, 1982. **257**(23): p. 14035-40.
32. Weis, W.I. and B.K. Kobilka, *The Molecular Basis of G Protein-Coupled Receptor Activation.* Annu Rev Biochem, 2018. **87**: p. 897-919.
33. Spengler, D., et al., *Differential signal transduction by five splice variants of the PACAP receptor.* Nature, 1993. **365**(6442): p. 170-5.
34. Aellig, W.H., *Pindolol--a beta-adrenoceptor blocking drug with partial agonist activity: clinical pharmacological considerations.* Br J Clin Pharmacol, 1982. **13**(Suppl 2): p. 187S-192S.
35. Watson, C., et al., *The use of stimulus-biased assay systems to detect agonist-specific receptor active states: implications for the trafficking of receptor stimulus by agonists.* Mol Pharmacol, 2000. **58**(6): p. 1230-8.
36. Deupi, X., X.D. Li, and G.F. Schertler, *Ligands stabilize specific GPCR conformations: but how?* Structure, 2012. **20**(8): p. 1289-90.
37. Benovic, J.L., et al., *Beta-adrenergic receptor kinase: primary structure delineates a multigene family.* Science, 1989. **246**(4927): p. 235-40.
38. Brown, A.J., et al., *The Orphan G protein-coupled receptors GPR41 and GPR43 are activated by propionate and other short chain carboxylic acids.* J Biol Chem, 2003. **278**(13): p. 11312-9.
39. Simon, M.I., M.P. Strathmann, and N. Gautam, *Diversity of G proteins in signal transduction.* Science, 1991. **252**(5007): p. 802-8.
40. Asano, T., et al., *Activation of the inhibitory GTP-binding protein of adenylate cyclase, Gi, by beta-adrenergic receptors in reconstituted phospholipid vesicles.* J Biol Chem, 1984. **259**(15): p. 9351-4.
41. Daaka, Y., L.M. Luttrell, and R.J. Lefkowitz, *Switching of the coupling of the beta2-adrenergic receptor to different G proteins by protein kinase A.* Nature, 1997. **390**(6655): p. 88-91.

42. Fisher, A., et al., *Selective signaling via unique M1 muscarinic agonists.* Ann N Y Acad Sci, 1993. **695**: p. 300-3.
43. Whistler, J.L. and M. von Zastrow, *Morphine-activated opioid receptors elude desensitization by beta-arrestin.* Proc Natl Acad Sci U S A, 1998. **95**(17): p. 9914-9.
44. Christopoulos, A., et al., *International Union of Basic and Clinical Pharmacology. XC. multisite pharmacology: recommendations for the nomenclature of receptor allosterism and allosteric ligands.* Pharmacol Rev, 2014. **66**(4): p. 918-47.
45. Silvestri, S., et al., *Increased dopamine D2 receptor binding after long-term treatment with antipsychotics in humans: a clinical PET study.* Psychopharmacology (Berl), 2000. **152**(2): p. 174-80.
46. Vincent, J., et al., *Pharmacological tolerance to alpha 1-adrenergic receptor antagonism mediated by terazosin in humans.* J Clin Invest, 1992. **90**(5): p. 1763-8.
47. DeLander, G.E., P.S. Portoghese, and A.E. Takemori, *Role of spinal mu opioid receptors in the development of morphine tolerance and dependence.* J Pharmacol Exp Ther, 1984. **231**(1): p. 91-6.
48. Pathan, H. and J. Williams, *Basic opioid pharmacology: an update.* Br J Pain, 2012. **6**(1): p. 11-6.
49. Gendron, L., et al., *Recent advances on the delta opioid receptor: from trafficking to function.* Br J Pharmacol, 2015. **172**(2): p. 403-19.
50. Sison, E.A., et al., *Plerixafor as a chemosensitizing agent in pediatric acute lymphoblastic leukemia: efficacy and potential mechanisms of resistance to CXCR4 inhibition.* Oncotarget, 2014. **5**(19): p. 8947-58.
51. Uy, G.L., et al., *A phase 1/2 study of chemosensitization with the CXCR4 antagonist plerixafor in relapsed or refractory acute myeloid leukemia.* Blood, 2012. **119**(17): p. 3917-24.
52. Griffith, J.W., C.L. Sokol, and A.D. Luster, *Chemokines and chemokine receptors: positioning cells for host defense and immunity.* Annu Rev Immunol, 2014. **32**: p. 659-702.
53. Zlotnik, A. and O. Yoshie, *Chemokines: a new classification system and their role in immunity.* Immunity, 2000. **12**(2): p. 121-7.
54. Ransohoff, R.M., *Chemokines and chemokine receptors: standing at the crossroads of immunobiology and neurobiology.* Immunity, 2009. **31**(5): p. 711-21.
55. O'Hayre, M., et al., *Emerging concepts and approaches for chemokine-receptor drug discovery.* Expert Opin Drug Discov, 2010. **5**(11): p. 1109-22.
56. Chatterjee, S., B. Behnam Azad, and S. Nimmagadda, *The intricate role of CXCR4 in cancer.* Adv Cancer Res, 2014. **124**: p. 31-82.
57. Bleul, C.C., et al., *The lymphocyte chemoattractant SDF-1 is a ligand for LESTR/fusin and blocks HIV-1 entry.* Nature, 1996. **382**(6594): p. 829-33.
58. Coakley, E., C.J. Petropoulos, and J.M. Whitcomb, *Assessing chemokine co-receptor usage in HIV.* Curr Opin Infect Dis, 2005. **18**(1): p. 9-15.
59. Balkwill, F., *The significance of cancer cell expression of the chemokine receptor CXCR4.* Semin Cancer Biol, 2004. **14**(3): p. 171-9.
60. Dar, A., O. Kollet, and T. Lapidot, *Mutual, reciprocal SDF-1/CXCR4 interactions between hematopoietic and bone marrow stromal cells regulate human stem cell migration and development in NOD/SCID chimeric mice.* Exp Hematol, 2006. **34**(8): p. 967-75.
61. Ma, Q., D. Jones, and T.A. Springer, *The chemokine receptor CXCR4 is required for the retention of B lineage and granulocytic precursors within the bone marrow microenvironment.* Immunity, 1999. **10**(4): p. 463-71.
62. McGrath, K.E., et al., *Embryonic expression and function of the chemokine SDF-1 and its receptor, CXCR4.* Dev Biol, 1999. **213**(2): p. 442-56.

63. Mohle, R., et al., *The chemokine receptor CXCR-4 is expressed on CD34+ hematopoietic progenitors and leukemic cells and mediates transendothelial migration induced by stromal cell-derived factor-1.* Blood, 1998. **91**(12): p. 4523-30.
64. Onai, N., et al., *Impairment of lymphopoiesis and myelopoiesis in mice reconstituted with bone marrow-hematopoietic progenitor cells expressing SDF-1-intrakine.* Blood, 2000. **96**(6): p. 2074-80.
65. Ponomaryov, T., et al., *Induction of the chemokine stromal-derived factor-1 following DNA damage improves human stem cell function.* J Clin Invest, 2000. **106**(11): p. 1331-9.
66. Sugiyama, T., et al., *Maintenance of the hematopoietic stem cell pool by CXCL12-CXCR4 chemokine signaling in bone marrow stromal cell niches.* Immunity, 2006. **25**(6): p. 977-88.
67. Shirozu, M., et al., *Structure and chromosomal localization of the human stromal cell-derived factor 1 (SDF1) gene.* Genomics, 1995. **28**(3): p. 495-500.
68. Yu, L., et al., *Identification and expression of novel isoforms of human stromal cell-derived factor 1.* Gene, 2006. **374**: p. 174-9.
69. Oberlin, E., et al., *The CXC chemokine SDF-1 is the ligand for LESTR/fusin and prevents infection by T-cell-line-adapted HIV-1.* Nature, 1996. **382**(6594): p. 833-5.
70. Nagasawa, T., et al., *Defects of B-cell lymphopoiesis and bone-marrow myelopoiesis in mice lacking the CXC chemokine PBSF/SDF-1.* Nature, 1996. **382**(6592): p. 635-8.
71. Zou, Y.R., et al., *Function of the chemokine receptor CXCR4 in haematopoiesis and in cerebellar development.* Nature, 1998. **393**(6685): p. 595-9.
72. Moser, B. and P. Loetscher, *Lymphocyte traffic control by chemokines.* Nat Immunol, 2001. **2**(2): p. 123-8.
73. Murphy, P.M., *The molecular biology of leukocyte chemoattractant receptors.* Annu Rev Immunol, 1994. **12**: p. 593-633.
74. Crump, M.P., et al., *Solution structure and basis for functional activity of stromal cell-derived factor-1; dissociation of CXCR4 activation from binding and inhibition of HIV-1.* EMBO J, 1997. **16**(23): p. 6996-7007.
75. Qin, L., et al., *Structural biology. Crystal structure of the chemokine receptor CXCR4 in complex with a viral chemokine.* Science, 2015. **347**(6226): p. 1117-22.
76. Brelot, A., et al., *Identification of residues of CXCR4 critical for human immunodeficiency virus coreceptor and chemokine receptor activities.* J Biol Chem, 2000. **275**(31): p. 23736-44.
77. Choi, W.T., et al., *Unique ligand binding sites on CXCR4 probed by a chemical biology approach: implications for the design of selective human immunodeficiency virus type 1 inhibitors.* J Virol, 2005. **79**(24): p. 15398-404.
78. Tian, S., et al., *Distinct functional sites for human immunodeficiency virus type 1 and stromal cell-derived factor 1alpha on CXCR4 transmembrane helical domains.* J Virol, 2005. **79**(20): p. 12667-73.
79. Zhou, N., et al., *Structural and functional characterization of human CXCR4 as a chemokine receptor and HIV-1 co-receptor by mutagenesis and molecular modeling studies.* J Biol Chem, 2001. **276**(46): p. 42826-33.
80. Busillo, J.M. and J.L. Benovic, *Regulation of CXCR4 signaling.* Biochim Biophys Acta, 2007. **1768**(4): p. 952-63.
81. Abrahamsen, H., T. Vang, and K. Tasken, *Protein kinase A intersects SRC signaling in membrane microdomains.* J Biol Chem, 2003. **278**(19): p. 17170-7.
82. Cheng, M., et al., *A critical role of Src family kinase in SDF-1/CXCR4-mediated bone-marrow progenitor cell recruitment to the ischemic heart.* J Mol Cell Cardiol, 2015. **81**: p. 49-53.

83. Vang, T., et al., *Combined spatial and enzymatic regulation of Csk by cAMP and protein kinase a inhibits T cell receptor signaling.* J Biol Chem, 2003. **278**(20): p. 17597-600.
84. Campbell, J.J., et al., *Chemokines and the arrest of lymphocytes rolling under flow conditions.* Science, 1998. **279**(5349): p. 381-4.
85. Constantin, G., et al., *Chemokines trigger immediate beta2 integrin affinity and mobility changes: differential regulation and roles in lymphocyte arrest under flow*. Immunity, 2000. **13**(6): p. 759-69.
86. Delgado-Martin, C., et al., *Chemokine CXCL12 uses CXCR4 and a signaling core formed by bifunctional Akt, extracellular signal-regulated kinase (ERK)1/2, and mammalian target of rapamycin complex 1 (mTORC1) proteins to control chemotaxis and survival simultaneously in mature dendritic cells.* J Biol Chem, 2011. **286**(43): p. 37222-36.
87. Peng, S.B., et al., *Akt activation, but not extracellular signal-regulated kinase activation, is required for SDF-1alpha/CXCR4-mediated migration of epitheloid carcinoma cells.* Mol Cancer Res, 2005. **3**(4): p. 227-36.
88. Haribabu, B., et al., *Regulation of human chemokine receptors CXCR4. Role of phosphorylation in desensitization and internalization.* J Biol Chem, 1997. **272**(45): p. 28726-31.
89. Streb, H., et al., *Release of Ca2+ from a nonmitochondrial intracellular store in pancreatic acinar cells by inositol-1,4,5-trisphosphate.* Nature, 1983. **306**(5938): p. 67-9.
90. Schonwasser, D.C., et al., *Activation of the mitogen-activated protein kinase/extracellular signal-regulated kinase pathway by conventional, novel, and atypical protein kinase C isotypes.* Mol Cell Biol, 1998. **18**(2): p. 790-8.
91. Orsini, M.J., et al., *Trafficking of the HIV coreceptor CXCR4. Role of arrestins and identification of residues in the c-terminal tail that mediate receptor internalization.* J Biol Chem, 1999. **274**(43): p. 31076-86.
92. Signoret, N., et al., *Phorbol esters and SDF-1 induce rapid endocytosis and down modulation of the chemokine receptor CXCR4.* J Cell Biol, 1997. **139**(3): p. 651-64.
93. Signoret, N., et al., *Differential regulation of CXCR4 and CCR5 endocytosis.* J Cell Sci, 1998. **111 (Pt 18)**: p. 2819-30.
94. Malik, R., et al., *Novel roles for the E3 ubiquitin ligase atrophin-interacting protein 4 and signal transduction adaptor molecule 1 in G protein-coupled receptor signaling.* J Biol Chem, 2012. **287**(12): p. 9013-27.
95. Fong, A.M., et al., *Defective lymphocyte chemotaxis in beta-arrestin2- and GRK6-deficient mice.* Proc Natl Acad Sci U S A, 2002. **99**(11): p. 7478-83.
96. Vroon, A., et al., *GRK6 deficiency is associated with enhanced CXCR4-mediated neutrophil chemotaxis in vitro and impaired responsiveness to G-CSF in vivo.* J Leukoc Biol, 2004. **75**(4): p. 698-704.
97. Cheng, Z.J., et al., *beta-arrestin differentially regulates the chemokine receptor CXCR4-mediated signaling and receptor internalization, and this implicates multiple interaction sites between beta-arrestin and CXCR4.* J Biol Chem, 2000. **275**(4): p. 2479-85.
98. Diaz, G.A., *CXCR4 mutations in WHIM syndrome: a misguided immune system?* Immunol Rev, 2005. **203**: p. 235-43.
99. Diaz, G.A. and A.V. Gulino, *WHIM syndrome: a defect in CXCR4 signaling.* Curr Allergy Asthma Rep, 2005. **5**(5): p. 350-5.
100. Hernandez, P.A., et al., *Mutations in the chemokine receptor gene CXCR4 are associated with WHIM syndrome, a combined immunodeficiency disease.* Nat Genet, 2003. **34**(1): p. 70-4.
101. Mueller, W., et al., *Hierarchical organization of multi-site phosphorylation at the CXCR4 C terminus.* PLoS One, 2013. **8**(5): p. e64975.

102. Tarasova, N.I., R.H. Stauber, and C.J. Michejda, *Spontaneous and ligand-induced trafficking of CXC-chemokine receptor 4.* J Biol Chem, 1998. **273**(26): p. 15883-6.
103. Marchese, A., et al., *The E3 ubiquitin ligase AIP4 mediates ubiquitination and sorting of the G protein-coupled receptor CXCR4.* Dev Cell, 2003. **5**(5): p. 709-22.
104. Marchese, A. and J.L. Benovic, *Agonist-promoted ubiquitination of the G protein-coupled receptor CXCR4 mediates lysosomal sorting.* J Biol Chem, 2001. **276**(49): p. 45509-12.
105. DeFea, K.A., et al., *beta-arrestin-dependent endocytosis of proteinase-activated receptor 2 is required for intracellular targeting of activated ERK1/2.* J Cell Biol, 2000. **148**(6): p. 1267-81.
106. Sun, Y., et al., *Beta-arrestin2 is critically involved in CXCR4-mediated chemotaxis, and this is mediated by its enhancement of p38 MAPK activation.* J Biol Chem, 2002. **277**(51): p. 49212-9.
107. Farzan, M., et al., *The role of post-translational modifications of the CXCR4 amino terminus in stromal-derived factor 1 alpha association and HIV-1 entry.* J Biol Chem, 2002. **277**(33): p. 29484-9.
108. Berson, J.F., et al., *A seven-transmembrane domain receptor involved in fusion and entry of T-cell-tropic human immunodeficiency virus type 1 strains.* J Virol, 1996. **70**(9): p. 6288-95.
109. Wang, J., et al., *N-linked glycosylation in the CXCR4 N-terminus inhibits binding to HIV-1 envelope glycoproteins.* Virology, 2004. **324**(1): p. 140-50.
110. Zhou, H. and H.H. Tai, *Characterization of recombinant human CXCR4 in insect cells: role of extracellular domains and N-glycosylation in ligand binding.* Arch Biochem Biophys, 1999. **369**(2): p. 267-76.
111. Sloane, A.J., et al., *Marked structural and functional heterogeneity in CXCR4: separation of HIV-1 and SDF-1alpha responses.* Immunol Cell Biol, 2005. **83**(2): p. 129-43.
112. Ziarek, J.J., et al., *Sulfopeptide probes of the CXCR4/CXCL12 interface reveal oligomer-specific contacts and chemokine allostery.* ACS Chem Biol, 2013. **8**(9): p. 1955-63.
113. Schols, D., et al., *Bicyclams, a class of potent anti-HIV agents, are targeted at the HIV coreceptor fusin/CXCR-4.* Antiviral Res, 1997. **35**(3): p. 147-56.
114. Schols, D., et al., *Inhibition of T-tropic HIV strains by selective antagonization of the chemokine receptor CXCR4.* J Exp Med, 1997. **186**(8): p. 1383-8.
115. Donzella, G.A., et al., *AMD3100, a small molecule inhibitor of HIV-1 entry via the CXCR4 co-receptor.* Nat Med, 1998. **4**(1): p. 72-7.
116. De Clercq, E., et al., *Potent and selective inhibition of human immunodeficiency virus (HIV)-1 and HIV-2 replication by a class of bicyclams interacting with a viral uncoating event.* Proc Natl Acad Sci U S A, 1992. **89**(12): p. 5286-90.
117. De Clercq, E., et al., *Highly potent and selective inhibition of human immunodeficiency virus by the bicyclam derivative JM3100.* Antimicrob Agents Chemother, 1994. **38**(4): p. 668-74.
118. National Cancer Institute. *FDA approval for Plerixafor*. 2013, July 3; Available from: https://www.cancer.gov/about-cancer/treatment/drugs/fda-plerixafor.
119. Hatse, S., et al., *Chemokine receptor inhibition by AMD3100 is strictly confined to CXCR4.* FEBS Lett, 2002. **527**(1-3): p. 255-62.
120. Ahn, J.Y., et al., *The prognostic value of CXCR4 in acute myeloid leukemia.* Appl Immunohistochem Mol Morphol, 2013. **21**(1): p. 79-84.
121. Lee, H.H., V. Bellat, and B. Law, *Chemotherapy induces adaptive drug resistance and metastatic potentials via phenotypic CXCR4-expressing cell state transition in ovarian cancer.* PLoS One, 2017. **12**(2): p. e0171044.

122. Li, J., et al., *Overexpression of CXCR4 is significantly associated with cisplatin-based chemotherapy resistance and can be a prognostic factor in epithelial ovarian cancer.* BMB Rep, 2014. **47**(1): p. 33-8.
123. Matsuo, H., et al., *CXCR4 Overexpression is a Poor Prognostic Factor in Pediatric Acute Myeloid Leukemia With Low Risk: A Report From the Japanese Pediatric Leukemia/Lymphoma Study Group.* Pediatr Blood Cancer, 2016. **63**(8): p. 1394-9.
124. Scala, S., et al., *Expression of CXCR4 predicts poor prognosis in patients with malignant melanoma.* Clin Cancer Res, 2005. **11**(5): p. 1835-41.
125. Sison, E.A., et al., *Dynamic chemotherapy-induced upregulation of CXCR4 expression: a mechanism of therapeutic resistance in pediatric AML.* Mol Cancer Res, 2013. **11**(9): p. 1004-16.
126. Xu, C., et al., *CXCR4 overexpression is correlated with poor prognosis in colorectal cancer.* Life Sci, 2018. **208**: p. 333-340.
127. Ho, T.K., et al., *Stromal-Cell-Derived Factor-1 (SDF-1)/CXCL12 as Potential Target of Therapeutic Angiogenesis in Critical Leg Ischaemia.* Cardiol Res Pract, 2012. **2012**: p. 143209.
128. Janowski, M., *Functional diversity of SDF-1 splicing variants.* Cell Adh Migr, 2009. **3**(3): p. 243-9.
129. Muller, A., et al., *Involvement of chemokine receptors in breast cancer metastasis.* Nature, 2001. **410**(6824): p. 50-6.
130. Society, A.C., *Leukemia at a Glance.* 2019.
131. Sison, E.A. and P. Brown, *The bone marrow microenvironment and leukemia: biology and therapeutic targeting.* Expert Rev Hematol, 2011. **4**(3): p. 271-83.
132. Vianello, F., et al., *Bone marrow mesenchymal stromal cells non-selectively protect chronic myeloid leukemia cells from imatinib-induced apoptosis via the CXCR4/CXCL12 axis.* Haematologica, 2010. **95**(7): p. 1081-9.
133. Komazawa, Y., et al., *Tolerance to famotidine and ranitidine treatment after 14 days of administration in healthy subjects without Helicobacter pylori infection.* J Gastroenterol Hepatol, 2003. **18**(6): p. 678-82.
134. Olsen, C.K., L.T. Brennum, and M. Kreilgaard, *Using pharmacokinetic-pharmacodynamic modelling as a tool for prediction of therapeutic effective plasma levels of antipsychotics.* Eur J Pharmacol, 2008. **584**(2-3): p. 318-27.
135. Gilchrist, A., et al., *Identifying bias in CCR1 antagonists using radiolabelled binding, receptor internalization, beta-arrestin translocation and chemotaxis assays.* Br J Pharmacol, 2014. **171**(22): p. 5127-38.
136. Magnan, R., et al., *Distinct CCK-2 receptor conformations associated with beta-arrestin-2 recruitment or phospholipase-C activation revealed by a biased antagonist.* J Am Chem Soc, 2013. **135**(7): p. 2560-73.
137. Trott, O. and A.J. Olson, *AutoDock Vina: improving the speed and accuracy of docking with a new scoring function, efficient optimization, and multithreading.* J Comput Chem, 2010. **31**(2): p. 455-61.
138. Delaglio, F., et al., *NMRPipe: a multidimensional spectral processing system based on UNIX pipes.* J Biomol NMR, 1995. **6**(3): p. 277-93.
139. Veldkamp, C.T., et al., *Monomeric structure of the cardioprotective chemokine SDF-1/CXCL12.* Protein Sci, 2009. **18**(7): p. 1359-69.
140. Kroeze, W.K., et al., *PRESTO-Tango as an open-source resource for interrogation of the druggable human GPCRome.* Nat Struct Mol Biol, 2015. **22**(5): p. 362-9.
141. Robert, X. and P. Gouet, *Deciphering key features in protein structures with the new ENDscript server.* Nucleic Acids Res, 2014. **42**(Web Server issue): p. W320-4.

142. Schneider, C.A., W.S. Rasband, and K.W. Eliceiri, *NIH Image to ImageJ: 25 years of image analysis.* Nat Methods, 2012. **9**(7): p. 671-5.
143. Spoo, A.C., et al., *CXCR4 is a prognostic marker in acute myelogenous leukemia.* Blood, 2007. **109**(2): p. 786-91.
144. Williams, J.T., et al., *Regulation of mu-opioid receptors: desensitization, phosphorylation, internalization, and tolerance.* Pharmacol Rev, 2013. **65**(1): p. 223-54.
145. De Clercq, E., *Inhibition of HIV infection by bicyclams, highly potent and specific CXCR4 antagonists.* Mol Pharmacol, 2000. **57**(5): p. 833-9.
146. Kim, H.Y., et al., *The CXCR4 Antagonist AMD3100 Has Dual Effects on Survival and Proliferation of Myeloma Cells In Vitro.* Cancer Res Treat, 2010. **42**(4): p. 225-34.
147. Zhang, W.B., et al., *A point mutation that confers constitutive activity to CXCR4 reveals that T140 is an inverse agonist and that AMD3100 and ALX40-4C are weak partial agonists.* J Biol Chem, 2002. **277**(27): p. 24515-21.
148. Hatse, S., et al., *Mutations at the CXCR4 interaction sites for AMD3100 influence anti-CXCR4 antibody binding and HIV-1 entry.* FEBS Lett, 2003. **546**(2-3): p. 300-6.
149. Rosenkilde, M.M., et al., *Molecular mechanism of AMD3100 antagonism in the CXCR4 receptor: transfer of binding site to the CXCR3 receptor.* J Biol Chem, 2004. **279**(4): p. 3033-41.
150. Sachpatzidis, A., et al., *Identification of allosteric peptide agonists of CXCR4.* J Biol Chem, 2003. **278**(2): p. 896-907.
151. Kofuku, Y., et al., *Structural basis of the interaction between chemokine stromal cell-derived factor-1/CXCL12 and its G-protein-coupled receptor CXCR4.* J Biol Chem, 2009. **284**(50): p. 35240-50.
152. Allegretti, M., M.C. Cesta, and M. Locati, *Allosteric Modulation of Chemoattractant Receptors.* Front Immunol, 2016. **7**: p. 170.
153. Strelow, J., et al., *Mechanism of Action Assays for Enzymes*, in *Assay Guidance Manual*, G.S. Sittampalam, et al., Editors. 2004: Bethesda (MD).
154. Drury, L.J., et al., *Monomeric and dimeric CXCL12 inhibit metastasis through distinct CXCR4 interactions and signaling pathways.* Proc Natl Acad Sci U S A, 2011. **108**(43): p. 17655-60.
155. Allouche, S., F. Noble, and N. Marie, *Opioid receptor desensitization: mechanisms and its link to tolerance.* Front Pharmacol, 2014. **5**: p. 280.
156. Gomes, B.A., et al., *Mu-opioid receptor down-regulation and tolerance are not equally dependent upon G-protein signaling.* Pharmacol Biochem Behav, 2002. **72**(1-2): p. 273-8.
157. He, L., et al., *Regulation of opioid receptor trafficking and morphine tolerance by receptor oligomerization.* Cell, 2002. **108**(2): p. 271-82.
158. Carnec, X., et al., *Anti-CXCR4 monoclonal antibodies recognizing overlapping epitopes differ significantly in their ability to inhibit entry of human immunodeficiency virus type 1.* J Virol, 2005. **79**(3): p. 1930-3.
159. Ge, B., et al., *Single-molecule imaging reveals dimerization/oligomerization of CXCR4 on plasma membrane closely related to its function.* Sci Rep, 2017. **7**(1): p. 16873.
160. Lao, J., et al., *Single-Molecule Imaging Demonstrates Ligand Regulation of the Oligomeric Status of CXCR4 in Living Cells.* J Phys Chem B, 2017. **121**(7): p. 1466-1474.
161. Oh, B.J., et al., *Differences in donor CXCR4 expression levels are correlated with functional capacity and therapeutic outcome of angiogenic treatment with endothelial colony forming cells.* Biochem Biophys Res Commun, 2010. **398**(4): p. 627-33.
162. Gonzalez, N., et al., *SDF-1/CXCL12 production by mature dendritic cells inhibits the propagation of X4-tropic HIV-1 isolates at the dendritic cell-T-cell infectious synapse.* J Virol, 2010. **84**(9): p. 4341-51.

163. Cole, S.W., B.D. Jamieson, and J.A. Zack, *cAMP up-regulates cell surface expression of lymphocyte CXCR4: implications for chemotaxis and HIV-1 infection.* J Immunol, 1999. **162**(3): p. 1392-400.
164. Cristillo, A.D., et al., *Up-regulation of HIV coreceptor CXCR4 expression in human T lymphocytes is mediated in part by a cAMP-responsive element.* FASEB J, 2002. **16**(3): p. 354-64.
165. Hu, X.M., et al., *Chemokine receptor CXCR4 regulates CaMKII/CREB pathway in spinal neurons that underlies cancer-induced bone pain.* Sci Rep, 2017. **7**(1): p. 4005.
166. Johannessen, M., M.P. Delghandi, and U. Moens, *What turns CREB on?* Cell Signal, 2004. **16**(11): p. 1211-27.
167. Yang, L., et al., *Blocking CXCR4-mediated cyclic AMP suppression inhibits brain tumor growth in vivo.* Cancer Res, 2007. **67**(2): p. 651-8.
168. Seamon, K.B. and J.W. Daly, *Forskolin: a unique diterpene activator of cyclic AMP-generating systems.* J Cyclic Nucleotide Res, 1981. **7**(4): p. 201-24.
169. Seamon, K.B., W. Padgett, and J.W. Daly, *Forskolin: unique diterpene activator of adenylate cyclase in membranes and in intact cells.* Proc Natl Acad Sci U S A, 1981. **78**(6): p. 3363-7.
170. Comb, M., et al., *A cyclic AMP- and phorbol ester-inducible DNA element.* Nature, 1986. **323**(6086): p. 353-6.
171. Tan, Y., et al., *FGF and stress regulate CREB and ATF-1 via a pathway involving p38 MAP kinase and MAPKAP kinase-2.* EMBO J, 1996. **15**(17): p. 4629-42.
172. Joo, E.K., et al., *Enhancement of cell survival by stromal cell-derived factor-1/CXCL12 involves activation of CREB and induction of Mcl-1 and c-Fos in factor-dependent human cell line MO7e.* Stem Cells Dev, 2004. **13**(5): p. 563-70.
173. Moore, N., et al., *Impact of CXCR4/CXCL12 Blockade on Normal Plasma Cells In Vivo.* Am J Transplant, 2017. **17**(6): p. 1663-1669.
174. Bonvini, P., et al., *Bortezomib-mediated 26S proteasome inhibition causes cell-cycle arrest and induces apoptosis in CD-30+ anaplastic large cell lymphoma.* Leukemia, 2007. **21**(4): p. 838-42.
175. Macia, E., et al., *Dynasore, a cell-permeable inhibitor of dynamin.* Dev Cell, 2006. **10**(6): p. 839-50.
176. Sanchez-Martin, L., P. Sanchez-Mateos, and C. Cabanas, *CXCR7 impact on CXCL12 biology and disease.* Trends Mol Med, 2013. **19**(1): p. 12-22.
177. Rajagopal, S., et al., *Beta-arrestin- but not G protein-mediated signaling by the "decoy" receptor CXCR7.* Proc Natl Acad Sci U S A, 2010. **107**(2): p. 628-32.
178. Kalatskaya, I., et al., *AMD3100 is a CXCR7 ligand with allosteric agonist properties.* Mol Pharmacol, 2009. **75**(5): p. 1240-7.
179. Singh, A.K., et al., *Chemokine receptor trio: CXCR3, CXCR4 and CXCR7 crosstalk via CXCL11 and CXCL12.* Cytokine Growth Factor Rev, 2013. **24**(1): p. 41-9.
180. Toth, P.T., D. Ren, and R.J. Miller, *Regulation of CXCR4 receptor dimerization by the chemokine SDF-1alpha and the HIV-1 coat protein gp120: a fluorescence resonance energy transfer (FRET) study.* J Pharmacol Exp Ther, 2004. **310**(1): p. 8-17.
181. Wang, J., et al., *Dimerization of CXCR4 in living malignant cells: control of cell migration by a synthetic peptide that reduces homologous CXCR4 interactions.* Mol Cancer Ther, 2006. **5**(10): p. 2474-83.
182. Bonneterre, J., et al., *Analysis of Arrestin Recruitment to Chemokine Receptors by Bioluminescence Resonance Energy Transfer.* Methods Enzymol, 2016. **570**: p. 131-53.
183. Wu, B., et al., *Structures of the CXCR4 chemokine GPCR with small-molecule and cyclic peptide antagonists.* Science, 2010. **330**(6007): p. 1066-71.

184. Hatse, S., et al., *Mutation of Asp(171) and Asp(262) of the chemokine receptor CXCR4 impairs its coreceptor function for human immunodeficiency virus-1 entry and abrogates the antagonistic activity of AMD3100.* Mol Pharmacol, 2001. **60**(1): p. 164-73.
185. Amendola, V., et al., *The interaction of Mozobil with carboxylates.* Org Biomol Chem, 2016. **14**(3): p. 905-12.
186. Labrosse, B., et al., *Determinants for sensitivity of human immunodeficiency virus coreceptor CXCR4 to the bicyclam AMD3100.* J Virol, 1998. **72**(8): p. 6381-8.
187. Monsigny, M., et al., *Sugar-lectin interactions: how does wheat-germ agglutinin bind sialoglycoconjugates?* Eur J Biochem, 1980. **104**(1): p. 147-53.
188. Martinez-Munoz, L., et al., *Separating Actin-Dependent Chemokine Receptor Nanoclustering from Dimerization Indicates a Role for Clustering in CXCR4 Signaling and Function.* Mol Cell, 2018. **71**(5): p. 873.
189. Ray-Saha, S., T. Huber, and T.P. Sakmar, *Antibody epitopes on g protein-coupled receptors mapped with genetically encoded photoactivatable cross-linkers.* Biochemistry, 2014. **53**(8): p. 1302-10.
190. Delgado, M.B., et al., *Rapid inactivation of stromal cell-derived factor-1 by cathepsin G associated with lymphocytes.* Eur J Immunol, 2001. **31**(3): p. 699-707.
191. Kufareva, I., et al., *Stoichiometry and geometry of the CXC chemokine receptor 4 complex with CXC ligand 12: molecular modeling and experimental validation.* Proc Natl Acad Sci U S A, 2014. **111**(50): p. E5363-72.
192. Tamamis, P. and C.A. Floudas, *Elucidating a key component of cancer metastasis: CXCL12 (SDF-1alpha) binding to CXCR4.* J Chem Inf Model, 2014. **54**(4): p. 1174-88.
193. Doranz, B.J., et al., *Identification of CXCR4 domains that support coreceptor and chemokine receptor functions.* J Virol, 1999. **73**(4): p. 2752-61.
194. Veldkamp, C.T., et al., *Structural basis of CXCR4 sulfotyrosine recognition by the chemokine SDF-1/CXCL12.* Sci Signal, 2008. **1**(37): p. ra4.
195. Contento, R.L., et al., *CXCR4-CCR5: a couple modulating T cell functions.* Proc Natl Acad Sci U S A, 2008. **105**(29): p. 10101-6.
196. Combadiere, C., S.K. Ahuja, and P.M. Murphy, *Cloning and functional expression of a human eosinophil CC chemokine receptor.* J Biol Chem, 1996. **271**(18): p. 11034.
197. Combadiere, C., et al., *Cloning and functional expression of CC CKR5, a human monocyte CC chemokine receptor selective for MIP-1(alpha), MIP-1(beta), and RANTES.* J Leukoc Biol, 1996. **60**(1): p. 147-52.
198. Hebert, T.E., et al., *A peptide derived from a beta2-adrenergic receptor transmembrane domain inhibits both receptor dimerization and activation.* J Biol Chem, 1996. **271**(27): p. 16384-92.
199. Huang, K.S., et al., *Refolding of an integral membrane protein. Denaturation, renaturation, and reconstitution of intact bacteriorhodopsin and two proteolytic fragments.* J Biol Chem, 1981. **256**(8): p. 3802-9.
200. Jakubik, J. and J. Wess, *Use of a sandwich enzyme-linked immunosorbent assay strategy to study mechanisms of G protein-coupled receptor assembly.* J Biol Chem, 1999. **274**(3): p. 1349-58.
201. Kahn, T.W. and D.M. Engelman, *Bacteriorhodopsin can be refolded from two independently stable transmembrane helices and the complementary five-helix fragment.* Biochemistry, 1992. **31**(26): p. 6144-51.
202. Kobilka, B.K., et al., *Chimeric alpha 2-,beta 2-adrenergic receptors: delineation of domains involved in effector coupling and ligand binding specificity.* Science, 1988. **240**(4857): p. 1310-6.

203. Maggio, R., Z. Vogel, and J. Wess, *Reconstitution of functional muscarinic receptors by co-expression of amino- and carboxyl-terminal receptor fragments.* FEBS Lett, 1993. **319**(1-2): p. 195-200.
204. Osuga, Y., et al., *Co-expression of defective luteinizing hormone receptor fragments partially reconstitutes ligand-induced signal generation.* J Biol Chem, 1997. **272**(40): p. 25006-12.
205. Ridge, K.D., S.S. Lee, and L.L. Yao, *In vivo assembly of rhodopsin from expressed polypeptide fragments.* Proc Natl Acad Sci U S A, 1995. **92**(8): p. 3204-8.
206. Schoneberg, T., et al., *Functional rescue of mutant V2 vasopressin receptors causing nephrogenic diabetes insipidus by a co-expressed receptor polypeptide.* EMBO J, 1996. **15**(6): p. 1283-91.
207. Schoneberg, T., J. Liu, and J. Wess, *Plasma membrane localization and functional rescue of truncated forms of a G protein-coupled receptor.* J Biol Chem, 1995. **270**(30): p. 18000-6.
208. Tarasova, N.I., W.G. Rice, and C.J. Michejda, *Inhibition of G-protein-coupled receptor function by disruption of transmembrane domain interactions.* J Biol Chem, 1999. **274**(49): p. 34911-5.
209. Tarasov, S.G., et al., *Structural plasticity of a transmembrane peptide allows self-assembly into biologically active nanoparticles.* Proc Natl Acad Sci U S A, 2011. **108**(24): p. 9798-803.
210. Lee, Y., et al., *The structure of monomeric components of self-assembling CXCR4 antagonists determines the architecture of resulting nanostructures.* Nanotechnology, 2011. **22**(50): p. 505101.
211. Smith, M.C., et al., *CXCR4 regulates growth of both primary and metastatic breast cancer.* Cancer Res, 2004. **64**(23): p. 8604-12.
212. Follesa, P. and M.K. Ticku, *NMDA receptor upregulation: molecular studies in cultured mouse cortical neurons after chronic antagonist exposure.* J Neurosci, 1996. **16**(7): p. 2172-8.
213. Kang, D.S., X. Tian, and J.L. Benovic, *Role of beta-arrestins and arrestin domain-containing proteins in G protein-coupled receptor trafficking.* Curr Opin Cell Biol, 2014. **27**: p. 63-71.
214. Marchese, A. and J. Trejo, *Ubiquitin-dependent regulation of G protein-coupled receptor trafficking and signaling.* Cell Signal, 2013. **25**(3): p. 707-16.
215. Busillo, J.M., et al., *Site-specific phosphorylation of CXCR4 is dynamically regulated by multiple kinases and results in differential modulation of CXCR4 signaling.* J Biol Chem, 2010. **285**(10): p. 7805-17.
216. Percherancier, Y., et al., *Bioluminescence resonance energy transfer reveals ligand-induced conformational changes in CXCR4 homo- and heterodimers.* J Biol Chem, 2005. **280**(11): p. 9895-903.
217. Ahn, S., et al., *Differential kinetic and spatial patterns of beta-arrestin and G protein-mediated ERK activation by the angiotensin II receptor.* J Biol Chem, 2004. **279**(34): p. 35518-25.
218. Quoyer, J., et al., *Pepducin targeting the C-X-C chemokine receptor type 4 acts as a biased agonist favoring activation of the inhibitory G protein.* Proc Natl Acad Sci U S A, 2013. **110**(52): p. E5088-97.
219. Beautrait, A., et al., *A new inhibitor of the beta-arrestin/AP2 endocytic complex reveals interplay between GPCR internalization and signalling.* Nat Commun, 2017. **8**: p. 15054.
220. Kohout, T.A., et al., *beta-Arrestin 1 and 2 differentially regulate heptahelical receptor signaling and trafficking.* Proc Natl Acad Sci U S A, 2001. **98**(4): p. 1601-6.

221. Ikeda, S.R., *Voltage-dependent modulation of N-type calcium channels by G-protein beta gamma subunits.* Nature, 1996. **380**(6571): p. 255-8.
222. Hitchinson, B., et al., *Biased antagonism of CXCR4 avoids antagonist tolerance.* Sci Signal, 2018. **11**(552).
223. Grozdanovic, M., et al., *Novel peptide nanoparticle-biased antagonist of CCR3 blocks eosinophil recruitment and airway hyperresponsiveness.* J Allergy Clin Immunol, 2019. **143**(2): p. 669-680 e12.
224. Tripathi, A., et al., *Heteromerization of chemokine (C-X-C motif) receptor 4 with alpha1A/B-adrenergic receptors controls alpha1-adrenergic receptor function.* Proc Natl Acad Sci U S A, 2015. **112**(13): p. E1659-68.
225. Berchiche, Y.A., et al., *Direct assessment of CXCR4 mutant conformations reveals complex link between receptor structure and G(alpha)(i) activation.* J Biol Chem, 2007. **282**(8): p. 5111-5.
226. Feng, Y.H., et al., *Mechanism of constitutive activation of the AT1 receptor: influence of the size of the agonist switch binding residue Asn(111).* Biochemistry, 1998. **37**(45): p. 15791-8.
227. Castaldo, C., et al., *CXCR4 Antagonists: A Screening Strategy for Identification of Functionally Selective Ligands.* J Biomol Screen, 2014. **19**(6): p. 859-69.
228. Zhang, L., et al., *Alpha-1 adrenoceptor up-regulation induced by prazosin but not KMD-3213 or reserpine in rats.* Br J Pharmacol, 2002. **135**(7): p. 1757-64.
229. Aarons, R.D., et al., *Elevation of beta-adrenergic receptor density in human lymphocytes after propranolol administration.* J Clin Invest, 1980. **65**(5): p. 949-57.
230. Ohkuma, S., et al., *Expression of beta-adrenergic receptor up-regulation is mediated by two different processes.* Brain Res, 2006. **1112**(1): p. 114-25.
231. Ngai, J., et al., *Interplay between the heterotrimeric G-protein subunits Galphaq and Galphai2 sets the threshold for chemotaxis and TCR activation.* BMC Immunol, 2009. **10**: p. 27.
232. Martinez-Martin, N., et al., *Herpes simplex virus enhances chemokine function through modulation of receptor trafficking and oligomerization.* Nat Commun, 2015. **6**: p. 6163.
233. Barwinska, D., et al., *AMD3100 ameliorates cigarette smoke-induced emphysema-like manifestations in mice.* Am J Physiol Lung Cell Mol Physiol, 2018. **315**(3): p. L382-L386.
234. McDermott, D.H., et al., *A phase 1 clinical trial of long-term, low-dose treatment of WHIM syndrome with the CXCR4 antagonist plerixafor.* Blood, 2014. **123**(15): p. 2308-16.
235. Grundler, R., et al., *Dissection of PIM serine/threonine kinases in FLT3-ITD-induced leukemogenesis reveals PIM1 as regulator of CXCL12-CXCR4-mediated homing and migration.* J Exp Med, 2009. **206**(9): p. 1957-70.
236. Elorza, A., et al., *MAPK-dependent degradation of G protein-coupled receptor kinase 2.* J Biol Chem, 2003. **278**(31): p. 29164-73.
237. Loudon, R.P., B. Perussia, and J.L. Benovic, *Differentially regulated expression of the G-protein-coupled receptor kinases, betaARK and GRK6, during myelomonocytic cell development in vitro.* Blood, 1996. **88**(12): p. 4547-57.
238. Luo, Y., et al., *SDF1alpha/CXCR4 signaling, via ERKs and the transcription factor Egr1, induces expression of a 67-kDa form of glutamic acid decarboxylase in embryonic hippocampal neurons.* J Biol Chem, 2008. **283**(36): p. 24789-800.
239. Kremer, K.N., et al., *Stromal cell-derived factor-1 signaling via the CXCR4-TCR heterodimer requires phospholipase C-beta3 and phospholipase C-gamma1 for distinct cellular responses.* J Immunol, 2011. **187**(3): p. 1440-7.
240. Lefkowitz, R.J. and S.K. Shenoy, *Transduction of receptor signals by beta-arrestins.* Science, 2005. **308**(5721): p. 512-7.

241. Tohgo, A., et al., *beta-Arrestin scaffolding of the ERK cascade enhances cytosolic ERK activity but inhibits ERK-mediated transcription following angiotensin AT1a receptor stimulation.* J Biol Chem, 2002. **277**(11): p. 9429-36.
242. Luo, J., J.M. Busillo, and J.L. Benovic, *M3 muscarinic acetylcholine receptor-mediated signaling is regulated by distinct mechanisms.* Mol Pharmacol, 2008. **74**(2): p. 338-47.
243. Jung, S.R., et al., *Muscarinic receptor regulates extracellular signal regulated kinase by two modes of arrestin binding.* Proc Natl Acad Sci U S A, 2017. **114**(28): p. E5579-E5588.
244. Zhao, M., et al., *Arrestin regulates MAPK activation and prevents NADPH oxidase-dependent death of cells expressing CXCR2.* J Biol Chem, 2004. **279**(47): p. 49259-67.
245. Grundmann, M., et al., *Lack of beta-arrestin signaling in the absence of active G proteins.* Nat Commun, 2018. **9**(1): p. 341.
246. Liebick, M., et al., *Functional consequences of chemically-induced beta-arrestin binding to chemokine receptors CXCR4 and CCR5 in the absence of ligand stimulation.* Cell Signal, 2017. **38**: p. 201-211.
247. O'Reilly, L.A., et al., *MEK/ERK-mediated phosphorylation of Bim is required to ensure survival of T and B lymphocytes during mitogenic stimulation.* J Immunol, 2009. **183**(1): p. 261-9.
248. Ramachandran, R., et al., *Targeting proteinase-activated receptors: therapeutic potential and challenges.* Nat Rev Drug Discov, 2012. **11**(1): p. 69-86.

APPENDIX A

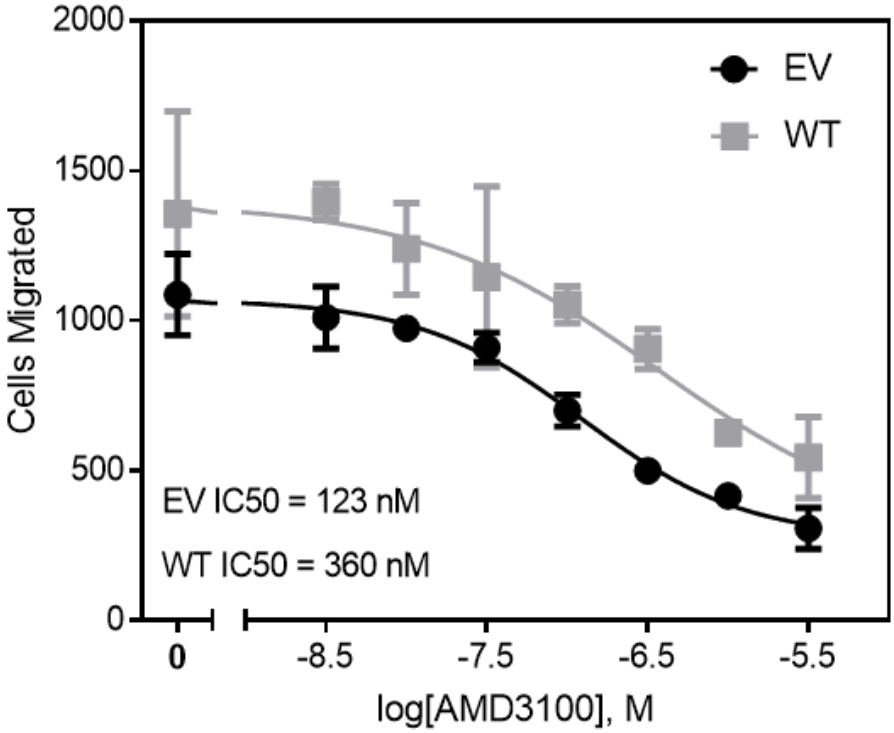

Figure 1: Transient overexpression of CXCR4 increases chemotaxis of Jurkat cells.

Jurkat cells were electroporated with 2 µg pcDNA3.1-EV or pcDNA3.1-Ha-CXCR4. After 36 hours, cells were subjected to a chemotaxis assay with stimulation by 20 nM CXCL12 and increasing concentrations of AMD3100.

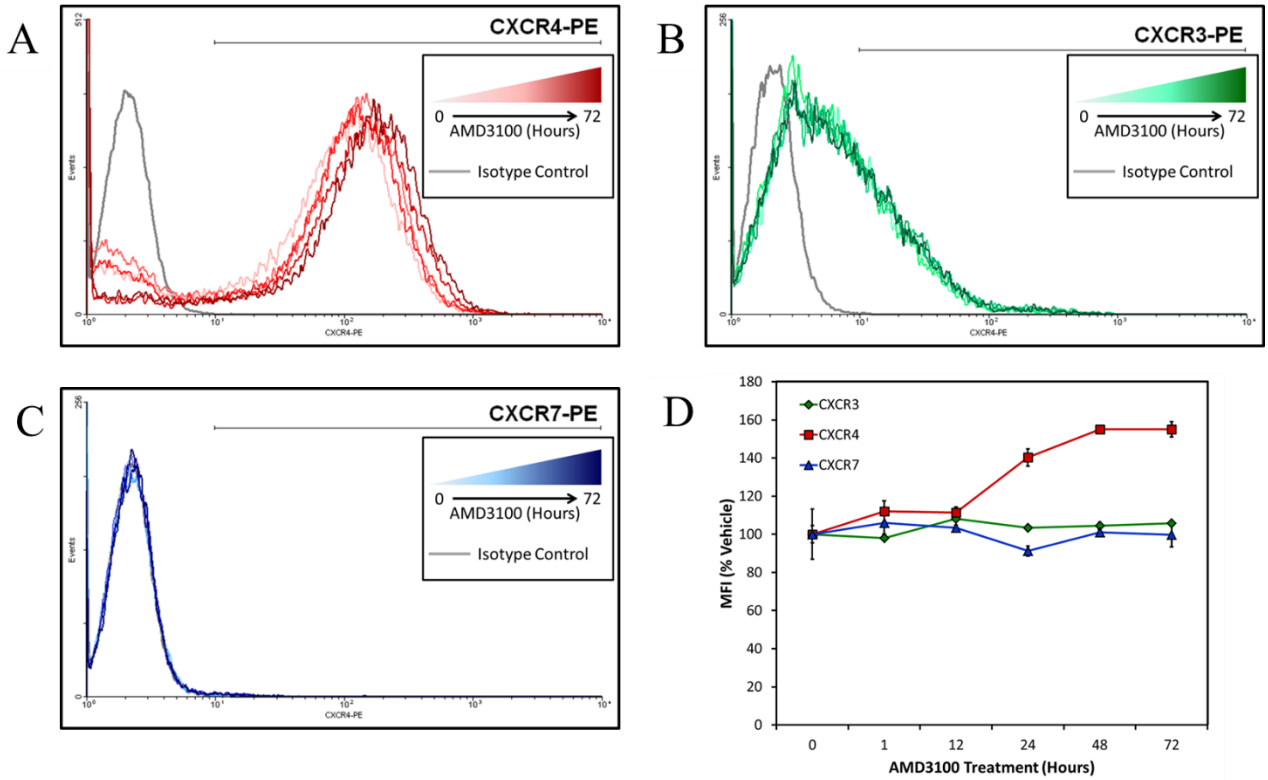

Figure 2: CXCR4 but not CXCR3 or AKCR7 increase in at the cell surface after prolonged exposure to AMD3100.

Jurkat cells were treated with AMD3100 for 1, 24, 48 and 72 hours with 1 µM AMD3100 and flow cytometry used to identify changes in the cell surface expression of the chemokine receptors (A) CXCR4, (B) CXCR3 and (C) AKCR7. MFI was quantified and plotted (D).

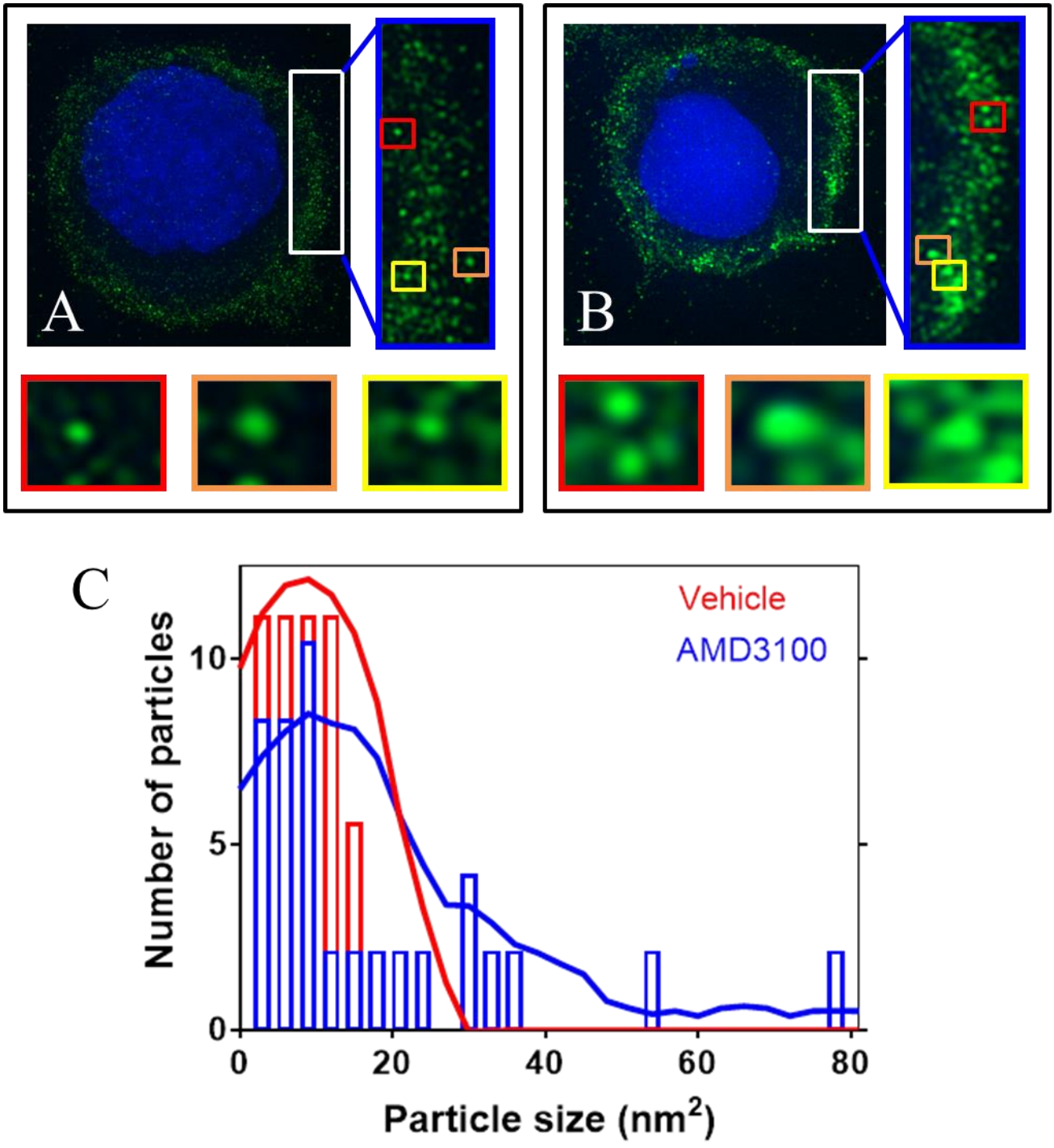

Figure 3: Structure illumination microscopy reveals clustering of CXCR4 after prolonged exposure to AMD3100.

Jurkat cells were treated with 1 µM AMD3100 for (A) 0 or (B) 72 hours. Cells were fixed onto coverslips and stained for CXCR4 using the anti-CXCR4 antibody 4G10. (C) Particle size was analysed by image J and plotted as a histogram.

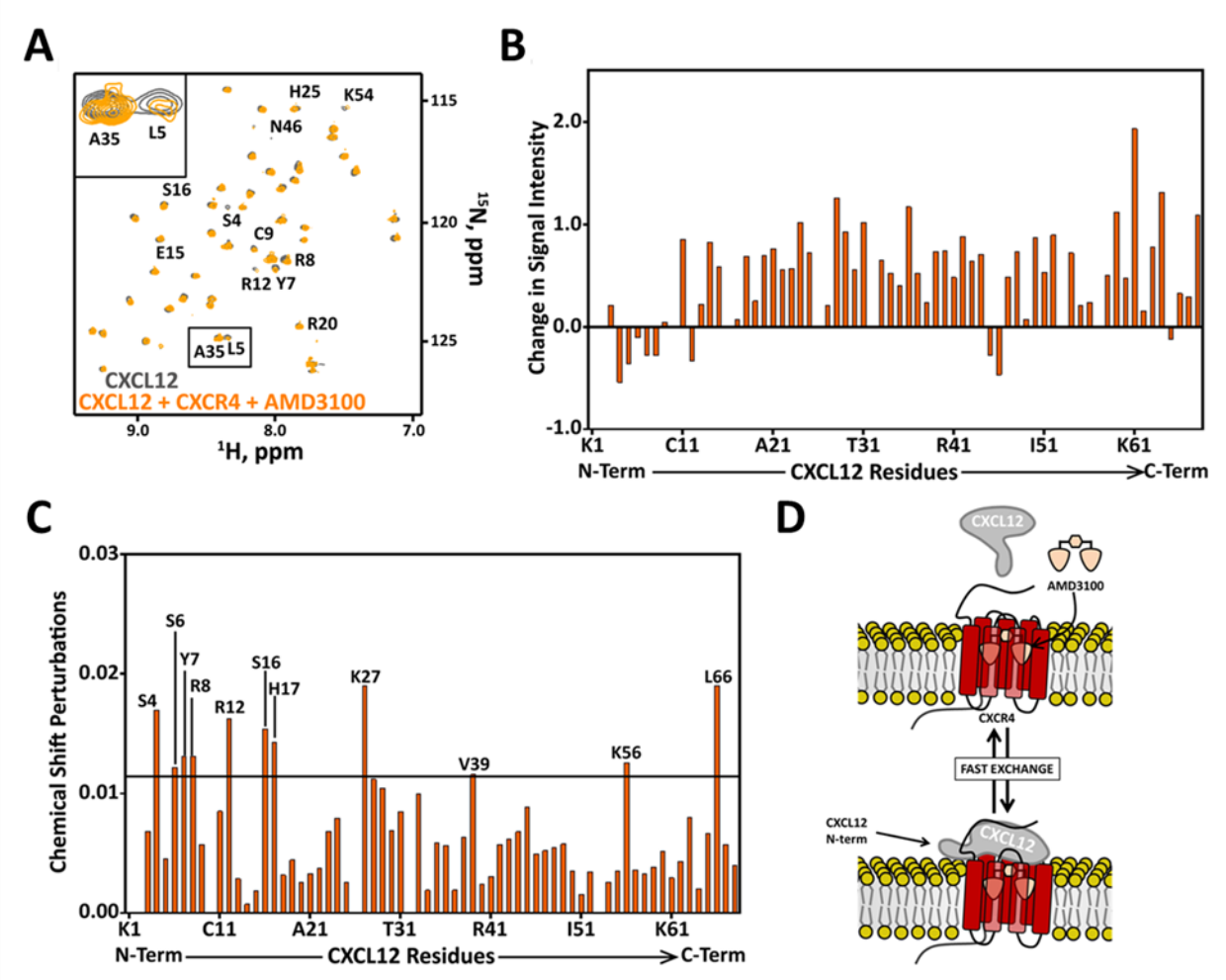

Figure 4: AMD3100 displaces the CXCL12 N-terminus from the CXCR4 binding site. (A) Superimposition of 1H-15N HSQC NMR spectra of 100 µM CXCL12 (grey) and 100 µM CXCL12 plus 20 µg of membrane preparations containing CXCR4 and 1 µM AMD3100 (orange). Residues affected by the addition of CXCR4 only are annotated for comparison. (B) The difference in signal intensity in CXCL12 spectra caused by the addition of CXCR4 and 1 µM AM3100 are graphed. (C) Chemical shift perturbation (CSP) analysis of CXCL12 1H-15N HSQC spectra upon addition of CXCR4 and AM3100 are graphed. Significant CSPs are those greater than the average CSP plus one standard deviation, denoted by the horizontal black line. (D) Models of the interaction between CXCR4, CXCL12 and AMD3100 showing displacement of the CXCL12 N-terminus from the receptor transmembrane helical bundle are depicted as cartoons.

STATEMENT OF PERMISSION FOR USE OF PREVIOUSLY PUBLISHED MATERIAL

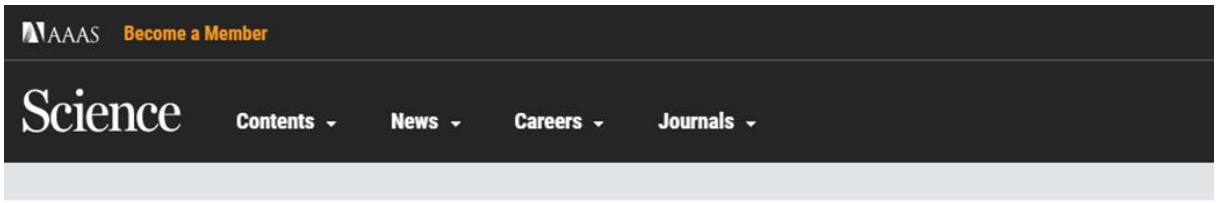

Reprints and Permissions

Using AAAS material in a thesis or dissertation

NOTE: If you are the original author of the AAAS article being reproduced, please refer to your License to Publish for rules on reproducing your paper in a dissertation or thesis. AAAS permits the use of content published in its journals *Science, Science Immunology, Science Robotics, Science Signaling, and Science Translational Medicine*, but only provided the following criteria are met:

1. If you are using figure(s)/table(s), permission is granted for use in print and electronic versions of your dissertation or thesis.
2. A full-text article may be used only in print versions of a dissertation or thesis. AAAS does not permit the reproduction of full-text articles in electronic versions of theses or dissertations.
3. The following credit line must be printed along with the AAAS material: "From [Full Reference Citation]. Reprinted with permission from AAAS."
4. All required credit lines and notices must be visible any time a user accesses any part of the AAAS material and must appear on any printed copies that an authorized user might make.
5. The AAAS material may not be modified or altered except that figures and tables may be modified with permission from the author. Author permission for any such changes must be secured prior to your use.
6. AAAS must publish the full paper prior to your use of any of its text or figures.
7. If the AAAS material covered by this permission was published in *Science* during the years 1974–1994, you must also obtain permission from the author, who may grant or withhold permission, and who may or may not charge a fee if permission is granted. See original article for author's address. This condition does not apply to news articles.
8. If you are an original author of the AAAS article being reproduced, please refer to your License to Publish for rules on reproducing your paper in a dissertation or thesis.

VITA

Ben Hitchinson

617 S. Lytle Street, Chicago, IL 60607

Cell: (312) 771-5539 *Email:* benhitchinson@gmail.com

Independent and enthusiastic biochemist with 8 years of experience in biochemistry research. Successfully managed thesis research and several collaborative projects resulting in publications in multiple areas.

KEY TECHNICAL SKILLS

- **Molecular and Cell Biology:** Confocal microscopy, flow cytometry, SDS-PAGE, western blotting, ELISA, immunoprecipitation, PCR, cloning, mutagenesis, proliferation assays, chemotaxis assays, cell fractionation.
- **Mammalian Cell Culture:** Experience with a range of cell lines including CHO, HEK, HeLa, Jurkat cells, stable and transient transfections.
- **Protein Biochemistry:** Recombinant protein expression and purification, chromatography and SPR.
- **Spectroscopy:** NMR, Fluorescence and UV.
- **Other:** Fluency in Microsoft office and Graphpad Prism, ability to organize and present complex data, to communicate with a range of audiences, and to work as part of a diverse team.

EDUCATION

Ph.D. Biochemistry	University of Illinois at Chicago (UIC), Chicago, IL USA	2012-2018
M.Res. Cancer Biology	Imperial College London, London, UK	2010-2011
B.Sc. (Hons) Biological Sciences	University of Teesside, Middlesbrough, UK	2007-2010

SELECTED PEER-REVIEWED PUBLICATIONS AND PATENTS

- **Hitchinson, B.** *et al.* (2018). Biased antagonism of CXCR4 avoids antagonist tolerance. Sci Signal 11.
- Halasi, M., **Hitchinson, B.** *et al.* (2018). Honokiol is a FOXM1 antagonist. Cell death & disease 9, 84.
- Jang, H., Abraham, S. J., Chavan, T. S., **Hitchinson, B.** *et al.* (2015). Mechanisms of membrane binding of small GTPase K-Ras4B farnesylated hypervariable region. J Biol. Chem. 290, 9465-9477.
- Adams, C., Cazzanelli, G., Rasul, S., **Hitchinson, B.** *et al.* (2015). Apoptosis inhibitor TRIAP1 is a novel effector of drug resistance. Oncology reports 34, 415-422.
- Grozdanovic, M., Laffey, K.G., Abdelkarim, H., **Hitchinson, B.** *et al.* (2018). Peptide nanoparticle-biased antagonist of CCR3 blocks eosinophil recruitment and airway hyperresponsiveness. JACI 18, 30709-7.
- Ackerman, S., Laffey, F., **Hitchinson, B.** *et al,* 2016. Peptide inhibition of ccr3-mediated diseases or conditions. U.S. Patent 62/115,880 filed February 13, 2015 and issued February 12, 2016.

AWARDS AND FUNDING

Dr. Gary Kruh Cancer Research Symposium Poster Prize Winner	2018
UIC Center for Clinical and Translational Science Grant	2015-2016
UIC Molecular Biology Research Symposium Poster Prize Winner	2015
UIC Biochemistry Retreat Poster Prize Winner	2014 & 2012
University of Illinois Cancer Center Poster Prize Winner	2013

Presented work at more than 5 national and international conferences.